HYDROLOGICAL ANALYSIS AND IMPROVED BRIDGE SCOUR PREDICTION FOR SELECTED STREAMS IN HAWAII

A THESIS SUBMITTED TO THE GRADUATE DIVISION OF THE UNIVERSITY OF HAWAI'I IN PARTIAL FULFILLMENT OF THE REQUIREMENTS FOR THE DEGREE OF

MASTER OF SCIENCE

IN

CIVIL ENGINEERING

May 2013

By

Nicholas Tecca

Thesis Committee:

Michelle H. Teng, Chairperson
Pao-Shin Chu
Oceana Francis
Phillip Ooi

ACKNOWLEDGEMENTS

I would like to express my gratitude and appreciation for all of the time, energy and hard work put into this project by Dr. Michelle Teng. The patient instruction and helpful advice offered by Dr. Teng was invaluable in the completion of this thesis. I would like to thank Dr. Phillip Ooi for sharing his geotechnical expertise critical to completing this thesis research. I also want to express my appreciation to Dr. Pao-Shin Chu and Dr. Oceana Francis for their help, support and guidance in completing this project.

I would like to thank Mr. Reza Rahimnejad for his assistance with the geotechnical lab work critical to the completion of this project. For assistance in collecting soil samples and conducting site investigations, I would like to thank Nelson Fernandez, Melia Iwamoto, Todd Kawamoto, Jarrett Yanagida, Isaiah Sato, Zoey Malaluan, Ame Masutomi, and Tony Shing.

I am very grateful to Mr. Gavin Masaki and Mr. James Nakamura for the excellent research conducted in previous studies that laid the foundation for this project. I would also like to thank Mr. Curtis Matsuda, Hydraulic Design Section Chief at the Hawaii Department of Transportation, for his continued support of this project.

Finally, I would like to thank all of my family and friends who have patiently supported me in the completion of this thesis and throughout my academic career.

This thesis was funded by Hawaii Department of Transportation (HDOT) contract number DOT-08-004. The opinions expressed in this report are solely those of the author and do not necessarily reflect the opinions of HDOT.

ABSTRACT

Flood induced bridge scour is the erosion of soil sediments around a bridge structure caused by the increased velocity of a stream during a flood event and turbulent flows caused by any sub-structure in the stream bed. Bridge scour is the leading cause of bridge failure in the United States, responsible for 60% of all bridge failures. Since 1988 the Federal Highway Administration (FHWA) has required that all new bridges be designed to resist scour. An over prediction in scour depth can result in a significant, possibly prohibitive, increase in construction cost and difficulty. An under prediction in scour depth can result in a bridge that is unsafe over the life of the structure. The FHWA recommends using the Hydraulic Engineering Circular 18 (HEC-18) design manual to predict bridge scour. The HEC-18 manual includes a series of empirical equations to predict maximum scour depth based on laboratory experiments in non-cohesive soils. Researchers have shown that for certain situations, the HEC-18 method over predicts the depth of scour, sometimes by a large margin. Researchers from Texas A&M University have proposed the Scour Rate in COhesive Soils Erosion Function Apparatus (SRICOS-EFA) method that accounts the development of scour over time and a wider range of soil properties than the HEC-18 method. The SRICOS-EFA requires an erosion rate curve to define the soil properties, whereas the HEC-18 method only requires the median grain size. A hydrograph is also required for the SRICOS-EFA method whereas the HEC-18 method only requires a peak flow rate. The SRICOS-EFA method is still new and requires more data to evaluate and validate the accuracy of the scour predictions.

The primary objectives of this study were to evaluate the HEC-18 design manual and SRICOS-EFA scour prediction methods and assess the hydrologic analysis required for each method. The pier scour predictions for both methods were evaluated for a single flood event, as only one scour event was available for use in this study. The hydrologic methods required to perform each scour calculation will be analyzed. This hydrologic analysis will include different methods to predict peak flow, determination of appropriate rainfall and stream flow duration for a design event and development of design hydrograph.

Two case studies on the island of Oahu, Hawaii were conducted in this study. The first case study was conducted on the Kaelepulu Stream. A scour event was recorded on January 2nd, 2004. The HEC-18 method and SRICOS-EFA method were used to make predictions for the recorded event, and these predictions were compared with the recorded scour depth. The second case study was conducted on the Manoa-Palolo Stream. Flood frequency analysis was conducted on the Manoa-Palolo watershed to determine the 100 year peak flow rate using statistical analysis and rainfall-runoff models. The peak flow rates and design hydrographs generated by each of 6 different methods was compared and evaluated. The scour depth caused by the 100 year flood was predicted using both methods and these results were also compared.

Both the HEC-18 method and the SRICOS-EFA method required a range of hydrologic and geotechnical parameters. Hydrologic analysis was conducted to determine how to reasonably represent local hydrologic conditions in a scour design calculation. The sensitivity of the final scour depth to variations in different parameters including the effect of hydrograph duration, hydrograph shape and soil type was analyzed with respect to local hydrologic conditions.

The January 2nd, 2004 scour event in the Kaelepulu stream is utilized to validate the scour prediction methods. The SRICOS-EFA method provided a more accurate prediction of scour depth than the HEC-18 method for the January 2nd scour event in the Kaelepulu Stream. The SRICOS-EFA method and the HEC-18 method had similar maximum scour depths for soils that were highly erodible or for floods conditions that were sufficiently long. Soils with low erodibility were found to be more sensitive to variations in hydrograph duration and shape than soils with high erodibility.

TABLE OF CONTENTS

Section **Page**

LIST OF TABLES

Table **Page**

LIST OF FIGURES

Chapter 1 INTRODUCTION

1.1 Technical Background

Bridge scour is defined as the erosion of soil sediments induced by the flow of a river around a bridge structure. Scour is a dynamic process, and it consists of both the aggradation and degradation of soil. Bridge scour is often the largest during flood events, when the velocity of the flow has increased relative to the base flow. Scour can occur across the width of the channel, induced by the bridge structure contracting the channel causing an increase in velocity in the bridge section relative to the upstream and downstream reaches. Turbulent flow around piers and abutments are also major factors in scour potential. The focus of this thesis is primarily on predicting the total depth of scour at a pier during a single flood event.

Scour is the leading cause of bridge failure in the United States, responsible for approximately 60% of all bridge failures (Federal Highway Administration, 1988). A catastrophic bridge failure can result in significant transportation difficulties, a large burden on the taxpayers, and potentially the loss of lives of those on or near the bridge when it fails. An accurate assessment of the scour potential can ensure that existing bridges are safe and that new bridges are constructed safely and economically. Scour potential is often the controlling parameter in the design of foundation depth. An over prediction in scour depth can result in a significant, possibly prohibitive, increase in the cost of building the bridge and the difficulty in construction. An under prediction of scour depth can lead to a new bridge that is unsafe.

Since 1988 the Federal Highway Administration (FHWA) has required that all new bridges are designed to withstand scour caused by large flood events. The most recent version of the Hydraulic Engineering Circular 18 design manual recommends applying risk-based approach to scour design that incorporates the need to provide safe infrastructure with the economic consequences of bridge failure (Arneson, Zevenbergen, Lagasse, & Clopper, 2012). The HEC-18 manual requires that all bridges remain serviceable during the scour design flood frequency, and stable during the scour design check flood frequency. The frequencies are a function of the return period of the design

flood. Table 1-1 shows the design frequencies as recommended by HEC-18, where the return period of the flood is denoted in the subscript. The HEC-18 manual states that it is almost always more cost effective to use a larger design event and prevent failure even in the case of very large flood events. The Hawaii Department of Transportation (HDOT) recommends different design flood frequencies based on the type of roadway functional classification shown in Figure 1-1. The HDOT design flood frequency and HEC-18 manual scour design flood frequency should be used together to determine the appropriate design flood for a particular structure located on the island of Oahu.

Table 1-1 Hydraulic design, scour design and scour design check flood frequencies (Arneson, Zevenbergen, Lagasse, & Clopper, 2012)

Hydraulic Design Flood Frequency, Q_D	Scour Design Flood Frequency, Q_S	Scour Design Check Flood Frequency, Q_C
Q_{10}	Q_{25}	Q_{50}
Q_{25}	Q_{50}	Q_{100}
Q_{50}	Q_{100}	Q_{200}
Q_{100}	Q_{200}	Q_{500}

Note: Q_{xx} denotes the flow rate for a particular river with the return period, XX, in years

RECURRENCE INTERVALS (yrs)			
Functional Classification*	Bridge/Culvert Crossing	Roadway (at grade)	Roadway (sump)
Interstate	50 **	25	50
Freeway/Expressway	50 **	25	50
Arterial	50 **	25	25
Collector	25	10	10
Local	10	10	10

* Refer to the current State Route System *(Straight Line Diagram)* prepared by the Department of Transportation for the roadway functional classification.

** 100 year interval for sites covered under the Flood Insurance Rate Map (FIRM). The Design Engineer shall comply with the National Flood Insurance Program's regulations and requirements.

- Designated recurrence intervals shall include associated ramps and auxiliary lanes.
- All bridge structures shall be analyzed for both 50 and 100 year storm event.

Figure 1-1 Hawaii Department of Transportation design flood frequency (Hawaii Department of Transportation Highways Division, 2010)

The FHWA recommends using the Hydraulic Engineering Circular 18 (HEC-18) design manual to predict design scour depth (Arneson, Zevenbergen, Lagasse, & Clopper, 2012). The HEC-18 method is an empirical equation based on laboratory experiments using sand as the stream bed. The equation predicts maximum scour depth under peak flow conditions, and does not account for the development of scour over time. For these reasons the HEC-18 equation has been the subject of significant research to evaluate its validity and accuracy (Conaway, 2007, Larsen, Francis & Jones, 2011, Polasik, 2004). Researchers have been able to show that the HEC-18 method over predicts scour depth when compared to observed field data, sometimes by as much as a factor of 10 (Masaki, 2004). The HEC-18 method will be discussed further in Section 2.1.

Recently, researchers at Texas A&M University have developed an alternative method for predicting maximum scour depth. The Scour Rate in Cohesive Soils – Erosion Function Apparatus (SRICOS-EFA) method accounts for site specific soil properties and

the time dependence of the development of scour (Briaud et al, 1999, 2004, 2011). Shelby tubes taken from a bridge location are analyzed using the erosion function apparatus (EFA), and a curve relating bed shear stress to erosion rate is developed. The SRICOS-EFA method requires a stream hydrograph for the period of interest, which allows the method to account for development of scour over time. Since it is relatively new, the SRICOS-EFA requires more field data to validate the method. The SRICOS-EFA method will be discussed further in Section 2.2.

Both of the scour prediction methods that are investigated in this study require numerous input parameters related to stream geometry, local hydraulics, bridge geometry and soil media. The majority of these parameters can be obtained by looking at bridge plans, site visits and lab work. The hydrology input to both methods can pose a fundamental issue. The HEC-18 method requires the velocity upstream of the bridge. For a historic event on a gaged stream, the stream records can be utilized. To predict scour caused by a design event, statistical analysis of historic records can produce the 100 year peak flow rate, or the appropriate flood frequency as determined by Table 1-1. The Log-Pearson III and Gumbel distributions will be utilized in a flood frequency analysis. A hydraulic software model can then be used to convert the flow rate to a stream velocity. Predicting scour depth for a design event (e.g., 100 year flood) on an ungaged stream can be more difficult. Hydrologic methods that are applicable for peak flow prediction in ungaged watersheds and will be studied include the rational method, TR-55, regional regression equations and HEC-HMS software. All 6 of the hydrologic methods mentioned will be applied to a single watershed to evaluate the peak flow rates predicted by each method. The SRICOS-EFA method requires a complete hydrograph for the period of interest to predict scour depth, not just the peak flow rate. For analyzing historic scour on a gaged stream, this can be relatively simple, if sufficiently long records are available. However to predict scour induced by a design hydrograph, whether the stream is gaged or ungaged, is difficult. Is hydrograph duration equal to the life of the bridge with the 100 year peak flow inserted reasonable? This is conservative but would ignore the effects of aggradation in the stream. It has been observed that a single large flood event (e.g., 100 year flood) may result in nearly the entire scour depth for the life of the

bridge (Ghelardi, 2004). Therefore it may be reasonable to only analyze the 100 year flood event. But what is a reasonable and conservative duration of the 100 year flood? Is a watershed specific duration (e.g., time of concentration) or a standard duration (e.g., 24 hours) a reasonable estimate of flood duration? Current design standards from the FHWA do not mention standard design duration. What is the shape of the hydrograph of a 100 year flood? Using a rectangular hydrograph with peak equal to the 100 year peak flow is conservative, but a unit hydrograph, triangular hydrograph or a recorded hydrograph scaled to the 100 year peak may be more accurate while still conservative. If routing procedures are utilized to predict the 100 year flow rate from rainfall data, what duration of rainfall is required to induce the 100 year flow rate? Is it reasonable to assume the 100 year rainfall induces the 100 year flood? These hydrologic issues have not been fully investigated in existing studies and will be further discussed in Chapter 3.

1.2 Literature Review

1.2.1 Scour in Non-Cohesive Soils

Early attempts to predict bridge scour relied on data from laboratory experiments with a limited number of parameters. Inglis (1949) developed a scour equation based solely on pier width and flow depth. This equation was developed based on flume experiments that only utilized sand with a median grain size of 0.29 mm and a single pier.

Laursen and Toch (1956) conducted flume experiments to determine the importance of flow, pier size and alignment, approach flow velocity and depth and sediment size on scour depth. The researchers concluded that flow velocity and sediment size did not have a significant effect on scour depth, and maximum scour depth was a function of the bridge geometry.

Several studies have been conducted to evaluate the accuracy of published empirical bridge scour equations, including the equations presented by Inglis (1949), Laursen and Toch (1956) and the HEC-18 design equation. Miller and Wilson (1996) evaluated 20 bridge sites using 14 published pier scour equations in Indiana. Scour depth

was determined using ground-penetrating radar and the observed scour depth was assumed to be caused by the peak historic discharge over the life of the bridge. The author's assumptions do not account for effects of aggradation that may result in the authors observed scour depth being smaller than the true maximum scour depth. The authors found that combining contraction scour and pier scour often led to overly large scour depths, however only analyzing pier scour led to numerous underestimates of scour depth. Debris piles at piers were observed to have a very large effect on observed scour depth. The depth of scour was measured to be greater at low flows with debris present than at high flow with debris removed. The authors found that none of the 14 equations that were studied accurately represented the historic pier scour at all of the bridge sites included in the study.

Jackson (1996) studied 84 cases of pier scour at 22 different bridge sites in Ohio including both cohesive and non-cohesive soils. Observed scour depth ranged from 0.5 to 6.1 feet and was used to evaluate the accuracy of 17 published scour equations. All of the published scour equations were inconsistent in accurately predicting scour depth, often including underestimates of scour depth or unrealistic overestimates. The Froehlich design equation was found to be the best scour design equation.

Masaki (2004) studied the development of bridge scour in Hawaii. Scour monitoring devices were installed on two bridges on Oahu. A scour event was recorded in real time by a sliding magnetic collar type scour monitoring device. Stream discharge was computed using the Muskingum routing method from a nearby rain gage. The methods described in the HEC-18 design manual predicted a scour depth of 11.03 feet compared to the 1 foot of scour that was recorded.

Some research has been focused on modifying the HEC-18 equation rather than creating a different model. There has been some success in reducing design scour depth and increasing accuracy by using multi-dimensional hydraulic models, physical models, and analysis of existing scour data.

Polasik (2005) conducted a case study for a design build of the new Tacoma Narrows Bridge to attempt to reduce the design scour depth to the minimum reasonable depth to minimize construction cost. Scour for the existing bridge was found to be about

half of the HEC-18 predicted scour, 63 years after construction. A one-dimensional model (HEC-RAS) for scour prediction, a two-dimensional model (RMA2) for hydraulic analysis, and a physical model to predict scour depth were all utilized to predict a reasonable design scour depth. Video inspection of the channel bed showed that large stones are present on the channel bed armoring the bed against scour. Scour depth predicted by the physical model were used to predict the bridge scour depth using a formula that includes a ratio of model and site bed material. Using the prediction from the physical model and the RMA2 model, the design scour depth was reduced by about 10 m from the original HEC-18 scour prediction.

Calappi et al. (2010) used data from the National Bridge Scour Database to perform non-linear regression and optimize the HEC-18 design equation for non-cohesive soils. The data was separated based on approach depth ratio, and for each range of approach depth ratios regression parameters were optimized, and a factor of safety was added to create a design equation. The proposed equation was able to reduce the mean square error for the validation data set significantly compared to the original HEC-18 design equation.

Nakamura (2010) revisited the scour event recorded by Masaki (2004). The Scour Rate in Cohesive Soils Erosion Function Apparatus method was used to predict scour depth and the results were compared to the scour depth prediction made using the HEC-18 method. The soil sediments in the stream are non-cohesive and therefore the median grain size is believed to be the controlling soil property for scour depth. Three erosion function curves for a clay, fine sand and sand were taken from the literature with a median grain size similar to the median grain size observed at the site. The scour depth predicted by the SRICOS-EFA method for the silty clay, fine sand and sand are 0.03 ft, 0.896 ft and 4.89 ft, respectively. The SRICOS-EFA method significantly improved the accuracy of the scour depth prediction relative to the HEC-18 method prediction of 11.03 feet and compared to the observed scour depth of 1 foot.

1.2.2 Scour in Cohesive Soils and Clay/Sand Mixtures

Only a limited number of studies have been conducted on bridge scour in cohesive soils. The SRICOS-EFA method proposed by Briaud et al (1999, 2001, 2004, 2011) is one of the major studies on this topic and will be discussed in detail in section 2.2. In addition to that work, several other studies have attempted to improve the scour depth prediction for clay type soils. These findings are discussed in this section.

Jiang et al. (2004) used a linear empirical erosion flux equation to determine scour depth for a single case study. The erosion rate was determined using the Simulator of Erosion Rate Function (SERF). SERF is an instrument that tests erodability of clay type soils. A cylindrical sample, that has sufficient cohesion to stand under its own strength, is suspended in a larger cylinder from a load cell and submerged in water. The outside cylinder is then rotated, causing the water to generate shear stress on the surface of the clay sample. The erosion flux is then calculated by the amount of mass lost during the test. The researchers utilized a clay soil with similar characteristics to the in-situ soil. The bathymetry of the scour hole observed in the field was compared with the scour hole predicted by the erosion flux equation. The researchers found the area of the hole at each depth contour was fairly comparable between estimated and measured values, showing that their method may be useful at determining both scour depth and dimensions.

Ghelardi (2004) estimated the long term scour at five bridges in Maryland using the SRICOS-EFA method. Synthetic hydrographs with a 160 year duration using a statistical analysis that had the correct distribution of daily flows were utilized. Four of the five sites did not have a flood that exceeded the 100 year flood event in their statistically generated hydrographs. Therefore the discharge equal to the 100 year event was manually inserted to the hydrographs of all five streams to ensure the worst case scenario was included and to allow for more accurate comparison to the HEC-18 method scour depth prediction for the 100 year event. The SRICOS-EFA method predicted a lower scour depth than the HEC-18 method in the case of all five bridges. It is important to note that no actual scour measurements were included in this report so the accuracy of either scour prediction method cannot be assessed.

Debnath and Chaudhuri (2010) conducted laboratory experiments to estimate the maximum scour depth and diameter of the scour hole for circular piers in clay-sand sediments. Velocity was near the threshold velocity for the sand, and clay content and water content were varied in the flume experiment. Equations based on laboratory results were proposed based on the Froude number, clay content, water content and bed shear strength. It was observed that increasing the clay content reduced the scour depth and shifted the location of maximum depth from the front of the pier to the sides. In general good agreement was observed between measured and computed scour depth and diameter of the scour hole. The authors recommended adding a factor of safety of 25% to the pier width to account for maximum scour depth after a prolonged time. This model may provide a good estimate of the dimensions of a scour hole for clay-sand mixtures.

1.2.3 Regression Models

A number of studies have been conducted attempting to predict scour using regression models rather than empirical equations. These models use existing scour data to optimize their model. All of these models create a best fit, where scour is both over and under estimated, requiring a factor of safety if these models are to be used for design. None of these models included any input parameters related to the soil characteristics except the median grain size. The mathematical models generally were more accurate than empirical equations, however the models are unlikely to be able to predict scour for conditions that vary from the data that was used to train them. This is supported by the lack of agreement between different proposed models in the selection of input variables, number of input variables, number of nodes in the hidden layer, and sensitivity analysis as to which variable has the most significant impact on scour depth. It is also of note that many of the researchers compared their model to the HEC-18 method, but not the SRICOS-EFA method.

Choi and Cheong (2006) investigated utilizing an artificial neural network (ANN) as an alternative to existing empirical equations. Input parameters include properties of the flow, sediments and pier geometry. The calibration using laboratory scour data was most accurate with 5 nodes in the hidden layer. The verification data set of laboratory

data produced a mean absolute percent error (MAPE) of 14.63%, which is lower than the 5 existing empirical equations that were compared with the ANN. The ANN was applied to 212 data points from field data, and the MAPE increased (66.30%) relative to the laboratory data sets, but was still more accurate than the empirical equations.

Bateni et al. (2007) utilized two different ANN models as well as artificial neuro-fuzzy inference system (ANFIS) to attempt to improve scour prediction over a broad range of conditions when compared to existing empirical equations. The researchers found the ANN model that utilized multi-layer perception using back propagation (MLP/BP) with 16 nodes in a single hidden layer out performed both the ANN model utilizing radial basis using orthogonal least-squares algorithm (RBF/OLS) and the ANFIS model. A sensitivity analysis demonstrated that pier diameter has the largest effect on scour depth.

Lee et al. (2007) studied artificial neural networks using Back-Propagation Neural Network (BPN) using 380 local scour observations from 13 US states to train and validate the model. Inputs relate to flow hydraulics, bridge geometry and soil properties. The model was optimized with 5 non-dimensional inputs and 6 nodes in the hidden layer. The proposed BPN model showed a lower root mean square error and higher correlation coefficient than 5 existing empirical equations for the same data set. The BPN model generally over predicted scour depth, with only a small number of cases under predicted.

Zounemat-Kermani et al. (2009) studied two ANN models, feed forward back propagation (FFBP) and radial basis function (RBF), and an ANFIS model to improve equilibrium scour depth prediction around pile groups. Sensitivity analysis determined the input with the largest impact on scour depth being the pile diameter. The FFBP model with a single hidden layer containing 17 nodes was found to be the most accurate model studied. The FFBP model was able to outperform 4 existing empirical equations, showing this model may be an improvement over existing equations.

Kaya (2010) used a three layer feed forward back propagation ANN to improve pier scour estimates. The number of variables included was varied between 2 and 14. The highest coefficient of determination (R^2) was found with only 4 inputs (pier skew, pier width, flow velocity and flow depth) suggesting some of the variables do not have as

significant of an impact as suggested by other studies. No comparison between the proposed ANN and existing empirical equations was made in this study.

Firat and Gungor (2009) studied generalized regression neural networks (GRNN) and feed forward neural network (FFNN) ANN to improve scour depth predictions around circular bridge piers. Both models used 8 input variables. The ANN was optimized to include 10 hidden neurons in a single hidden layer. A sensitivity analysis showed that for this model pier dimension and mean grain size had the largest effect on scour prediction while flow depth and flow velocity had the smallest effect. The GRNN model performed better than the FFNN, multiple linear regression analysis, and five empirical equations.

Najafzadeh and Barani (2011) studied group method of data handling (GMDH) as a new method to predict pier scour depth. Two different models were compared, namely genetic programming (GP) and back propagation (BP). Both models had seven site specific properties combined into five non-dimensional inputs. Both the GP and BP models outperformed five empirical equations, and the GP model was found to be the most accurate. A sensitivity analysis determined the ratio of pier diameter to flow depth had the most significant impact, whereas Froude's number had the least impact on the accuracy of scour predictions.

1.2.4 Effects of Multi-Dimensional Hydraulic Analysis on Scour Prediction

A one dimensional hydraulic model may not accurately represent the stream velocity in a complex stream system. Research has been conducted to determine if a higher dimension hydraulic model can be used as the input to scour prediction models and result in greater accuracy than a one dimensional hydraulic model or quasi-one dimensional models like HEC-RAS.

Huang et al. (2009) investigated the HEC-18 scour equation validity with respect to large bridge piers. To study the large scale model, three dimensional computational fluid dynamics (3D CFD) models of both full scale and small scale were studied. The small scale CFD model maintained Froude similarity to the large scale model, but ignored Reynolds number similarity, as is common practice in physical modeling. The

study found that ignoring Reynolds number similarity can result in a significant error in scour predictions around large bridge piers. Therefore 3D CFD may provide more accurate scour predictions around large bridge piers than small scale physical models, which existing empirical equations such as HEC-18 are based.

Larsen et al. (2011) performed a scour prediction case study on a section of the Big Sioux River Bridge at Flandreau, SD. The site has a complex stream and flood plain geometry. The researchers compared scour predictions from a 1-dimensional model (HEC-RAS) with a depth averaged 2-dimensional model (Finite-Element Surface-Water Modeling, FESWMS) to predict approach flow velocity and the SRICOS-EFA method for scour prediction. The 1-dimensional model was found to predict a lower approach velocity than the 2-dimensional model, due to the complex stream geometry. The actual velocity distribution across the stream was not recorded during the flood event to compare the accuracy of the velocity predictions. However it was found that even with the higher velocity from the 2-dimensional model, the SRICOS-EFA method was closer to observed scour predictions than the HEC-18 method, although both methods over predicted the scour depth. The observed scour for the period from March 28 to July 7, 1993 was 7-8 ft, measured after the storm and may not account for aggradation after the flood receded. The SRICOS-EFA method predicted 14.5 ft with hydrograph duration of 102 days while the HEC-18 method predicted 17.1 ft.

Yu et al. (2011) compared the 1-dimensional HEC-RAS software to the 2-dimensional finite element model Flo2dh (part of FESWMS). Both models showed a spatial distribution of the velocity, but multidimensional models have the advantage of realistically simulating the flow field distribution. The HEC-RAS analysis used the maximum velocity for scour prediction rather than calculating the scour at each pier based on the local flow conditions. The design scour depth determined using the higher dimension model and the Froehlich equation was 28.82 ft, compared to 32.52 ft for HEC-RAS and the Colorado State University equation. Utilizing Flo2dh and the Colorado State University equation, the predicted scour depth is significantly reduced at the center pier (19.4 ft), compared to the scour depth predicted at the outside piers (31.21 ft). No observed scour data was available for comparison in this study.

1.2.5 Time Dependent Scour

Scour is a dynamic process, and maximum scour depth does not occur instantaneously. Temporal development of scour may provide a more accurate prediction of scour depth than empirical equations that assume equilibrium was reached. SRICOS-EFA is one method that accounts for this temporal development, and will be discussed in section 2.2. Some studies have proposed methods for time dependent scour depth that were more accurate than empirical equations for the dataset analyzed. Other studies have analyzed real time monitoring of existing bridges to show that empirical equations often overestimate scour depth and do not account for all variables that effect scour processes.

Conaway (2007) conducted a four year field study of 17 bridges in Alaska. Each bridge was equipped with sonar scour monitoring device on the pier and a transducer to measure river stage, allowing for real-time stream and scour monitoring. Floods exceeding the 100 year recurrence interval occurred at 5 of the sites during monitoring. Four of these five sites experienced scour less than those predicted during the measured large flood event. The effects of bed armoring and change in flow distribution are believed to be responsible for these over predictions. Seasonal aggradation and degradation, channel migration and long term channel change were also shown to have significant effects on observed scour and are not accounted for in traditional empirical scour prediction equations.

Lu et al. (2008) proposed a temporally variable model to predict scour that accounts for general scour, contraction scour and local scour based on observed field data. Observed data was obtained using three different scour monitoring techniques for two typhoon events in a fluvial river, the lower Cho-Shui River located in Taiwan. The proposed model was calibrated using one typhoon, and validated using the second. The temporal variations in scour depth were calculated for the validation model, and a close comparison between the simulated scour depth and measured scour depth was observed. The researchers also used ten commonly used formulas for equilibrium scour depth, and the accuracy of the proposed model compared well with the accuracy of existing formulas.

Govindasamy et al. (2008) proposed a new method using observed scour at existing bridges for evaluating the scour risk of existing bridges utilizing the hydrograph and scour experienced during the life of the bridge, as well as time dependent scour equations. Using this tiered method, the scour risk of a bridge can be analyzed using the actual scour measurements from the site (BSA 1). Then if the bridge is determined to be at risk, maximum scour (BSA 2) and time dependent scour (BSA 3) can be calculated without the need for site specific soil testing. Time dependent scour is calculated using the SRICOS-EFA method. To avoid site specific soil testing, a chart was presented that allows initial erosion rate to be estimated as a function of stream velocity or shear stress and soil type. Flood duration equal to the life of the bridge would show if the bridge was scour critical. Case studies to validate the proposed method are described in Govindasamy et al (2010).

Govindasamy et al. (2010) conducted a follow-up study on Govindasamy (2008) providing 11 case studies to validate BSA 1. Historic stream flow and scour measurements were used to predict current scour depths. Good agreement existed between the predicted scour and the measured scour, suggesting BSA 1 is a valid method for evaluating existing bridges. The researchers then evaluated ten bridges determined to be scour critical by the HEC-18 method, and of these ten bridges, six were found to be stable by the BSA 1 method.

Hager and Unger (2010) present a dynamic equation based on Froude's number for predicting time dependent scour. The time variable is introduced as a dimensionless quantity, where the time of interest is divided by time to peak of the flood. Similar to the existing HEC-18 method, the median grain size is the only soil parameter considered in the governing equation. For experiments conducted on non-cohesive soils, the experimental data are within +/- 25% of the proposed prediction equation. The proposed equation is applied to scour data recorded in Central Switzerland, and produced an overestimate of measured end scour of 14%.

Tregnaghi et al. (2011) studied time dependent scouring at bed sills. The study found that with the appropriate normalization, temporal scour evolution can be collapsed onto a dimensionless curve, assuming the time dependent scour can be modeled as a

series of steady state conditions, and the scour profiles at the bed sills are geometrically similar. The data presented from physical experiments agreed well with the simulation results. The researchers suggest the model should be able to be applied to varying scour events, as long as the proper normalization is utilized.

1.2.6 Hydrologic Modeling for Scour Prediction

Time dependent scour prediction methods require the duration of a flood in addition to the peak flow. Only a limited number of studies have been conducted on the duration of a design flood event. The studies that have been completed vary in their recommendations due to the characteristics of the watersheds that were included in the study. While a consensus on the duration of a flood event does not exist, the methods used to determine an appropriate duration may be applicable to a broad range of watersheds.

Levy and McCuen (1999) studied six Maryland watersheds to determine if a specified duration (e.g. 24 hours) or a watershed specific duration (e.g., time of concentration) is a better representation of the rainfall duration that causes the peak discharge. The duration of rainfall that induced the annual maximum discharge for each of the six watersheds over 19 years were analyzed. The study investigated 24 hour duration because this is commonly used by practicing engineers, as in the Soil Conservation Survey (SCS) design storms. The study concludes that for watersheds ranging in area from 2-50 sq mi the 24 hour duration provides a reasonably accurate estimate of rainfall characteristics compared to the observed storms in the six watersheds included in this study. The study found the use of an area dependent duration such as time of concentration is likely to underestimate peak discharge. This underestimation is because the rational formula assumes the intensity is determined using the time of concentration and the local intensity-duration-frequency curve. Large watersheds have a longer time of concentration, which yields an unrealistically low intensity for the 100 year rain event. These findings may not be applicable to watersheds in different regions with different rainfall characteristics.

Cleveland et al. (2008) proposed a method to generate a synthetic unit hydrograph from topographic data (30-m digital elevation model (DEM)) and classification as either developed or undeveloped land use. Travel time from each cell in the DEM to the outlet is used to generate an arrival time distribution, which is converted to a dimensionless unit hydrograph. The proposed method was relatively comparable to conventional methods of generating a unit hydrograph at predicting observed peak flow and time to peak. This may allow unit hydrographs to be generated for watersheds without stream flow records.

Lau and Gali (2010) conducted a case study on an Illinois watershed on critical storm duration as related to flood control. The critical duration, as defined by the authors, is the duration which produces the highest peak flow and stage. FEMA defines the design storm as the storm that causes the highest flood discharge under a particular flood frequency. Critical duration was found to increase moving from upstream to downstream in a watershed, with duration for sub-watersheds varying between 6 and 48 hours. Streams without detention were found to have a more significant difference between short and long duration events than streams with detention storage. The study found that critical duration varies based on watershed characteristics but that generally larger watersheds require a longer critical duration.

Kimoto et al. (2011) compared locally developed and SCS design storms with observed storms in Southern Arizona. Design storms of 3 hour and 24 hour duration are recommended by the City of Tucson for watersheds less than and greater than 78 sq km, respectively. The study found that none of the design storms accurately represented observed large events based on temporal distribution, pattern index and intensity-duration relationship. The study also suggests that while it is a common practice, using the 100 year rainfall event of any duration to predict that 100 year discharge is not always accurate. Large flood events occur as a result of many complex processes that are not necessarily captured by simply assuming a large rain event.

1.3 Objectives of the Present Study

The specific objectives of the present study are to:

1. perform hydrological analysis and evaluate methods for predicting peak flows and storm duration of design flood events such as 100-year flood for scour prediction through computer simulation and modeling;
2. conduct lab experiments of soil properties and field survey of stream geometry for predicting stream hydraulics and bridge scour;
3. evaluate, compare and validate two different methods (the HEC-18 method and the SRICOS-EFA method) for scour prediction by comparing the predicted results with available field data;
4. examine the effects of storm duration and soil property on scour prediction;
5. examine the sensitivity of scour prediction to hydrograph shape, accuracy in velocity and erosion rate measurements;
6. make recommendations on improved methodology and procedure for scour prediction in engineering design.

Chapter 2 SCOUR PREDICTION METHODS

2.1 HEC-18 Method

The HEC-18 method is the current design standard recommended by the FHWA. The method was developed utilizing data from laboratory flume experiments with sand as the stream bed. Many researchers believe that this method over predicts scour for certain field situations (Masaki, 2004, Polasik, 2005). Some believe this to be a factor of safety for the design. However some over predictions are so large as to greatly increase the cost and difficulty of construction. The details of the HEC-18 method are discussed in Arneson et al. (2012).

2.1.1 Total Scour Prediction

The HEC-18 method predicts total scour by combining the effects of long-term degradation, contraction scour and local scour (i.e. pier scour and abutment scour). By considering each of these components to be independent and summing their values to generate a total scour estimate, the design scour depth is more conservative. Some researchers believe this summation may result in an unrealistic overestimate of scour depth (Briaud et al., 1999, 2004, 2011) For the purpose of this thesis, only contraction scour and pier scour will be considered, as shown in equation 2.1. Long-term degradation is not included because this degradation is generally induced by changing land use within the watershed or changes in the stream, such as the addition of dams, and is not caused by a single large flood event.

$$y_{s,total} = y_{s,contraction} + y_{s,pier} \tag{2.1}$$

where:

$y_{s,total}$ = total depth of scour

$y_{s,contraction}$ = depth of scour caused by channel contraction

$y_{s,pier}$ = depth of scour caused by turbulent flow around pier

2.1.2 Contraction Scour

Contraction scour occurs when the width of a stream is reduced thus causing an increase in stream velocity through the bridge section. This increase in velocity causes the streambed to erode. The response of a stream to a contraction depends on the streams condition as either live-bed or clear-water. Live-bed contraction scour occurs when the stream is transporting bed material from upstream of the contracted section. Clear-water contraction scour occurs when either no bed material is being transported from upstream or the bed material being transported from upstream is in suspension and at less than the capacity of the flow.

2.1.2.1 Live-Bed Contraction Scour

Live-bed contraction scour continues until the flow of sediments from the contracted section is equal to the sediment transported into the contracted section. The depth of scour can be determined by subtracting the average depth in the contracted channel at equilibrium from the initial depth in the contracted section, shown in equation 2-2. The equilibrium depth of the channel is a function of flow, bottom width, water depth, shear stress and water density. This equilibrium scour depth can be calculated using equation 2-3.

$$y_s = y_2 - y_o \qquad \textbf{2-2}$$

$$\frac{y_2}{y_1} = \left(\frac{Q_2}{Q_1}\right)^{6/7} \left(\frac{w_1}{w_2}\right)^{k_1} \qquad \textbf{2-3}$$

where:

Table 2-1 Parameter k_1 selection for HEC-18 live-bed contraction scour equation

V*/ω	k_1	Mode of Bed Material Transport
<0.50	0.59	Mostly contact bed material discharge
0.50 to 2.0	0.64	Some suspended bed material discharge
>2.0	0.69	Mostly suspended bed material discharge

$$V^* = \left(\frac{\tau_o}{\rho}\right)^{1/2} = (g y_1 S_1)^{1/2} \qquad \textbf{2-4}$$

y_s = average contraction scour depth, ft (m)

y_2 = average depth in the contracted section at equilibrium, ft (m)

y_1 = average depth in the upstream main channel, ft (m)

y_o = average depth in contracted section before scour, ft (m)

Q_1 = flow in the upstream channel transporting sediment, ft^3/s (m^3/s)

Q_2 = flow in contracted section, ft^3/s (m^3/s)

W_1 = bottom width of upstream main channel that is transporting sediment, ft (m)

W_2 = bottom width of main channel in contracted section less sum of pier widths, ft (m)

k_1 = exponent determined by V* and ω

V* = shear velocity in the upstream section, ft/s (m/s)

ω = fall velocity of bed material on the D_{50}, m/s (for ft/s multiply ω by 3.28)

g = acceleration due to gravity, ft/s^2 (m/s^2)

S_1 = slope of energy grade line of main channel

τ_o = shear stress on the bed, lb/ft^2 (Pa)

ρ = density of water, $slugs/ft^3$ (kg/m^3)

2.1.2.2 Clear-Water Contraction Scour

Clear-water contraction scour is the degradation of the stream bed caused by a reduction in channel width when sediment transport does not occur. Contraction scour

generally continues until the stream velocity in the contracted section is equal to the critical velocity of the bed material. The critical velocity is the stream velocity at which bed material equal to a diameter D and smaller will be transported. Bed material is never perfectly homogeneous, therefore the median grain size, D_{50}, is used to determine if erosion of the bed will occur. The equation to predict critical velocity can be seen below as equation 2-5.

$$V_c = K_u y^{1/6} D^{1/3} \tag{2-5}$$

where:

V_c = critical velocity, ft/s (m/s)

K_u = 6.19 for SI units; 11.17 for English units

y = average depth of flow upstream of bridge, ft (m)

D = particle size, ft (m)

Equation 2-5 can be rearranged to calculate the equilibrium depth of scour, y_2, shown in equation 2-6. The depth of scour can then be calculated by subtracting the existing depth of the section from the equilibrium depth of scour, shown in equation 2-7.

$$y_2 = \left[\frac{K_u Q^2}{D_m^{2/3} w^2}\right]^{3/7} \tag{2-6}$$

$$y_s = y_2 - y_o \tag{2-7}$$

where:

y_s = average depth of contraction scour, ft (m)

y_2 = equilibrium depth in contracted section after scour, ft (m)

y_o = average existing depth in contracted section, ft (m)

K_u = 0.0077 for English units; 0.025 for SI units

Q = flow through the bridge contracted section, ft^3/s (m^3/s)

D_m = diameter of smallest non-transportable particle ($1.25*D_{50}$), ft (m)

W = bottom width of contracted section less pier widths, ft (m)

2.1.3 Pier Scour

Pier scour is the erosion around a pier structure induced by turbulent flows. Water will flow downward along the upstream edge of the pier, and a horseshoe vortex will develop along the sides of the pier. This downward flow and horseshoe vortex control the erosion process.

Many different factors affect the development of pier scour, including hydraulic properties, soil properties and the pier geometry. The HEC-18 equation for pier scour predicts maximum equilibrium scour depth for both live-bed and clear-water conditions. The HEC-18 equation to predict pier scour is shown below as equation 2-8. The HEC-18 equation can be modified for cases that include wide pier applications, complex substructure configurations, multiple columns skewed to the flow, scour caused by debris and scour in tidal waterways.

$$\frac{y_s}{y_1} = 2.0 K_1 K_2 K_3 \left(\frac{a}{y_1}\right)^{0.65} Fr_1^{0.43} \qquad \textbf{2-8}$$

where:

ys = scour depth, ft (m)

y_1 = depth of flow upstream of the pier, ft (m)

K_1 = correction factor for the pier nose shape, from Table 2-2

K_2 = correction factor for the angle of attack, from equation 2-9

K_3 = correction factor for the bed condition, from Table 2-3

a = pier width, ft (m)

L = pier length, ft (m)

Fr_1 = Froude number directly upstream of the pier = $V_1/(gy_1)^{1/2}$

V_1 = mean velocity of flow upstream of the pier, ft/s (m/s)

g = gravitational acceleration, ft/s^2 (m/s^2)

θ = angle of attack of the flow

Table 2-2 Correction factor K_1 for HEC-18 pier scour equation

Shape of Pier Nose	K_1
Square nose	1.1
Round nose	1.0
Circular cylinder	1.0
Group of cylinders	1.0
Sharp Nose	0.9

$$K_2 = \left(cos\theta + \frac{L}{a} sin\theta\right)^{0.65} \quad \text{2-9}$$

Table 2-3 Correction factor K_3 for HEC-18 pier scour equation

Bed Condition	Dune Height (ft)	K_3
Clear-water scour	N/A	1.1
Plane Bed and Antidune flow	N/A	1.1
Small Dunes	$10 > H \geq 2$	1.1
Medium Dunes	$30 > H \geq 10$	1.2 to 1.1
Large Dunes	$H \geq 30$	1.3

2.2 SRICOS-EFA Method

The Scour Rate in COhesive Soils – Erosion Function Apparatus (SRICOS-EFA) method was developed by researchers at Texas A&M (Briaud et al., 1999, 2001, 2004, 2011). This method estimates contraction and pier scour assuming that if contraction scour occurs, pier scour begins at the completion of contraction scour. Therefore the velocity used in pier scour calculations is not the actual velocity, but the critical velocity of the soil.

2.2.1 SRICOS-EFA Governing Equation

Similar to the HEC-18 method, the SRICOS-EFA method accounts for hydraulics at the site, soil properties, and bridge geometry. The SRICOS-EFA method also accounts for the development of scour over time. The equation for time dependent scour depth can be seen below in equation 2-10 (Briaud J.-L. , Chen, Li, Nurtjahyo, & Wang, 2004).

$$Z(t) = \frac{t}{\frac{1}{\dot{Z}_i} + \frac{t}{Z_{max}}} \qquad \textbf{2-10}$$

where:
Z(t) = time dependent scour depth, mm

$\dot{Z}_i$ = initial erosion rate, mm/hr

Z_{max} = maximum scour depth, mm

t = duration of flood event, hr

Equation 2-10 assumes that a single flood event with a constant velocity induces the erosion of bed material. For multiple flood events, including breaking a single hydrograph into components to allow for variable velocity, the concept of equivalent time must be utilized. Each of the sequential floods, called flood 1 and flood 2, can generate scour. However the scour depth generated by flood 1 could also have been generated by flood 2, and the time that it would have taken for flood 2 to scour the same depth as flood 1 is called the equivalent time. The equivalent time is then added to the duration of flood 2, and the scour depth for flood 2 is calculated using this new time value to determine the total scour at the end of flood 2 caused by both floods. The equation to determine equivalent time is shown below in equation 2-11. This process can be repeated as many times as required to fit the desired flood event.

$$t_e = \frac{t_1}{\frac{\dot{Z}_{i2}}{\dot{Z}_{i1}} + t_1 \dot{Z}_{i2}\left(\frac{1}{Z_{max1}} - \frac{1}{Z_{max2}}\right)} \qquad \textbf{2-11}$$

where:

t_e = equivalent time, hr

t_1 = duration of flood 1, hr

t_2 = duration of flood 2, hr

$\dot{Z}_{i1}$ = initial erosion rate of flood 1, mm/hr

$\dot{Z}_{i2}$ = initial erosion rate of flood 2, mm/hr

Z_{max1} = maximum scour depth of flood 1, mm

Z_{max2} = maximum scour depth of flood 2, mm

2.2.2 Calculation of Maximum Scour Depth, Z_{max}

The maximum scour depth is a combination of contraction scour depth and pier scour depth. The SRICOS-EFA maximum contraction scour is defined by equation 2-12.

$$Z_{max}(cont) = K_\theta K_L * 1.90\left(\frac{1.38\left(v_1\frac{B_1}{B_2}\right)}{\sqrt{gH_1}} - \frac{\left(\frac{\tau_c}{\rho}\right)^{0.5}}{gnH_1^{1/3}}\right)H_1 \geq 0 \qquad \textbf{2-12}$$

where:

Z_{max}(cont) = maximum depth of contraction scour (m)

K_θ = factor for influence of transition angle (equal to 1.0)

K_L = factor for influence of length of contracted channel (equal to 1.0)

V_1 = velocity in the uncontracted channel (m/s)

B_1 = width of the uncontracted channel (m)

B_2 = width of the contracted channel (m)

g = gravitational acceleration

H_1 = water depth in the uncontracted channel

τ_c = critical shear stress obtained from EFA (kg/m^2)

ρ = density of water (kg/m^3)

n = Manning's coefficient (s/m$^{1/3}$)

If no contraction scour occurs, then pier scour can be calculated using the velocity and water depth in the contracted section assuming the piers are not present. If contraction scour does occur, then the velocity for the pier scour calculation is the critical velocity for the soil and the water depth is the contraction scour added to the water depth, shown below in equation 2-13 and equation 2-14, respectively.

$$V = \begin{cases} v_c = \sqrt{\dfrac{\tau_c H_2^{\frac{1}{3}}}{\rho g n^2}}; & Z_{max}(cont) > 0 \\ V_{HEC}; & Z_{max}(cont) = 0 \end{cases} \quad \textbf{2-13}$$

$$H_2 = H_1 + Z_{max}(cont) \quad \textbf{2-14}$$

Using the appropriate values of velocity from equation 2-13, the maximum pier scour depth can be calculated using equation 2-15.

$$Z_{max}(pier) = 0.18 K_w K_{sp} K_{sh} R_e^{0.635} \quad \textbf{2-15}$$

$$K_w = \begin{cases} 0.85\left(\dfrac{H}{B}\right)^{0.34} & H/B \geq 1.6 \\ 1 & H/B < 1.6 \end{cases} \quad \textbf{2-16}$$

$$K_{sp} = \frac{B_1}{(B_1 - nB)} \quad \textbf{2-17}$$

$$R_e = \frac{V(L\sin \propto + B\cos \propto)}{\nu} \quad \textbf{2-18}$$

where:

Z_{max}(pier) = maximum pier scour depth (mm)

K_w = correction factor for pier scour water depth

K_{sp} = correction factor for pier spacing

K_{sh} = correction factor for shape (1.1 for rectangular with L/B>1, otherwise 1.0)

R_e = Reynold's number

H = water depth, as appropriate from equation 2-14 (m)

B = pier diameter (m)

B_1 = width of the uncontracted channel (m)

n = number of piers

L = length of pier (m)

α = angle of attack of the flow with respect to the pier

ν = kinematic viscosity of water (m^2/s)

The maximum bridge scour can be calculated using equation 2-19 which combines the scour depth caused by contraction scour and pier scour.

$$Z_{max} = Z_{max}(cont) + Z_{max}(pier) \quad \textbf{2-19}$$

2.2.3 Calculation of Initial Erosion Rate, $\dot{Z}_i$

The initial erosion rate is a function of maximum bed shear stress. A generic EFA curve is shown in Figure 2-1 to demonstrate this relationship. Soil testing using an erosion function apparatus (EFA) is required to generate a site specific EFA curve. From this curve, the initial erosion rate can be determined from the maximum bed shear stress. The maximum bed shear stress can be calculated using equation 2-20.

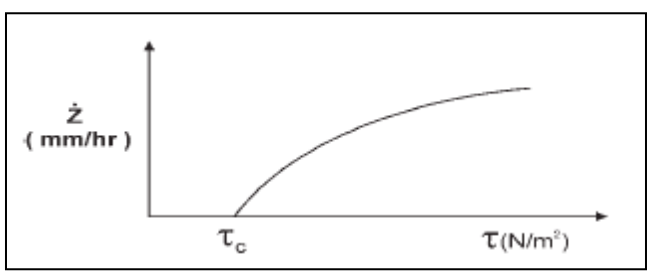

Figure 2-1 Generic EFA curve relating bed shear stress to initial erosion rate (Briaud J.-L. , Chen, Li, Nurtjahyo, & Wang, 2004)

$$\tau_{max} = k_w k_{sh} k_{sp} k_\alpha \rho V^2 \left[\frac{1}{logR_e} - \frac{1}{10}\right] \quad \textbf{2-20}$$

$$k_w = 1 + 16e^{-\frac{4H}{B}} \quad \textbf{2-21}$$

$$k_{sh} = 1.15 + 7e^{-\frac{4H}{B}}; or\ 1\ for\ circular\ shape \quad \textbf{2-22}$$

$$k_{sp} = 1 + 5e^{-1.1\frac{S}{B}} \quad \textbf{2-23}$$

$$k_\propto = 1 + 1.5\left(\frac{\propto}{90}\right)^{0.57} \quad \textbf{2-24}$$

$$V = \begin{cases} V_1; channel\ with\ no\ contraction \\ V_2; \quad channel\ with\ contraction \end{cases} \quad \textbf{2-25}$$

where:

H = water depth

B = pier diameter or projected width (if skewed to flow)

S = pier spacing, center-to-center

L = pier length

α = angle of attack of the flow

V_1 = velocity in the uncontracted channel (m/s)

V_2 = velocity in the contracted channel, without presence of pier (m/s)

V_2 can be obtained from HEC-RAS or a similar program, or from mass conservation using equation 2-26.

$$V_2 = 1.14V_1\left(\frac{B_1}{B_2}\right) \quad \textbf{2-26}$$

In the case of a multi-layer soil system, the initial erosion rate can vary with the layer that is being eroded. If the erosion Z(t) has exceeded the depth of the soil layer, this is equivalent to having had layer 2 scoured for an equivalent time, using equation 2-11.

By using equivalent time and multiple EFA curves, a system can be constructed for multiple soil layers.

Chapter 3 HYDROLOGICAL ANALYSIS AND FLOOD PREDICTION FOR SELECTED WATERSHEDS AND STREAMS

Hydrologic analysis is required prior to predicting scour depth. Both scour prediction methods require the input of flow conditions at the bridge location. Specifically, the value of peak flow is required by the HEC-18 method and the flow hydrograph is required by the SRICOS-EFA method. Both methods require the flow to be converted to velocity and water depth to predict the bridge scour depth.

Bridges are required to resist the scour design flood frequency, (for example the 100 year flood), and be stable during the scour design check flood frequency (for example the 500 year flood); therefore both events must be analyzed for the particular stream. This usually requires statistical analysis of historical rainfall and stream flow records in order to calculate a particular return frequency, such as the 100-year event. Historically only peak flow discharge was considered in scour prediction by the HEC-18 design manual. The relatively new SRICOS-EFA method, however, requires more detailed flow conditions including the flood duration in order to construct proper hydrograph for scour prediction. While the statistical methodologies have been well established for calculating peak flows of different flood frequencies, there have been very few studies that have performed statistical analysis on storm durations. Direct statistical calculation of the peak flow is not possible for streams that do not have a gage. These ungaged sites require empirical methods, such as the rational method, TR-55 method and HEC-HMS, to predict peak flow by converting rainfall to flow rate.

This chapter presents the methodologies and results for predicting peak flow rate for flood of different return periods for selected streams in Hawaii. Both gaged and ungaged bridge sites are studied and discussed. A preliminary investigation of historical records on storm duration is also presented. It should be noted that climate change is not considered in any of the analysis of rainfall or stream flow records.

3.1 Statistical Study of Historical Data on Storm Duration in Hawaii

In most of the existing hydraulic engineering design such as bridge design, culvert design, and storm water drainage design engineers consider the peak flow as the dominant design parameter. The storm duration, and how the flow discharge changes with time, often are not considered in sizing the inlets, pipes, culverts, or bridge openings and foundation depth. In reality, both the peak flow and how long the flood lasts should have impact on the performance of the civil infrastructure such as bridges. The newly developed SRICOS-EFA method by the Texas A&M University for bridge scour prediction requires the input of a flood hydrograph that shows the flood duration and how the flood varies with time. Scour is caused by erosion of the stream bed under flood flow and soils with varied properties erode at different rates.

Since most of the existing hydraulic design does not consider the flood duration but only the peak flow, there has been very little research done on statistical analysis of rainfall and flood durations. There are no established statistical methods to determine reasonable flood duration for 100-year flood. Many researchers and engineers simply assume that the peak flow maintains for 24 hours to achieve a conservative prediction for bridge scour (Ghelardi, 2004). While a conservative prediction is good for bridge safety, a large overestimate can also increase the difficulty and cost in bridge design and construction.

This study investigates storm and flood duration by examining historical rainfall and stream flow records in Hawaii. The objective is to attempt to answer some of the unresolved questions related to this topic: what is the typical duration of rainfall in a watershed or elevated discharge in a stream in Hawaii? What is the longest possible duration of rainfall and elevated flow rate? What duration or rainfall and flood discharge is appropriate for evaluating the design scour event?

3.1.1. Historical Records Examined

Historic hourly rain gage data was obtained from the National Oceanic and Atmospheric Administration (NOAA) for the island of Oahu (National Oceanic and Atmospheric Administration, 2012). Rainfall events with large hourly rainfall, or extreme rainfall events, are of interest in this study. Only rain gages with a sufficiently long period of record were considered, in this case a minimum of 18 years of hourly data. NOAA provided data for 23 rain gages on the island of Oahu that met the minimum length of record. Table 3-1 shows the name and duration of the rain gages analyzed in this study. The location of the selected rain gages can be seen in Figure 3-1.

Table 3-1 Duration of rainfall at selected Oahu rain gages

Rain Gage ID	Name of Rain Gage	Years of Record
COOP:510055	AHUIMANU LOOP 839.12 HI US	43
COOP:510404	DOWSETT 775.4 HI US	28
COOP:510438	DOWSETT HIGHLANDS 78 HI US	20
COOP:510964	HALAWA SHAFT 771.2 HI US	46
COOP:511540	HOKULOA 725.2 HI US	46
COOP:511919	HONOLULU INTERNATIONAL AIRPORT HI US	49
COOP:512570	KAHUKU 912 HI US	46
COOP:512683	KAILUA FIRE STATION 791.3 HI US	46
COOP:515655	LULUKU 781.7 HI US	44
COOP:515758	MAKAHA COUNTRY CLUB HI US	24
COOP:515782	MAKAHA PUMP 800.2 HI US	18
COOP:516222	MAUNAWILI 787.1 HI US	46
COOP:516553	MOUNT KAALA 844 HI US	46
COOP:517150	OPAEULA 870 HI US	46
COOP:517942	PEARL COUNTRY CLUB HI US	34
COOP:518314	PUNALUU PUMP 905.2 HI US	39
COOP:518342	PUPUKEA HEIGHTS 896. HI US	43
COOP:518946	WAHIAWA DAM 863 HI US	46
COOP:518965	WAIAHOLE 837 HI US	46
COOP:519195	WAIALUA 847 HI US	46
COOP:519500	WAILUPE VALLEY SCHOOL 723.6 HI US	45
COOP:519534	WAIMANALO NONOKIO 795.2 HI US	39
COOP:519593	WAIMEA 892 HI US	46

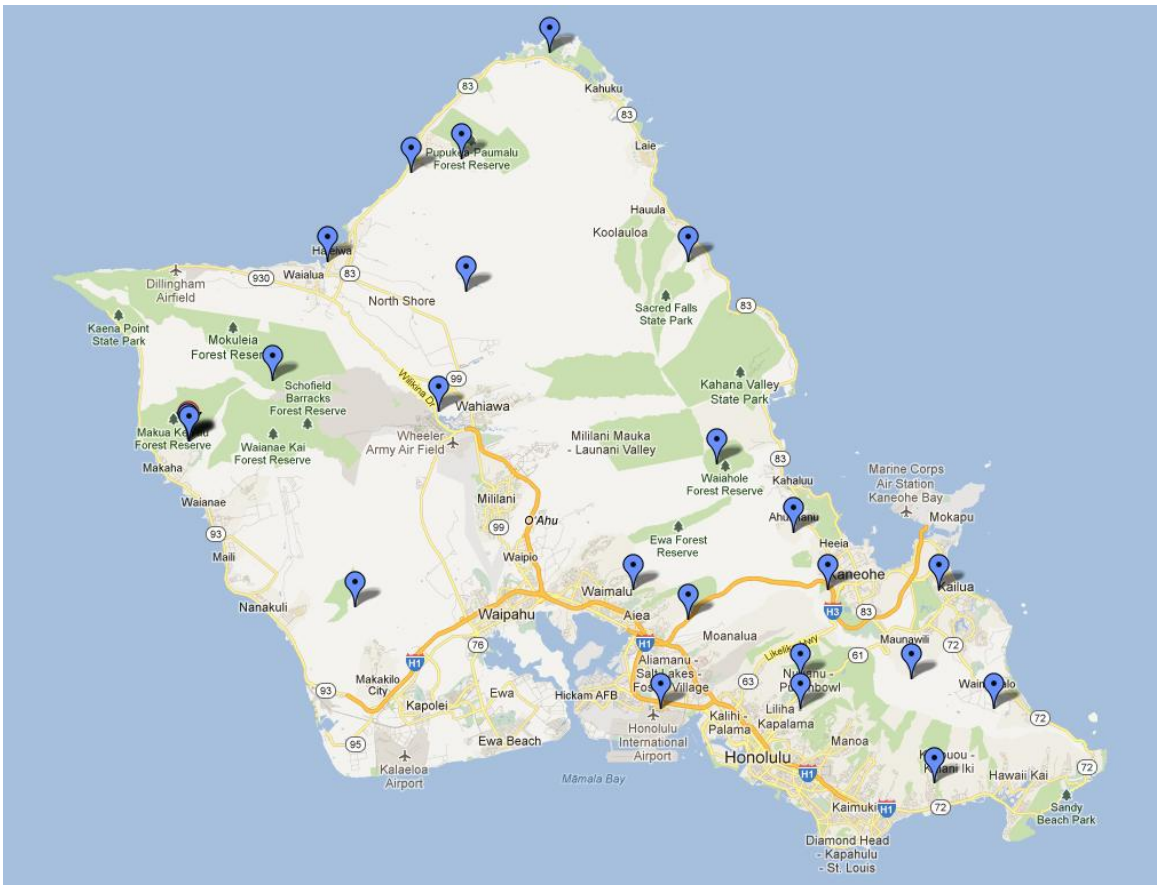

Figure 3-1 Location of selected rain gage stations

3.1.2. Statistical Results on Storm Duration

The determination of the typical rainfall duration for an extreme rainfall event is critical to hydrologic designs. The five extreme rainfall events with the highest peak hourly rainfall for each of the 23 selected rain gage stations were identified, resulting in a total of 115 rainfall events. The duration of the rainfall for each event was determined as beginning when the extreme event first increased significantly and sustained the increased level of rainfall. The event was assumed to conclude when the rainfall returned to a low base level of rainfall and the low level of rainfall was sustained. The hyetograph, which shows rainfall variations with time, recorded by the Mt. Kaala rain gage station on

January 8, 1980 is shown in Figure 3-2. The period of elevated rainfall is marked on the figure to show the criteria used to determine the beginning and ending of a rainfall event.

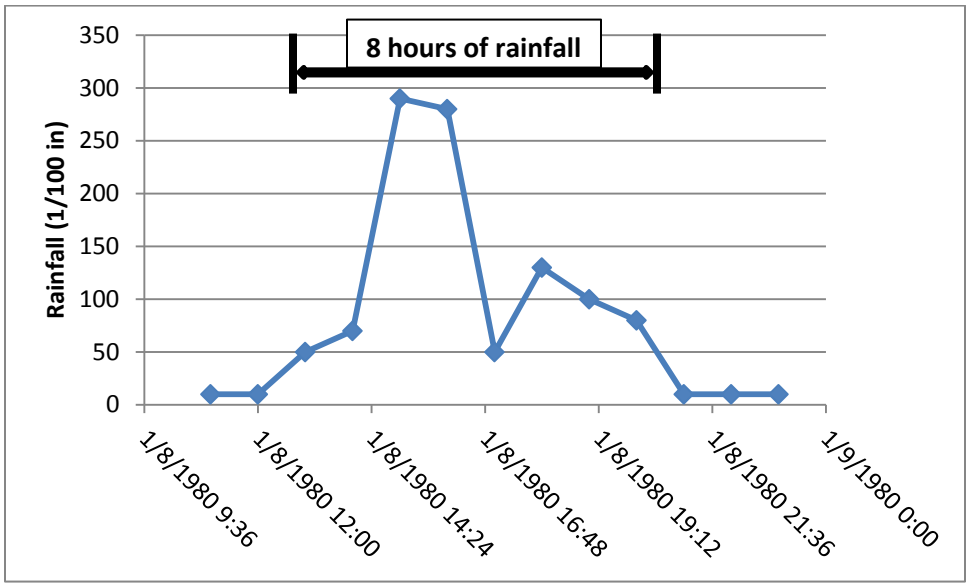

Figure 3-2 Hyetograph for rainfall event recorded by Mt. Kaala rain gage on January 8, 1980

The distribution of the duration and the rainfall intensity are shown in Table 3-2. There was no apparent pattern between rainfall intensity and duration, as seen by Figure 3-3. The island was split into five regions: Central, Leeward, North Shore, South Shore and Windward. As shown in Table 3-3, the duration in the Central region is slightly longer than any of the other regions. However based on the limited number of gages in each region, these results are not significant enough to draw engineering conclusions. It will therefore be assumed that duration does not vary significantly based on location on the island of Oahu.

Table 3-2 Distribution of extreme rainfall intensity and duration on Oahu

	Peak Hourly Rainfall (1/100 in)	Duration of hyetograph (hrs)
average	258.10	6.72
min	150	3
max	410	13
standard deviation	58.21	2.66

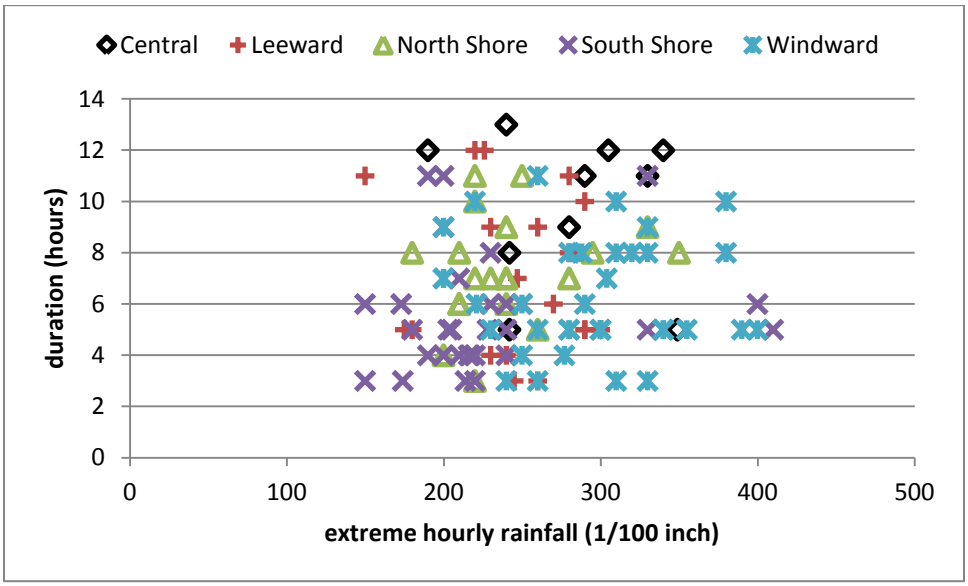

Figure 3-3 Plot of rainfall duration versus peak hourly rainfall by region of Oahu

Table 3-3 Distribution of extreme rainfall intensity and duration by region of Oahu

	Average Duration (hrs)	Standard Deviation of Duration (hrs)	Average Extreme Hourly Intensity (1/100 in)	Standard Deviation of Extreme Hourly Intensity (1/100 in)	Number of Gages
Central	9.80	2.94	280.80	51.82	2
Leeward	6.95	3.03	248.15	42.96	4
North Shore	7.35	2.08	242.25	42.81	4
South Shore	5.60	2.31	228.33	62.28	6
Windward	6.31	2.23	291.86	54.54	7

3.2 Peak Flow Prediction for Gaged Manoa-Palolo Stream

Predicting the peak flow of a gaged stream with a sufficiently long historical discharge record is usually straight forward. This can be completed using a direct statistical calculation of the flow record by applying well established probability distributions such as the Gumbel or Log Pearson III distribution for analyzing annual extreme values.

If a stream is not gaged, then direct prediction of the peak flow by statistical analysis is not possible. In these cases, indirect methods to predict the peak flow through analysis of the rainfall record are required. Results of rainfall intensity are then used to predict stream peak flows through methods such as the rational method, TR-55, HEC-HMS or regression methods.

One of the bridge sites included in this study is the Kapiolani off ramp from the westbound H-1 freeway that crosses the Manoa-Palolo Stream. A USGS gaging station is located downstream of the bridge providing the needed historical stream record to calculate the 100-year peak flow directly. The direct statistical calculation of the peak flow for this particular site using Log-Pearson and Gumbel methods are performed and presented in section 3.2.2. In addition, the indirect prediction of peak flow by USGS regression equations and WMS (Watershed Modeling System) software for this site are included. Direct and indirect methods are applied for this site to evaluate and validate the indirect methods so that the method most applicable to ungaged sites can be selected and the same procedure can be applied to several other ungaged streams included in this study.

3.2.1 The Manoa-Palolo Watershed and the Manoa-Palolo Bridge Site

The Manoa-Palolo stream is located on the south shore of Oahu, on the leeward side of the Ko'olau mountain range. The watershed contributing to the stream includes both the Manoa and Palolo valleys, and the ridges that drain down to the valleys. The ridges that encompass each valley on three sides have very steep slopes and are thickly vegetated. Residential housing is the dominant land use on both valley floors. A satellite image of the Manoa-Palolo watershed and surrounding area can be seen in Figure 3-4.

Figure 3-4 The Manoa-Palolo Watershed and surrounding area

The streams that contribute to the river section of interest vary from upstream to downstream. Towards the back of the valleys, the streams are narrow, steep and natural with large volcanic rocks in the bed. As the water flows downstream many of the streams have steep or vertical man-made embankments on one or both sides. Sections of the Palolo stream are lined with concrete on the bottom as well as both sides.

The section of the Manoa-Palolo stream that contains the bridge pier of interest has steep man-made embankments on both sides. The streambed has coarse sand, gravel and cobbles, as well as sections that include finer material. The finer bed material often grows vegetation which diverts the flow to the sections without vegetation during low flows. Periodically, maintenance crews enter the stream to remove this vegetation. These

conditions are consistent both upstream and downstream of the location of the bridge pier of interest.

The USGS operates a stream gage station approximately 0.25 miles downstream of the pier of interest (USGS, 2013). The stream conditions at this gaging station are similar to the stream conditions at the study section. The gaging station data includes annual peak stream flow data from 1967 through 2010. The station also has 15 minute stream flow data from 1999 through 2012, although large sections of the 15 minute data are missing.

3.2.2 Direct Statistical Calculation of the 100-Year Peak Flow

Statistical distributions can be utilized to analyze peak annual stream discharge data to determine discharges for large flood events like the 100 year flood. The Log-Pearson III and Gumbel distributions are used to analyze the 43 years of available peak discharge data. The procedures for these statistical analyses are discussed in Masaki (2004) and Miyagi (2010).

The 100 year flood predicted by the Gumbel distribution is 10388 cfs. The Gumbel Extreme Value Curve is shown in Figure 3-5. The Log-Pearson III distribution predicts a 100 year flood of 12568 cfs and is shown in Figure 3-6. The Log-Pearson III distribution fits the data slightly better, particularly at higher flow rates. Both statistical analyses provide a reasonable estimate of the 100 year discharge; however the 100 year flow rate predicted by the Log-Pearson III distribution will be used for 100 year flood scour predictions in the Manoa-Palolo stream using both HEC-18 and SRICOS-EFA methods.

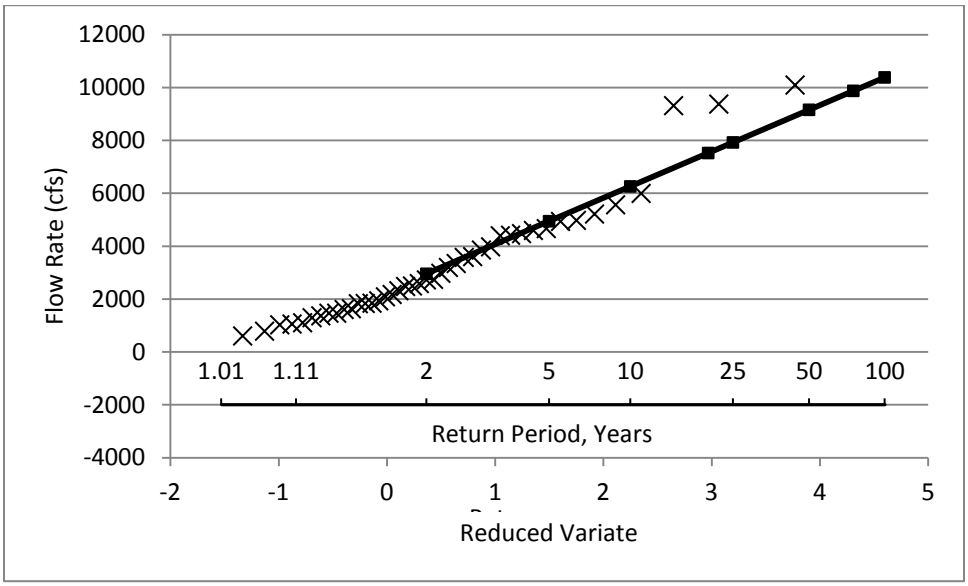

Figure 3-5 Gumbel extreme value curve for Manoa-Palolo Stream

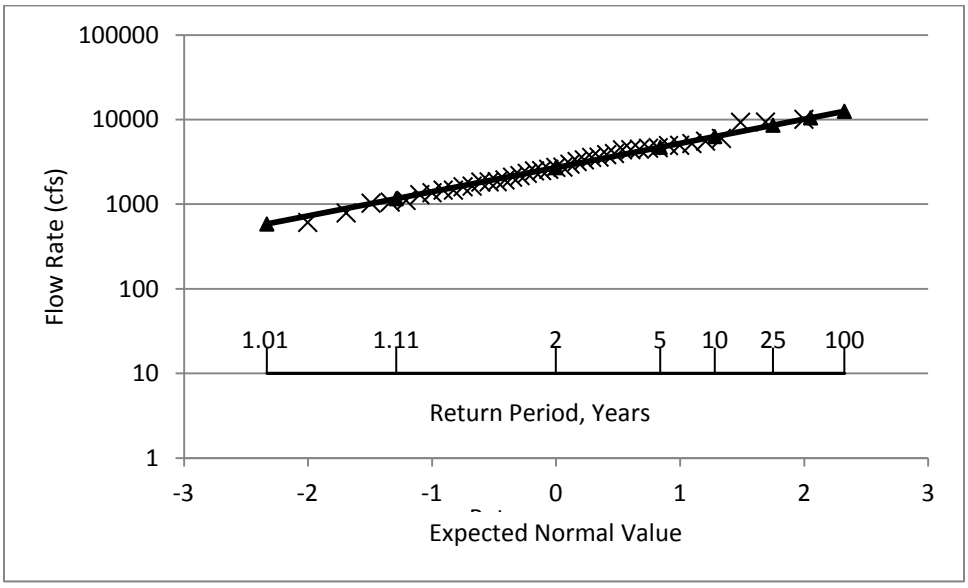

Figure 3-6 Log-Pearson III curve for Manoa-Palolo Stream

3.2.3 Indirect Prediction of the 100-Year Flow by USGS Regional Regression Equations

One method for the indirect prediction of peak flow of a certain flood frequency is by applying regional regression equations. The US Geologic Survey conducted a study for the state of Hawaii that estimates floods at different frequencies based on the cumulative stream flow records of streams in that hydrologic region. The island of Oahu was divided into windward and leeward hydrologic regions. Equation 3-1 estimates the 100 year flood for the windward side of Oahu, and equation 3-2 estimates the 100 year flood for the leeward side of Oahu (Oki, Rosa, & Yeung, 2010). It should be noted that the standard model error for the windward side and leeward side of Oahu are 44% and 38%, respectively.

$$Q_{100} = 3251 * DRNAREA^{0.726} \qquad for\ 0.04 \leq DRNAREA \leq 5.44 \tag{3-1}$$

$$Q_{100} = 539.5 * DRNAREA^{0.646} * PRECIP^{0.335} \qquad for\ 0.56 \leq DRNAREA \leq 252 \quad and\ 31.9 \leq PRECIP \leq 252 \tag{3-2}$$

where:
Q_{100} = peak discharge for 100 year recurrence interval, in cfs
DRNAREA = drainage area, in square miles
PRECIP = mean annual precipitation, in inches

The drainage area of a watershed in Hawaii can be delineated using a digital elevation model (DEM) and watershed modeling software, such as Watershed Modeling System (WMS).

The mean annual precipitation can be obtained from the 2011 Rainfall Atlas of Hawaii produced by the Department of Geography at the University of Hawaii at Manoa shown in Figure 3-7 (Giambelluca, et al., 2012). The drainage area of each watershed can be delineated on the rainfall atlas, and then an area averaged estimate of the mean annual rainfall across the entire watershed can be obtained.

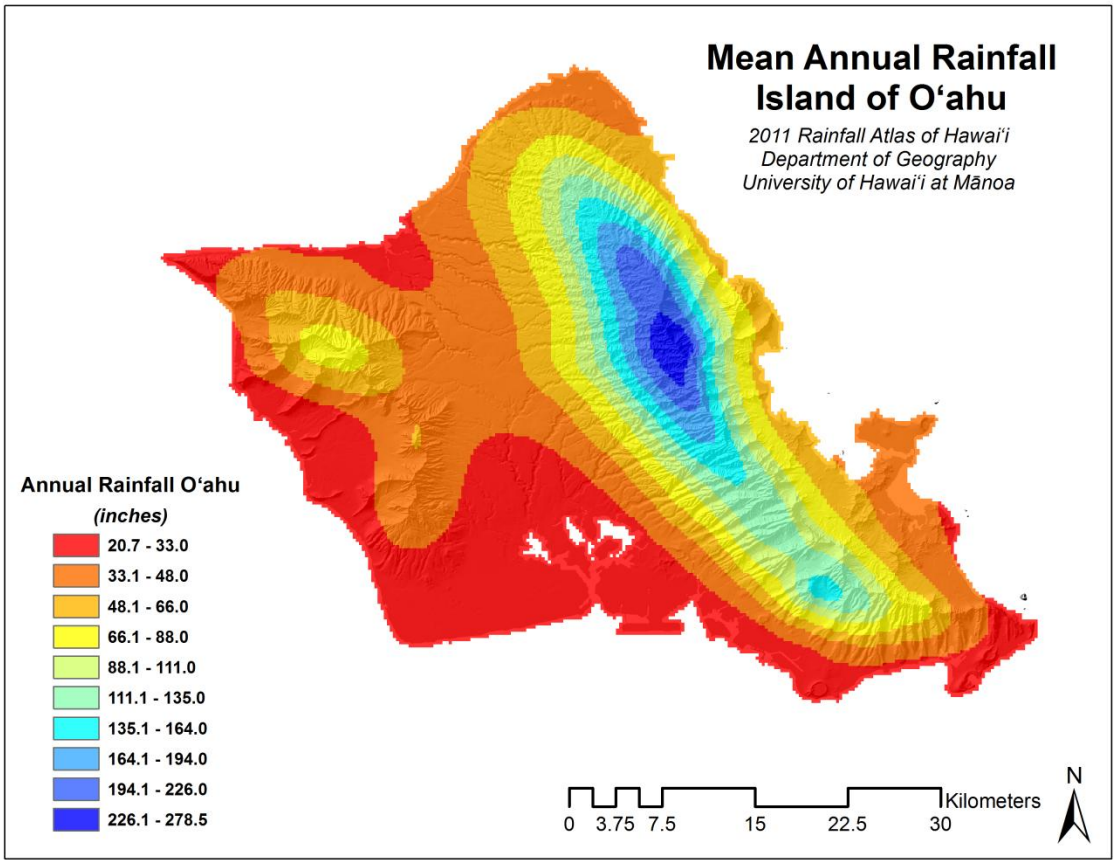

Figure 3-7 Mean annual rainfall for the island of Oahu (Giambelluca, et al., 2012)

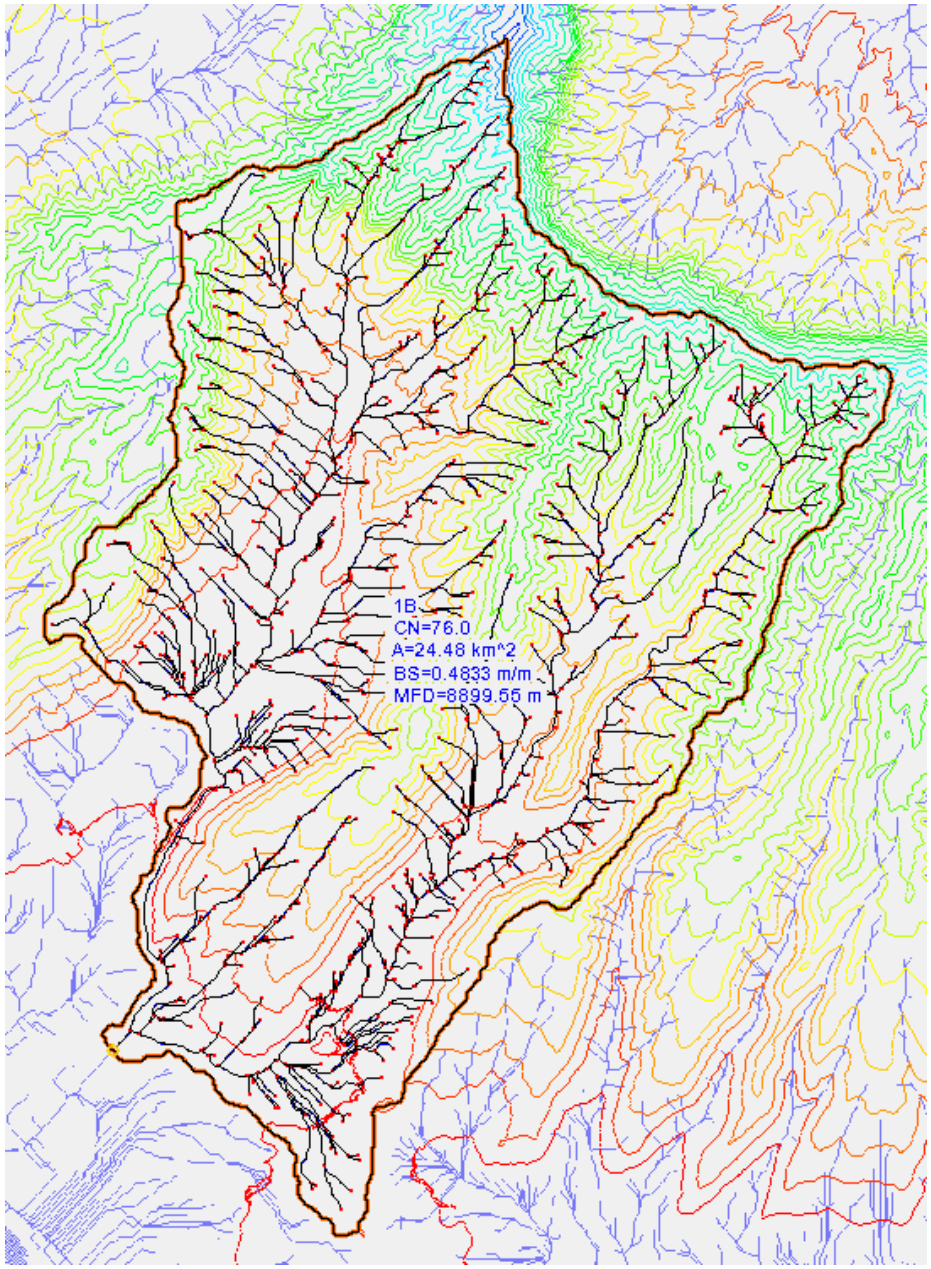

Figure 3-8 Drainage area and digital elevation model for the Manoa-Palolo Bridge. CN is the curve number, A is the drainage area, BS is the average slope and MFD is the longest travel path

The drainage area of the Manoa-Palolo Bridge is 24.48 square kilometers or 9.45 square miles and is shown in Figure 3-8. Estimating the area averaged annual rainfall for the drainage area, the mean annual rainfall was determined to be 91 inches. A summary of the values used to calculate the mean annual rainfall can be seen in Table 3-4. The watershed is on the Leeward side of Oahu, so equation 3-2 is applicable. The 100 year

flow rate at the Manoa-Palolo Bridge is predicted to be 10433 cfs using the USGS regression equations method.

Table 3-4 Mean annual rainfall drainage areas located on the leeward side of Oahu

		Fraction of Drainage Area in each Rainfall Range				
Range of Rainfall (in)	**Average of Rainfall Range (in)**	**Manoa-Palolo Stream**	**Kaoli Ditch**	**Halawa Stream**	**Moanlua Stream**	**West Loch Stream**
20.7-33	27		0.6	0.2	0.15	0.65
33.1-48	41	0.25	0.4	0.2	0.25	0.35
48.1-66	57	0.1		0.1	0.1	
66.1-88	77	0.15		0.1	0.1	
88.1-111	100	0.15		0.1	0.1	
111.1-135	123	0.15		0.3	0.3	
135.1-164	150	0.2				
164.1-194	179					
194.1-226	210					
226.1-278.5	252					
Mean Annual Rainfall (in)		91	32	74	74	32

3.2.4 Indirect Prediction of the 100 Year Flow by HEC-HMS

Hydraulic Engineering Circular – Hydrologic Modeling System (HEC-HMS) is a precipitation-runoff process modeling software (Feldman, 2000). HEC-HMS includes a basin model, meteorologic model and control model. The HEC-HMS software has numerous methods to define precipitation, convert rainfall to discharge, route a hydrograph between two points and estimate basin parameters like the lag time. This study evaluated the Manoa-Palolo watershed was evaluated using a single composite watershed, a sub-basin model with 11 sub-basins and a sub-basin model with 30 sub-basins. The composite model considers the rainfall and runoff from the entire basin as being part of a single drainage area. The sub-basin models consider the rainfall and runoff of each basin independent, and then the runoff at each outlet is routed to the outlet of the entire drainage area and combined with the runoff from the other sub-basins. The sub-basin models allow for variation of parameters like the curve number throughout the drainage area, however the sub-basin models require the addition of routing parameters

that are not required in the composited model. For the composite and sub-basin models the SCS runoff curve number was used as the loss rate method shown in equation 3-3. The SCS unit hydrograph method was used as the transform method and can be described by equation 3-4, equation 3-5 and the SCS unit hydrograph shown in Figure 3-9. The lag time was calculated using the basin geometry and the SCS Method shown in equation 3-6. The precipitation was defined using rain gages and the Thiessen polygon method to determine the weight of each gage. The mean areal precipitation for a given time interval using the Thiessen polygon approach to determine the weighting factor of each gage is shown in equation 3-9. The runoff from the sub-basin model was routed using the Muskingum-Cunge method, described by equation 3-10. Watershed Modeling System (WMS) 9.0 produced by Aquaveo was used to set up the HEC-HMS model and then the model was run using HEC-HMS 3.5.

$$P_e = \frac{(P - I_a)^2}{P - I_a + S} = \frac{\left(P - 0.2\left(\frac{1000}{CN} - 10\right)\right)^2}{P + 0.8\left(\frac{1000}{CN} - 10\right)} \qquad \textbf{3-3}$$

where:
P_e = cumulative excess precipitation or runoff at time t (in)
P = cumulative rainfall at time t (in)
I_a = initial abstraction (in)
I_a = 0.2S
S = potential maximum retention after runoff begins (in)
S = (1000/CN) – 10
CN = curve number, ranging from 0 to 100

The SCS unit hydrograph is defined by equation 3-4, 3-5 and Figure 3-9:

$$U_p = C\frac{A}{T_p} \qquad \textbf{3-4}$$

$$T_p = \frac{\Delta t}{2} + t_{lag} \qquad \textbf{3-5}$$

where:
U_p = unit hydrograph peak (cfs/in)

C = conversion constant: 484 in foot-pound
A = watershed area (mi^2)
T_p = time of unit hydrograph peak (hrs)
Δt = computational interval in HEC-HMS (hrs)
t_{lag} = lag time (hrs)

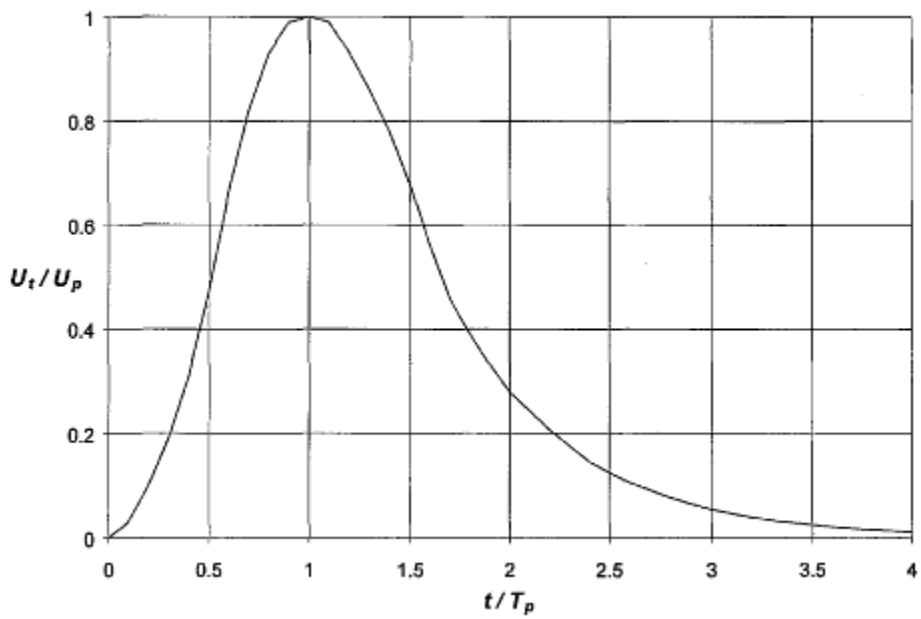

Figure 3-9 SCS unit hydrograph

$$t_{lag} = L^{0.8}\left[\frac{\left(\left(\frac{1000}{CN} - 10\right) + 1\right)^{0.7}}{1900\sqrt{S}}\right] \qquad \textbf{3-6}$$

where:
t_{lag} = lag time (hrs)
L = basin length (ft)
CN = curve number
S = average basin slope (%)

The rainfall distribution is weighted spatially and temporally as defined by equations 3-7, 3-8 and 3-9:

$$P_{MAP} = \frac{\sum_i w_i \sum_t p_i(t)}{\sum_i w_i} \qquad \textbf{3-7}$$

$$p_{pattern}(t) = \frac{\sum w_i(t) p_i(t)}{\sum w_i(t)} \quad \textbf{3-8}$$

$$P_{MAP}(t) = \frac{p_{pattern}(t)}{\sum p_{pattern}(t)} P_{MAP} \quad \textbf{3-9}$$

where:
P_{MAP} = total storm mean areal precipitation depth over basin
$P_{MAP}(t)$ = mean areal precipitation depth over basin at time t
$P_{pattern}(t)$ = precipitation pattern over time and basin area
w_i = weighting factor assigned to a rain gage
$p_i(t)$ = precipitation depth at time t at gage i

The Muskingum-Cunge Method, utilized to route the flow from the sub-basins to the drainage area outlet, is defined by equations 3-10 through 3-14:

$$O_t = C_1 I_{t-1} + C_2 I_t + C_3 O_{t-1} + C_4 q_L \Delta x \quad \textbf{3-10}$$

$$C_1 = \frac{\frac{\Delta t}{K} + 2X}{\frac{\Delta t}{K} + 2(1 - X)} \quad \textbf{3-11}$$

$$C_2 = \frac{\frac{\Delta t}{K} - 2X}{\frac{\Delta t}{K} + 2(1 - X)} \quad \textbf{3-12}$$

$$C_3 = \frac{2(1 - X) - \frac{\Delta t}{K}}{\frac{\Delta t}{K} + 2(1 - X)} \quad \textbf{3-13}$$

$$C_4 = \frac{2\left(\frac{\Delta t}{K}\right)}{\frac{\Delta t}{K} + 2(1 - X)} \quad \textbf{3-14}$$

where:
O = outflow
I = inflow
q_L = lateral inflow
Δx = length of channel
Δt = time interval
K = travel time = $\Delta x/c$
c = wave speed
$X = 0.5*(1-Q/(BS_o c\Delta x))$
B = channel top width
S_o = channel slope
Q = flow

The sub-basin boundaries were determined by overlaying soil type and land use shapefiles over the drainage area. Each sub-basin outlet in both sub-basin models was located to maintain relatively uniform soil type and land use and sub-basins that were relatively similar in size. The curve number for each individual combination of land use and soil type was determined and the composite curve number for each sub-basin was then calculated as an area averaged CN. The curve number for the composite watershed model was calculated as an area weighted average from the CN determined for each sub-basin. The composite model boundaries are shown in Figure 3-8 and the basin data used with HEC-HMS is shown in Table 3-5. The 11 sub-basin model and 30 sub-basin model boundaries are shown in Figure 3-10 and Figure 3-11, respectively. The basin data used in the HEC-HMS model is shown in Table 3-6 for the 11 sub-basin model and Table 3-7 for the 30 sub-basin model.

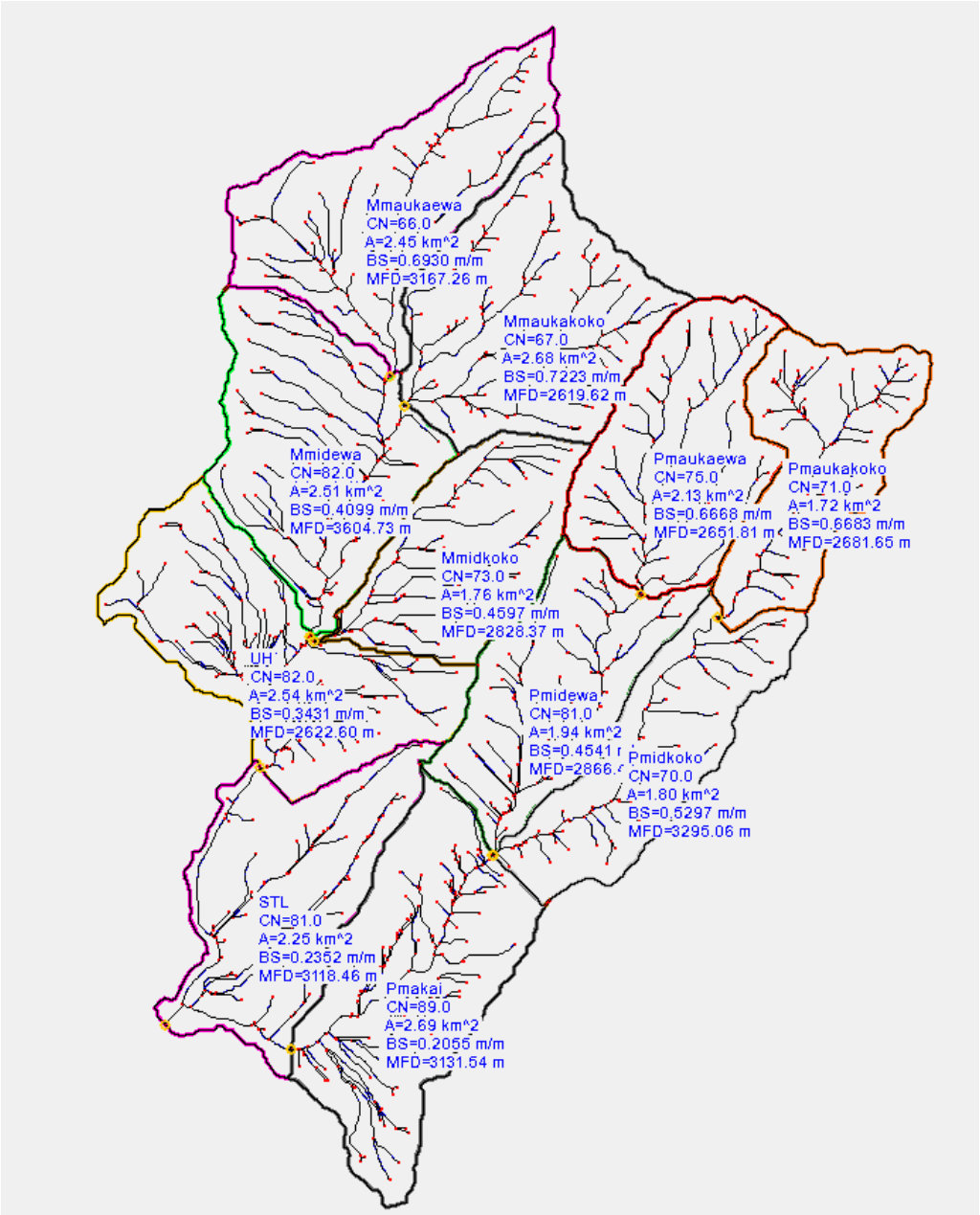

Figure 3-10 11 sub-basin model boundaries and curve numbers for the Manoa-Palolo watershed

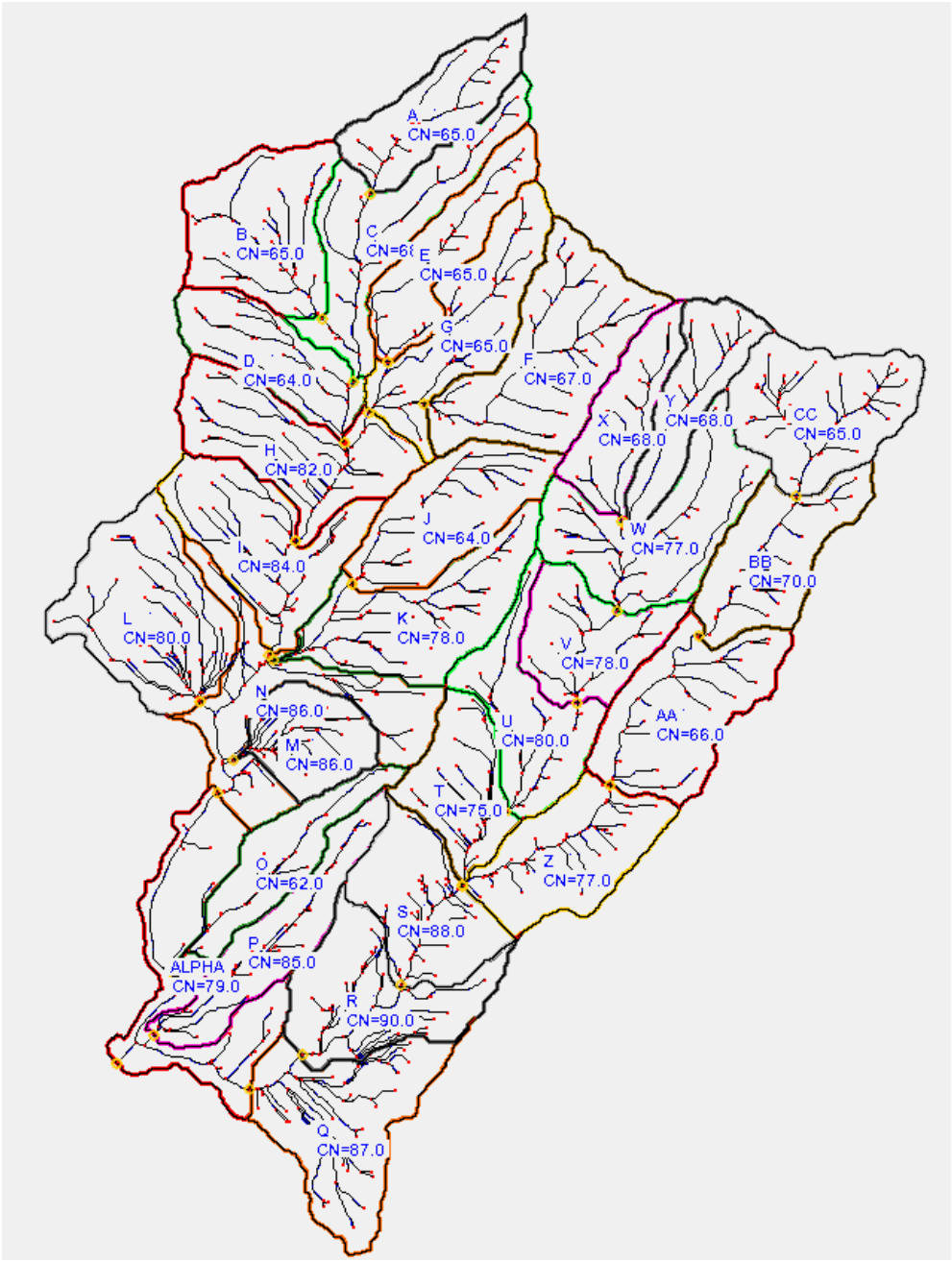

Figure 3-11 30 sub-basin model boundaries and curve numbers for the Manoa-Palolo Watershed

Table 3-5 Composite model data utilized with HEC-HMS

Basin Name	T_{lag} (hrs)	CN	A (km^2)	Basin Slope (m/m)	Maximum Flow Distance (m)
composite	0.7667	76	24.48	0.4833	8899.55

Table 3-6 11 sub-basin model data utilized with HEC-HMS

Sub-Basin Name	T_{lag} (hrs)	CN	A (km^2)	Basin Slope (m/m)	Maximum Flow Distance (m)
STL	0.4079	81	2.25	0.2352	3118.46
UH	0.2847	82	2.54	0.3431	2622.60
Mmidkoko	0.3423	73	1.76	0.4597	2828.37
Mmidewa	0.3360	82	2.51	0.4099	3604.73
Mmaukaewa	0.3686	66	2.45	0.6930	3167.29
Mmaukakoko	0.3021	67	2.68	0.7223	2619.62
Pmakai	0.3303	89	2.69	0.2055	3131.54
Pmidkoko	0.3423	70	1.80	0.5297	3295.06
Pmidewa	0.2745	81	1.94	0.4541	2866.47
Pmaukaewa	0.2551	75	2.13	0.6668	2651.81
Pmaukakoko	0.2875	71	1.72	0.6683	2681.65

Table 3-7 30 sub-basin model data utilized with HEC-HMS

Sub- Basin Name	T_{lag} (hrs)	CN	A (km^2)	Basin Slope (m/m)	Maximum Flow Distance (m)
A	0.0892	65	0.63	0.8788	1774.22
B	0.1005	65	0.94	0.5837	1789.17
C	0.1418	68	0.90	0.6730	2700.16
D	0.0990	64	0.63	0.5020	1844.46
E	0.1137	65	0.62	0.7112	2219.59
F	0.1187	67	1.21	0.8025	2212.64
G	0.1147	65	0.85	0.6159	2210.27
H	0.1246	82	0.95	0.4338	2086.66
I	0.1194	84	0.94	0.3242	1951.28
J	0.1239	64	0.81	0.4804	1998.76
K	0.1502	78	0.95	0.4421	2404.63
L	0.1069	80	1.13	0.3719	1679.82
M	0.1156	86	0.50	0.3575	1360.37
N	0.1924	86	0.91	0.2995	2622.60
O	0.1499	62	0.55	0.2544	2296.41
P	0.1672	85	0.70	0.2012	2464.50
Q	0.2147	87	1.05	0.0901	1843.14
R	0.1346	90	0.87	0.2265	1983.07
S	0.1129	88	0.77	0.3393	1703.98
T	0.1152	75	0.59	0.4543	1662.50
U	0.1232	80	0.70	0.4324	2042.30
V	0.0751	78	0.65	0.4773	1202.25
W	0.1270	77	1.02	0.5675	1875.45
X	0.0985	68	0.55	0.7708	1708.70
Y	0.1158	68	0.56	0.7460	1983.36
Z	0.1503	77	0.83	0.4603	1778.34
AA	0.1320	66	0.97	0.5884	1925.88
BB	0.1005	70	0.75	0.6860	1889.65
CC	0.0782	65	0.97	0.6546	1411.34
ALPHA	0.3825	79	1.00	0.2484	2603.77

The HEC-HMS model is very sensitive to variations in curve number. Therefore three rainfall-runoff events were used to validate the Manoa-Palolo watershed model. Rainfall was recorded at 15 minute intervals on December 19, 2010, May 2, 2011 and March 5, 2012 at the following rain gage stations: Manoa Lyon Arboretum, St. Stephens and Palolo Fire Station, available through the National Weather Service (National

Weather Service, 2013). The 15 minute discharge for the Manoa-Palolo stream for the specified events is available through the USGS (USGS, 2013). The models were evaluated in their ability to predict the peak flow and the time of peak. The results of this validation can be seen in Table 3-8 and Table 3-9. The rainfall distribution for the 3 rainfall events used in this validation can be seen in Table 3-11, Table 3-12 and Table 3-15. The modeled hydrographs are compared with the recorded hydrograph in Figure 3-15, Figure 3-16 and Figure 3-17. The sub-basin models and the composite model are shown to predict the peak flow with reasonable accuracy. The time of peak, which is used as an indicator of matching the hydrograph shape, also shows very good agreement for both models.

Table 3-8 Peak discharge validation of Manoa-Palolo HEC-HMS model

Flood Event	Stream gage	11 Sub Basin Model	30 Sub Basin Model	Composite model
December 19, 2010	4160	5365	5550	5436
March 5, 2012	5010	5835	6035	4946
May 2, 2011	2680	3090	3167	2119

Table 3-9 Time of peak discharge validation of Manoa-Palolo HEC-HMS model

Flood Event	Stream Gage	11 Sub Basin Model	30 Sub Basin Model	Composite Model
December 19, 2010	13:10	13:15	13:15	13:30
March 5, 2012	3:42	3:45	3:30	4:00
May 2, 2011	19:10	19:15	19:00	19:30

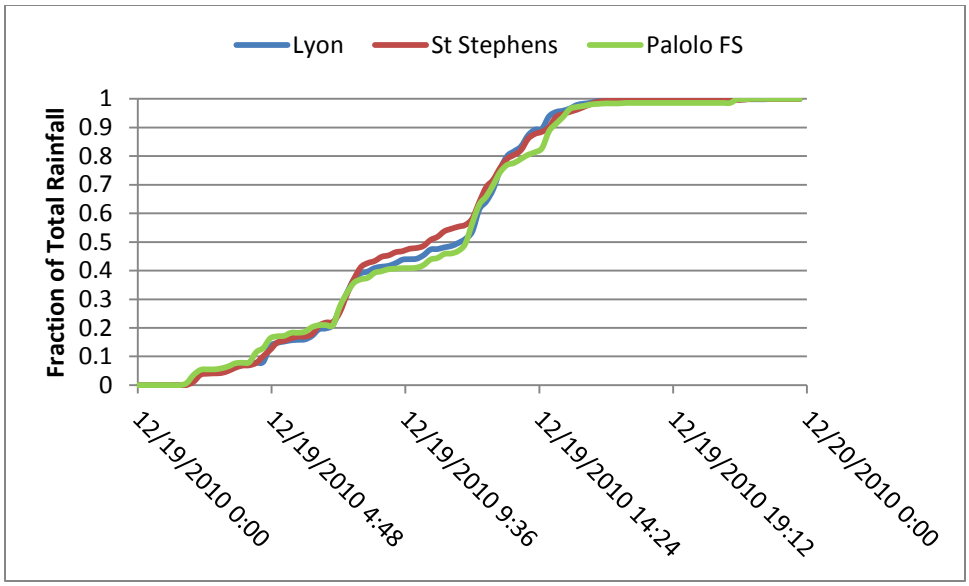

Figure 3-12 Rainfall distribution recorded at 3 different rain gages on December 19, 2010

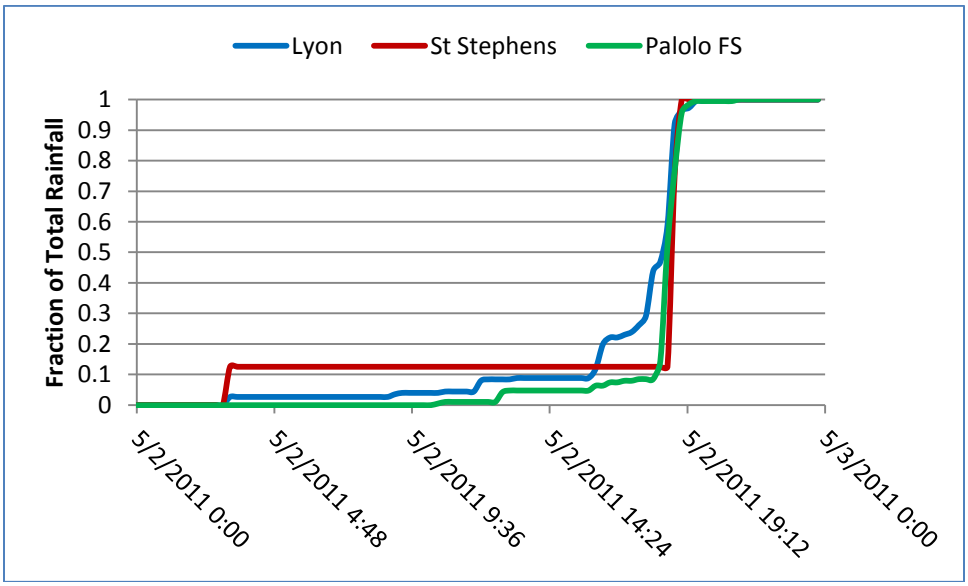

Figure 3-13 Rainfall distribution recorded at 3 different rain gages on May 2, 2011

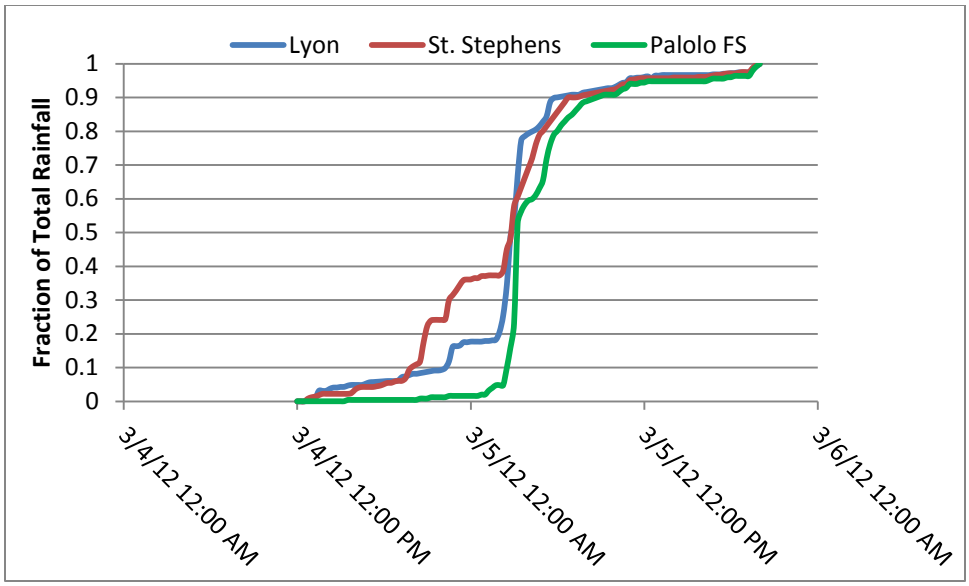

Figure 3-14 Rainfall distribution recorded at 3 different rain gages on March 5, 2012

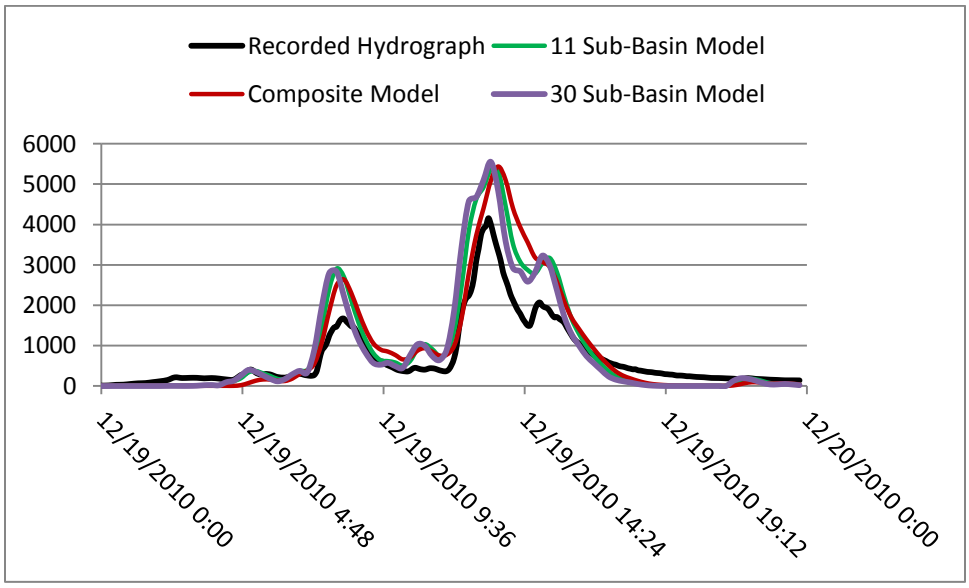

Figure 3-15 Validation of Manoa-Palolo sub-basin and composite HEC-HMS models for December 19, 2010 flood

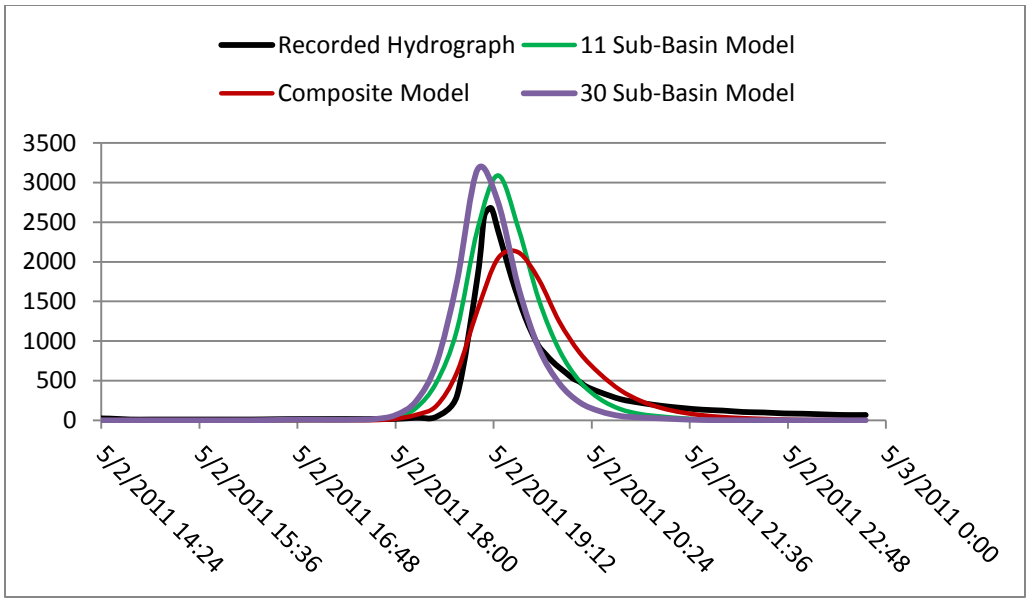

Figure 3-16 Validation of Manoa-Palolo sub-basin and composite HEC-HMS models for May 2, 2011 flood

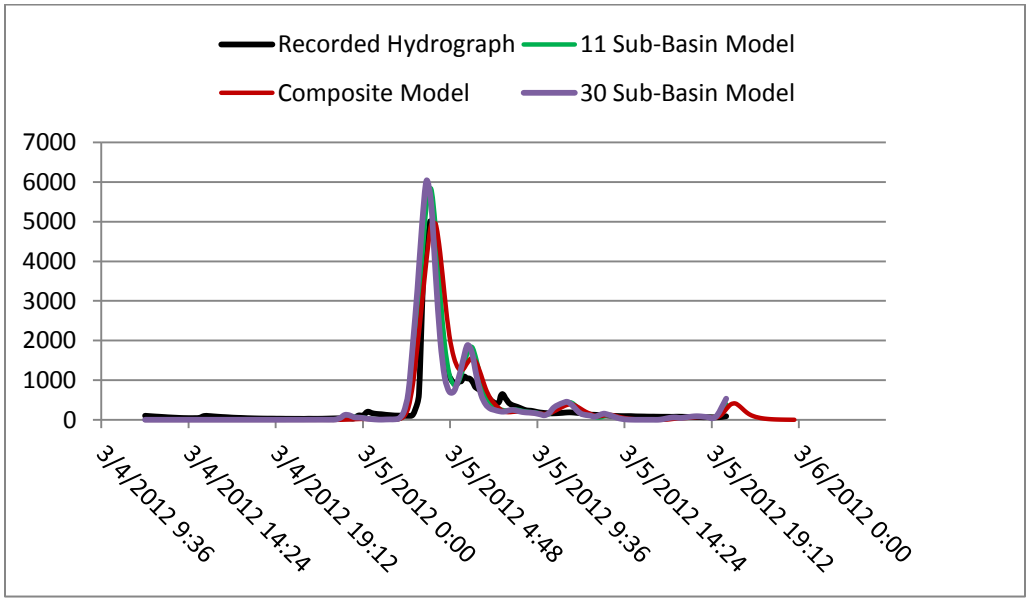

Figure 3-17 Validation of Manoa-Palolo sub-basin and composite HEC-HMS models for March 5, 2012 flood

All three models were used to make predictions of the 100 year flow rate. Two different temporal distributions were utilized; one based on NOAA Atlas 14 shown in Figure 3-18 and the other based on the SCS Type 1 curve shown in Figure 3-19. NOAA

Atlas 14 provides temporal distributions for 6, 12, 24 and 96 hour rainfall events (Perica, et al., 2011). An analysis of rainfall duration for large rainfall events shown in Table 3-2 shows the average rainfall duration on the island of Oahu is approximately 6.72 hours. The 6 hour duration with a 50% chance of occurrence was selected as representative of a typical large storm event, since the actual rainfall distribution is equally likely to fall on either side of the 50% distribution. The discharge hydrograph generated using the NOAA Atlas 14 temporal distribution does not necessarily represent the absolute 100 year peak flow rate; rather it is representative of the peak discharge induced by the 100 year 6 hour rainfall. A large rainfall gradient exists across the Manoa-Palolo watershed, and this rainfall gradient was represented by 8 different rain gages, shown in Table 3-10. The 6 hour precipitation is used with the NOAA Atlas 14 temporal distribution while the 24 hour precipitation is used with the SCS Type 1 temporal distribution.

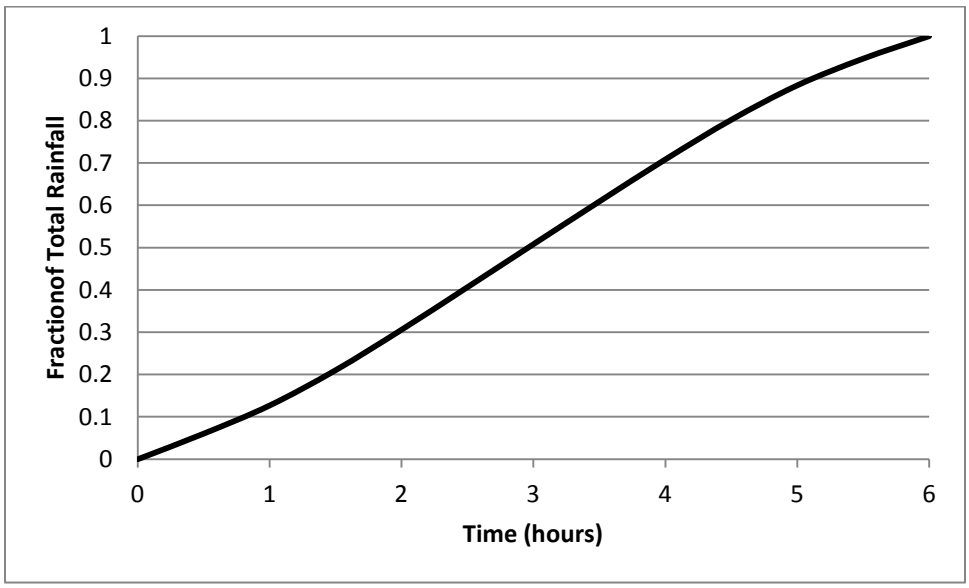

Figure 3-18 NOAA Atlas 14 rainfall duration – 6 hour duration and 50% chance of occurrence (Perica, et al., 2011)

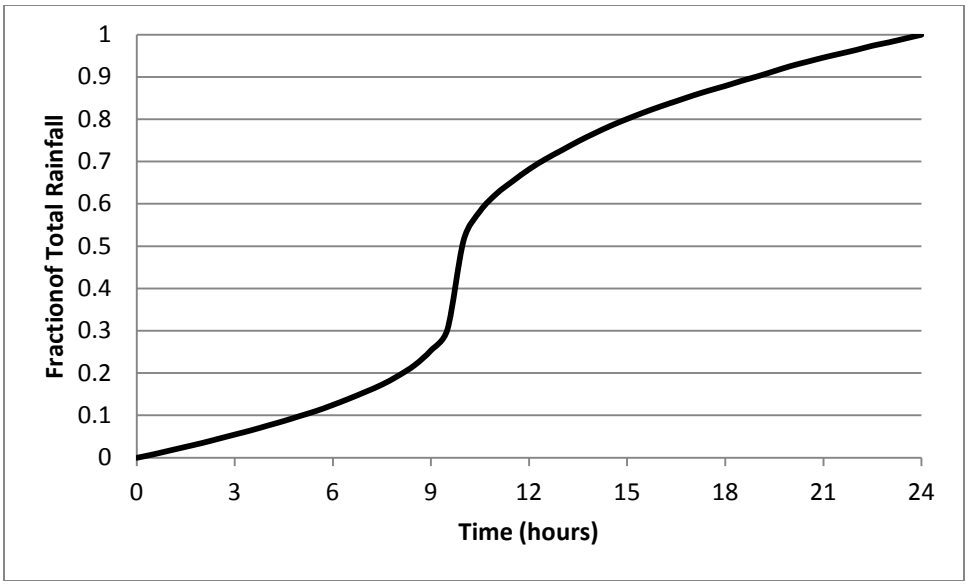

Figure 3-19 SCS Type 1 rainfall distribution

Table 3-10 Rain gages used to predict 100 year discharge with HEC-HMS (Perica, et al., 2011)

Rain Gage	UTM Easting	UTM Northing	100 Year - 6 Hour Precipitation (in)	100 Year – 24 hour Precipitation (in)
Lyon	624183	2359486	11.2	17.5
St. Stephens	626633	2363224	12	18.4
Kaimuki	624484	2353975	7.08	11.1
Spielgelberger	623414	2358395	10.2	16.0
Manoa Tunnel	625339	2358963	11.2	17.4
Palolo Valley	627365	2358425	11.4	17.5
Wilhelmia Rise	626059	2355714	8.51	13.3
University of Hawaii	622738	2355811	7.87	12.4

The 100 year discharge for the Manoa-Palolo watershed predicted by the different models and temporal distributions are shown in Table 3-11. The hydrograph for each model is shown in Figure 3-20 through Figure 3-25.

Table 3-11 Comparison of 100 year discharge predictions for the Manoa-Palolo HEC-HMS models

Model	Precipitation Temporal Distribution (duration)	Discharge (cfs)
Composite	NOAA Atlas 14 (6 hr)	10165
Composite	SCS Type 1 (24 hr)	20724
11 Sub-Basins	NOAA Atlas 14 (6 hr)	10341
11 Sub-Basins	SCS Type 1 (24 hr)	29740
30 Sub-Basin Model	NOAA Atlas 14 (6 hr)	10138
30 Sub-Basin Model	SCS Type 1 (24 hr)	36586

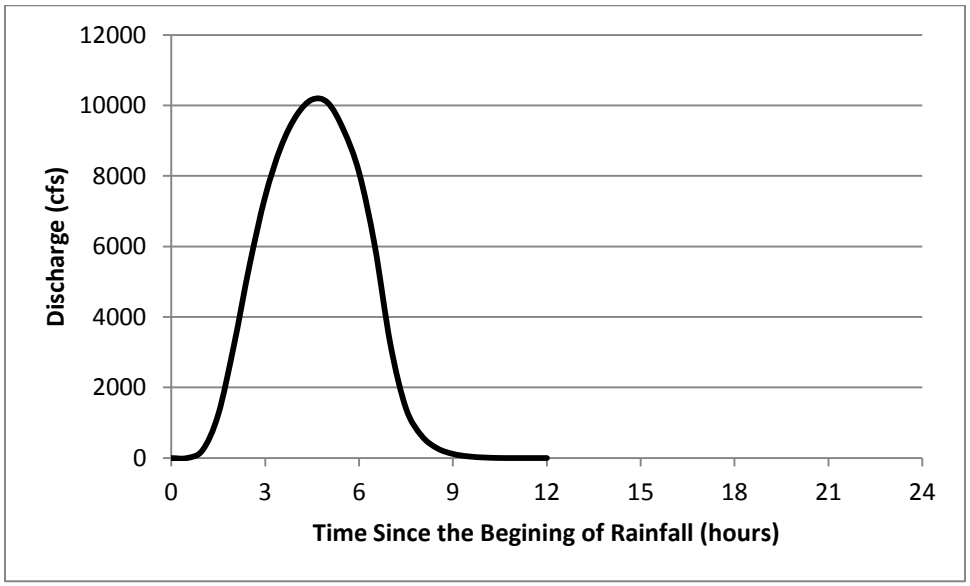

Figure 3-20 Hydrograph for the 100 year flood in the Manoa-Palolo Stream generated by HEC-HMS composite model and NOAA Atlas 14 6 hour rainfall distribution

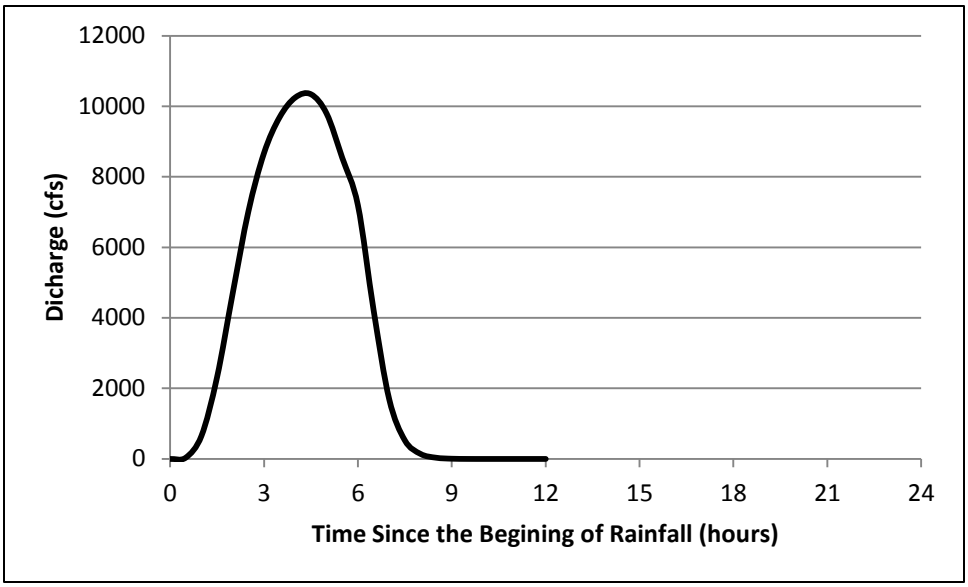

Figure 3-21 Hydrograph for the 100 year flood in the Manoa-Palolo Stream generated by the HEC-HMS 11 sub-basin model and NOAA Atlas 14 6 hour rainfall distribution

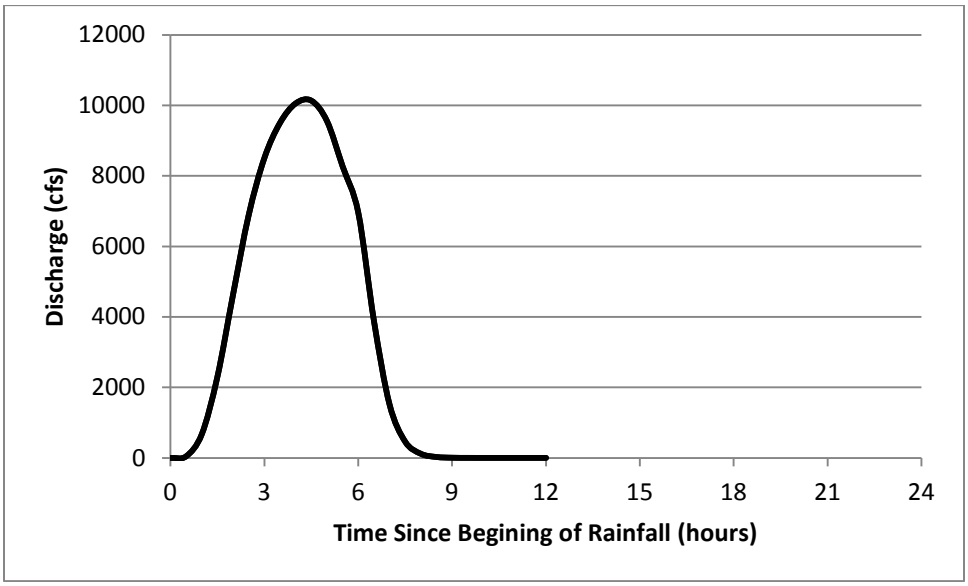

Figure 3-22 Hydrograph for the 100 year flood in the Manoa-Palolo Stream generated by the HEC-HMS 30 sub-basin model and NOAA Atlas 14 6 hour rainfall distribution

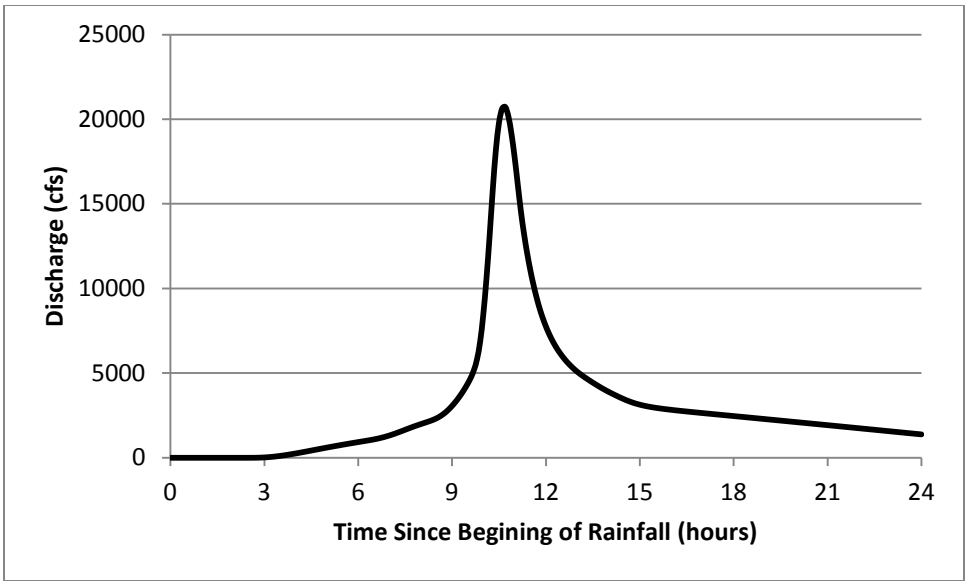

Figure 3-23 Hydrograph for the 100 year flood in the Manoa-Palolo Stream generated by the HEC-HMS composite model and SCS Type 1 24 hour rainfall distribution

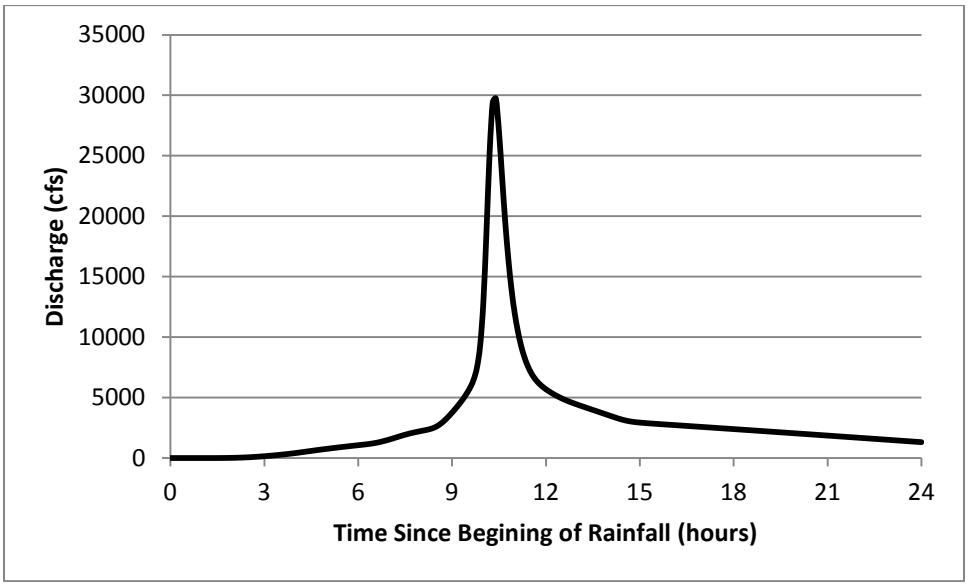

Figure 3-24 Hydrograph for the 100 year flood in the Manoa-Palolo Stream generated by the HEC-HMS 11 sub-basin model and SCS Type 1 24 hour rainfall distribution

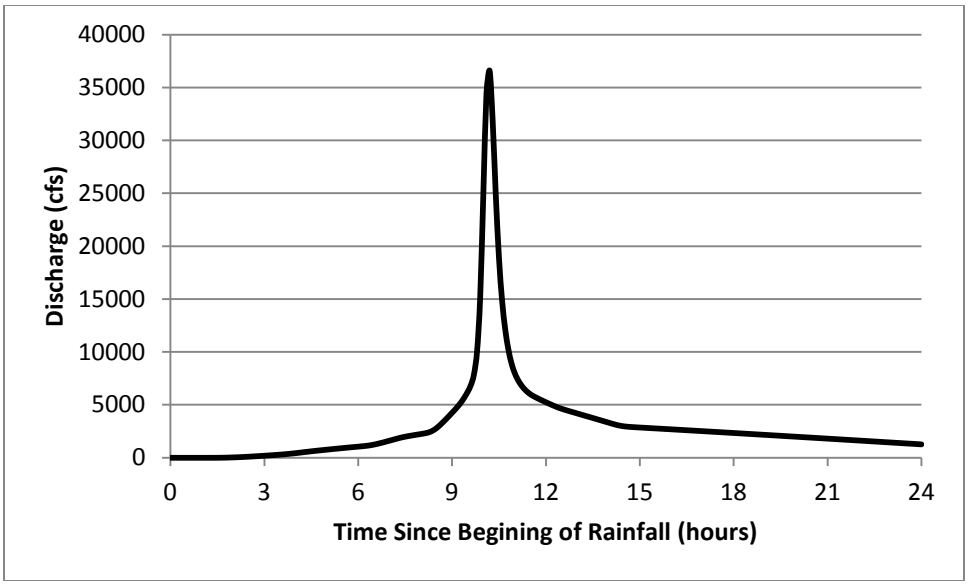

Figure 3-25 Hydrograph for the 100 year flood in the Manoa-Palolo Stream generated by the HEC-HMS 30 sub-basin model and SCS Type 1 24 hour rainfall distribution

3.2.5 Indirect Prediction of the 100 Year Flow by TR-55

Technical Release 55 (TR-55) is the second rainfall-runoff model that was used to predict the 100 year discharge for the Manoa-Palolo watershed (Soil Conservation Service, no Natural Resources Conservation Service, 1986). WMS was used to calculate the basin parameters, and the TR-55 tabular method was used to predict the peak flow and hydrograph. The TR-55 precipitation input requires a 24 hour rainfall with a temporal distribution based on the SCS 24 hour rainfall distribution. Rainfall in Hawaii is described by a Type 1 distribution.

The hydrograph developed using the TR-55 tabular method can be described by equation 3-15. The tabular unit discharge is a function of time of concentration and travel time for a drainage area and represents the discharge of a sub-basin routed to the outlet of the drainage area. Time of concentration is the time required for water to travel from the most hydraulically distant point within the sub-basin to the sub-basin outlet, while the travel time is the time required for water to travel from the sub-basin outlet to the outlet of the drainage area. Both times are calculated by dividing the flow path into uniform flow segments, calculating the time to travel along each segment then summing the required segments. TR-55 recommends calculating sheet flow travel time using equation

3-17, open channel flow using equation 3-18 and 3-19, and shallow concentrated flow using equation 3-18 and 3-20. The volume of direct runoff is a function of rainfall, initial abstraction of the soil and potential maximum retention of the soil. Precise values of initial abstraction and potential maximum retention are difficult to calculate and can be represented by a curve number which is related to both the soil and ground cover. The volume of direct runoff can be calculated using equation 3-16.

$$q = q_t A_m Q \tag{3-15}$$

where:
q = hydrograph coordinate at hydrograph time t (cfs)
q_t = tabular hydrograph unit discharge from TR-55 manual (csm/in)
A_m = drainage area (mi^2)
Q = runoff depth, equation 3-16 (in)

$$Q = \frac{\left(P - 0.2\left(\frac{1000}{CN} - 10\right)\right)^2}{P + 0.8\left(\frac{1000}{CN} - 10\right)} \tag{3-16}$$

$$T_{sheet\ flow} = \frac{0.007(nL)^{0.8}}{(P_2)^{0.5} S^{0.4}} \tag{3-17}$$

$$T_{shallow\ concentrated\ and\ open\ channel} = \frac{L}{3600V} \tag{3-18}$$

$$V_{open\ channel} = \frac{1.49 r^{2/3} S^{1/2}}{n} \tag{3-19}$$

$$V_{shallow\ concentrated} = \begin{cases} 16.1345\sqrt{S} & for\ unpaved\ surfaces \\ 20.3282\sqrt{S} & for\ paved\ surfaaces \end{cases} \tag{3-20}$$

where:
T = travel time (hrs)

n = Manning's roughness coefficient
L = flow length (ft)
P = precipitation (in)
P_2 = 2 year, 24 hour rainfall (in)
CN = curve number
s = slope of hydraulic grade line (approximately equal to land slope) (ft/ft)
V = velocity (ft/s)
r = hydraulic radius (ft) equal to the channel cross sectional area over wetted perimeter

A single composite basin model, an 11 sub-basin model and 30 sub-basin model were used with the TR-55 method. The sub-basin boundaries, overall drainage area boundaries and the curve numbers for each model were the same as the HEC-HMS model. NOAA Atlas 14 was used to determine the 100 year 24 hour rainfall (Perica, et al., 2011). An area weighted average of the 100 year 24 hour rainfall was utilized for the composite model and when a sub-basin was not accurately represented by a single rain gage. The parameters used to calculate the 100 year peak flow for the Manoa-Palolo watershed using the composite model, 11 sub-basin model and 30 sub-basin model are shown in Table 3-12, Table 3-13 and Table 3-14, respectively. The TR-55 composite model predicted a 100 year discharge of 18146 cfs and the hydrograph is shown in Figure 3-26. The TR-55 11 sub-basin model predicted a 100 year peak flow in the Manoa-Palolo stream of 28571 cfs, shown in Figure 3-27. The 100 year discharge predicted using the 30 sub-basin model was 21345 cfs and the hydrograph is shown in Figure 3-28.

Table 3-12 Parameters used in TR-55 tabular method computation of 100 year discharge for Manoa-Palolo composite model

Basin Name	T_c (hrs)	T_t (hrs)	P (in)	CN	A (mi^2)	Basin Slope (m/m)	Maximum Flow Distance (m)
composite	1.5	n/a	15	76	9.45	0.4833	8899.55

Table 3-13 Parameters used in TR-55 tabular method computation of 100 year discharge for Manoa-Palolo 11 sub-basin model

Sub-Basin Name	T_c (hrs)	T_t (hrs)	P (in)	CN	A (mi^2)	Basin Slope (m/m)	Maximum Flow Distance (m)
STL	0.4	n/a	12.4	81	0.87	0.2352	3118.46
UH	0.4	0.2	15.3	82	0.98	0.3431	2622.6
Mmidkoko	0.3	0.4	17	73	0.68	0.4597	2828.37
Mmidewa	0.4	0.4	16.6	82	0.97	0.4099	3604.73
Mmaukaewa	0.3	0.5	17.5	66	0.96	0.693	3167.29
Mmaukakoko	0.2	0.5	17.4	67	1.03	0.7223	2619.62
Pmakai	0.4	0.1	11.7	89	1.04	0.2055	3131.54
Pmidkoko	0.4	0.3	14.1	70	0.69	0.5297	3295.06
Pmidewa	0.3	0.3	14.5	81	0.75	0.4541	2866.47
Pmaukaewa	0.3	0.4	17.4	75	0.82	0.6668	2651.81
Pmaukakoko	0.3	0.4	17.5	71	0.66	0.6683	2681.65

Table 3-14 Parameters used in TR-55 tabular method computation of 100 year discharge for Manoa-Palolo 30 sub-basin model

Sub-Basin Name	T_c (hrs)	T_t (hrs)	P (in)	CN	A (mi^2)	Basin Slope (m/m)	Maximum Flow Distance (m)
A	0.1	1.5	17.5	65	0.63	0.8788	1774.22
B	0.2	1	17.5	65	0.94	0.5837	1789.17
C	0.2	1	17.5	68	0.9	0.673	2700.16
D	0.2	1	17.5	64	0.63	0.502	1844.46
E	0.2	1	17.5	65	0.62	0.7112	2219.59
F	0.2	1	17.4	67	1.21	0.8025	2212.64
G	0.2	1	17.5	65	0.85	0.6159	2210.27
H	0.2	1	16.7	82	0.95	0.4338	2086.66
I	0.02	1	16	84	0.94	0.3242	1951.28
J	0.2	1	17.4	64	0.81	0.4804	1998.76
K	0.3	0.75	16.8	78	0.95	0.4421	2404.63
L	0.2	0.75	16	80	1.13	0.3719	1679.82
M	0.2	0.75	14.2	86	0.5	0.3575	1360.37
N	0.3	0.75	14.9	86	0.91	0.2995	2622.6
O	0.2	0.2	12.4	62	0.55	0.2544	2296.41
P	0.3	0.1	12.4	85	0.7	0.2012	2464.5
Q	0.4	0.2	11.1	87	1.05	0.0901	1843.14
R	0.2	0.2	11.1	90	0.87	0.2265	1983.07
S	0.2	0.4	13.3	88	0.77	0.3393	1703.98
T	0.2	0.5	13.3	75	0.59	0.4543	1662.5
U	0.2	0.5	13.5	80	0.7	0.4324	2042.3
V	0.1	0.5	15.8	78	0.65	0.4773	1202.25
W	0.2	0.75	17.5	77	1.02	0.5675	1875.45
X	0.2	0.75	17.5	68	0.55	0.7708	1708.7
Y	0.2	0.75	17.5	68	0.56	0.746	1983.36
Z	0.3	0.5	13.3	77	0.83	0.4603	1778.34
AA	0.2	0.75	15.4	66	0.97	0.5884	1925.88
BB	0.2	0.75	17.5	70	0.75	0.686	1889.65
CC	0.1	1	17.5	65	0.97	0.6546	1411.34
ALPHA	0.5	0	12.2	79	1	0.2484	2603.77

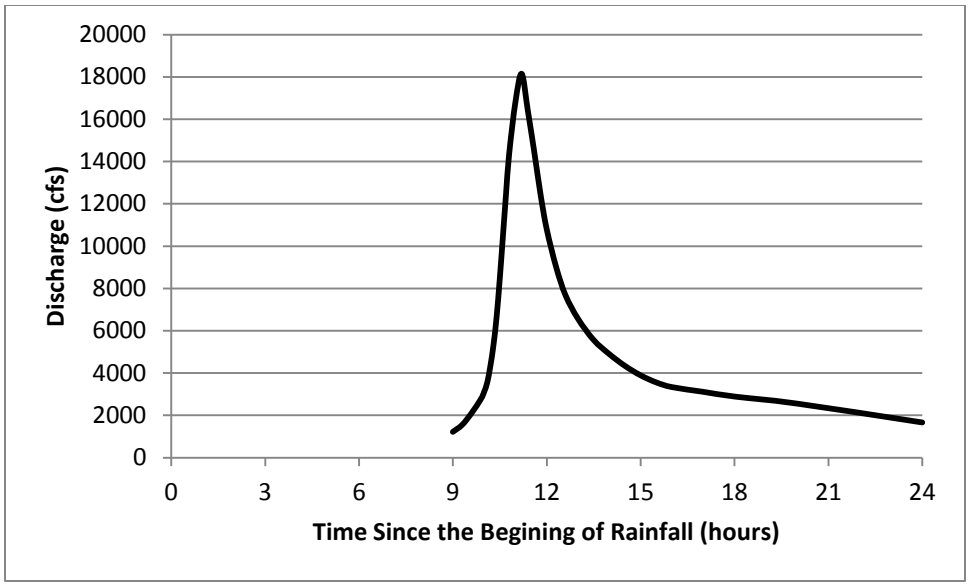

Figure 3-26 Hydrograph generated for the 100 year flood in the Manoa-Palolo Stream from the TR-55 composite model

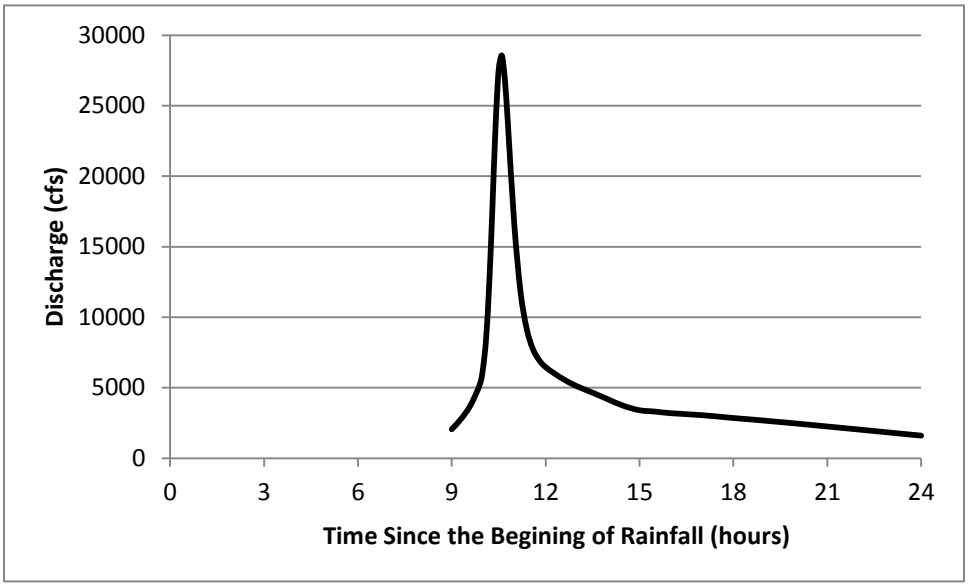

Figure 3-27 Hydrograph generated for the 100 year flood in the Manoa-Palolo Stream from the TR-55 11 sub-basin model

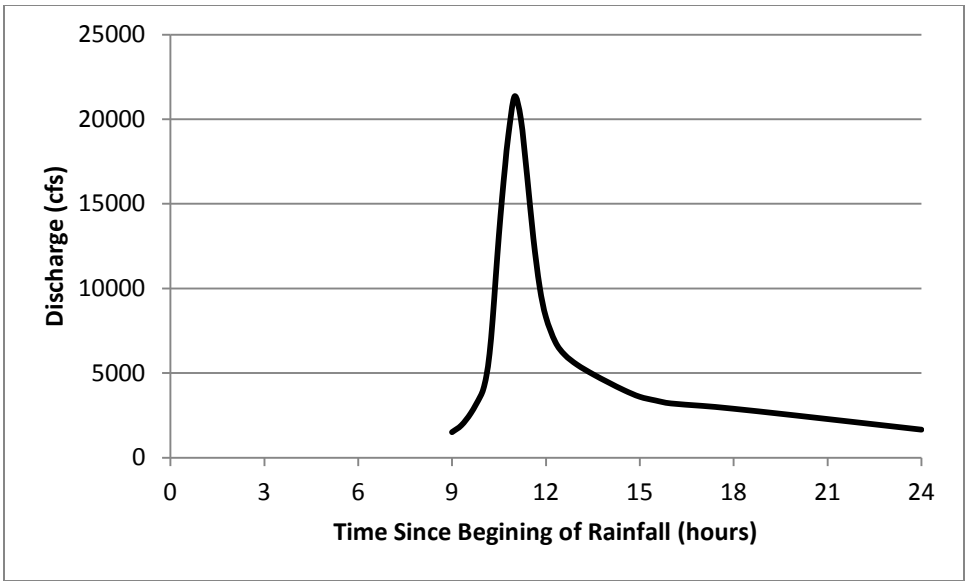

Figure 3-28 Hydrograph generated for the 100 year flood in the Manoa-Palolo Stream from the TR-55 30 sub-basin model

3.2.6 Indirect Prediction of the 100 Year Flow by Rational Method

The rational method is a commonly used equation to predict peak flow, particularly for the sizing of storm water drainage systems in small watersheds. The rational method requires a runoff coefficient that is related to the type of ground cover, the rainfall intensity and the drainage area as shown in equation 3-20. The rational method was designed for use in small watersheds, and the City & County of Honolulu does not recommend using the rational method for watersheds greater than 100 acres (City and County of Honolulu, 2000).

$$Q = ciA \qquad \textbf{3-20}$$

where:
Q = peak discharge (cfs)
c = runoff coefficient
i = intensity of rainfall with duration equal to the drainage basin time of concentration and frequency of the design event (in/hr)
A = area of the drainage basin (acres)

The Manoa-Palolo watershed has an area of 24.28 km^2, or 6050 acres. The watershed was split into sub-basins to apply the rational method to each sub-basin individually. The discharge at the outlet of each sub-basin was assumed to be represented

by a triangular hydrograph, with the peak equal to the peak discharge, the time of peak equal to the time of concentration and the total hydrograph duration equal to twice the time of concentration. The hydrograph from each outlet was combined using the Muskingum-Cunge routing method, shown in equation 3-10.

The Manoa-Palolo watershed was divided into 30 sub-basins. The resulting average sub-basin area is approximately 200 acres, which is twice the size recommended by the City & County of Honolulu. The error generated by having a basin that is larger than recommended was balanced against the potential errors in the application of the routing procedure. Thirty sub-basins were determined to create sub-basins that were small enough that the rational method for each sub-basin would be reasonably accurate without requiring too many sub-basins to be combined using the Muskingum-Cunge method. The outlet of each sub-basin was located to attempt to keep the land use of each sub-basin uniform and the area of each basin close to 200 acres.

The range of key parameters that were utilized in the rational method and Muskingum-Cunge routing method are summarized in Table 3-15. The peak flow rate predicted by the rational method and Muskingum-Cunge method is 9615 cfs. The hydrograph at the outlet of the Manoa-Palolo watershed is shown in Figure 3-29.

Table 3-15 Range of sub-basin variables used with Rational Method and Muskingum-Cunge Method

Runoff Coefficient	0.6 – 0.85
Area of Sub-basin (acres)	124 – 300
Time of Concentration of Sub-basin (min)	7 – 38
Rainfall Intensity (in/hr)	5.05 – 16.35
Sub-basin peak flow, Q_p (cfs)	813 – 2565
K, Muskingum-Cunge Routing Parameter (s)	120 – 2280
X, Muskingum-Cunge Routing Parameter	-0.25 – -0.004

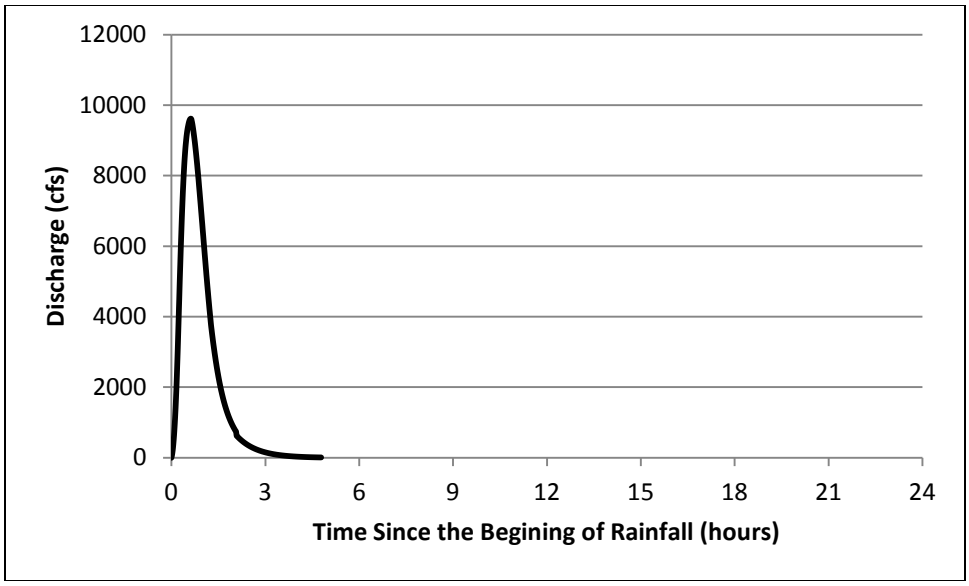

Figure 3-29 Hydrograph generated for the 100 year flood in the Manoa-Palolo Stream from the Rational Method and Muskingum-Cunge Method

3.2.7 Comparison and Validation of the Direct and Indirect Predictions

A summary of all predicted 100 year discharges for the Manoa-Palolo stream are shown in Table 3-16. Further analysis into the appropriate number of sub-basins required to accurately predict the 100 year discharge with each different method is necessary. HEC-HMS requires additional investigation to determine the appropriate precipitation input to generate the 100 year peak discharge. The potential effect of changing land use over the duration of a stream gage record as a result of increased development on the peak flow predicted by statistical methods should also be considered.

Table 3-16 Summary of 100 year discharge predicted for Manao-Palolo Watershed

Method	100 Year Peak Flow (cfs)
Gumbel Distribution	10388
Log-Pearson III Distribution	12568
USGS Regional Regression Equations	10433
HEC-HMS composite model – 6 hour rainfall	10165
HEC-HMS 11 sub-basin model – 6 hour rainfall	10341
HEC-HMS 30 sub-basin model – 6 hour rainfall	10138
HEC-HMS composite model – 24 hour rainfall	20724
HEC-HMS 11 sub-basin model – 24 hour rainfall	29740
HEC-HMS 30 sub-basin model – 24 hour rainfall	36586
TR-55 composite model	18146
TR-55 11 sub-basin model	28571
TR-55 30 sub-basin model	21345
Rational Method and Muskingum-Cunge Method	9615

3.3 100 Year Peak Flow Prediction for Ungaged Stream and Bridge Sites

The 100 year peak flow of five additional watersheds was included in this study. These streams either do not have a gage near the bridge of interest or the stream gage has an insufficient record for a statistically significant calculation of the 100 year discharge. The five ungaged streams are the Kaoli Ditch, Halawa Stream, Moanalua Stream, Waiahole Stream and West Loch Stream. The Kaoli Ditch is a drainage canal on the south shore of the island of Oahu, between Kapolei and Waipahu. A rail bridge is planned for this site near North-South Road south of Farrington Highway as part of the Honolulu Rail Transit Project. The ditch is dry except after a rain event and is vegetated on the gradually sloping sides. The Halawa Stream is located in Honolulu, HI. The bridge of interest that defines the drainage area outlet is the Kamehameha Highway located adjacent to the Pearl Harbor Memorial near where the Halawa stream empties into Pearl Harbor. The Moanalua Stream is located in Honolulu, HI near Ft. Shafter. The bridge that defines the basin outlet is the upstream side of the Keehi Interchange that includes the H-

1 freeway and Nimitz Highway. The Waiahole Stream is located on the windward coast of Oahu, north of Kaneohe. The bridge that defines the outlet of the drainage area is on Kamehameha Highway. The West Loch stream is located between Waipahu and Ewa, directly adjacent to Pearl Harbor on the Leeward side of Oahu. The bridge defining the outlet of the drainage area is Fort Weaver Road crossing the West Loch Golf Course.

3.3.1 Prediction of the 100 Year Peak Flow for Ungaged Watersheds using USGS Regional Regression Equations

The USGS regional regression equations for the island of Oahu are described in Section 3.2.3. The USGS regional regression equations were selected to predict the peak flow because they provide a reasonable estimate of the 100 year peak flow rate, even though the standard error associated with these equations is relatively large. This estimate can then be compared to the rainfall-runoff model and a relatively consistent prediction will show the 100 year flow rate is in the correct range. The five watersheds described above were delineated using WMS and the watershed boundaries are shown in Figure 3-30 through Figure 3-34. The mean annual rainfall was calculated using a weighted average and the 2011 Rainfall Atlas of Hawaii (Giambelluca, et al., 2012). Table 3-4 shows the area of each watershed in each rainfall range and the mean annual precipitation of each watershed. Waiahole stream is excluded from Table 3-4 because it is located on the windward side of Oahu and the USGS regional regression equation for the windward side does not require mean annual rainfall as an input. A summary of the required inputs to the USGS regional regression equation and the predicted 100 year discharge can be seen in Table 3-17.

Table 3-17 100 year discharge for ungaged watersheds using USGS regional regression equations

Stream	Location on Oahu	Mean Annual Precipitation (in)	Drainage Area (mi^2)	USGS regional regression equation 100 year discharge (cfs)
Kaoli Ditch	Leeward	32	4.52	4565
Halawa Stream	Leeward	74	9.61	9840
Moanalua Stream	Leeward	74	10.33	10311
Waiahole Stream	Windward	n/a	3.73	8454
West Loch Stream	Leeward	32	11.32	8260

3.3.2 Prediction of the 100 Year Peak Flow for Ungaged Watersheds using HEC-HMS

The HEC-HMS software utilizing a composite watershed model was selected as a second method for predicting the peak flow in the 5 ungaged watersheds. As seen in Table 3-16 the composite model showed good agreement and with the statistical analysis on the stream record. A composite model also does not require routing parameters to be estimated which is required with the sub-basin models. HEC-HMS was selected over the TR-55 method because HEC-HMS allowed for a variable rainfall distribution that is not possible with the TR-55 method. Both the 6 hour rainfall distribution and 24 hour rainfall distribution are included in this analysis. All techniques used to predict the 100 year discharge for the Manoa-Palolo stream using the HEC-HMS composite model were repeated for each of the ungaged watersheds. It is of note that the hydrographs generated using the 6 hour rainfall distribution in HEC-HMS represent the hydrograph induced by the 100 year 6 hour rainfall and may not be the absolute 100 year peak flow rate. The delineated watershed, drainage paths and rain gages used to calculate the 100 year discharge for each ungaged watershed are shown in Figure 3-30 through Figure 3-34.

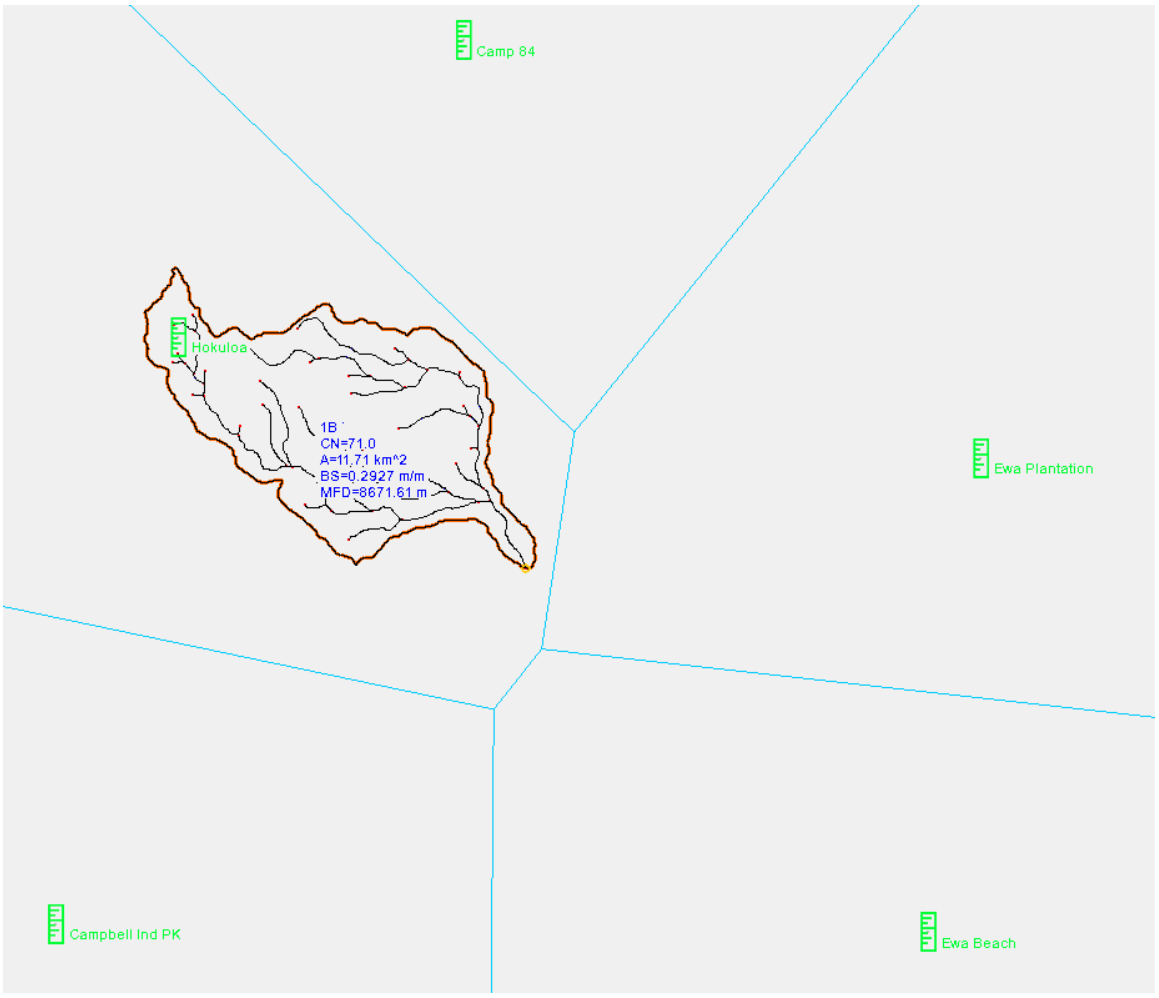

Figure 3-30 Drainage pathways and rain gage locations for Kaoli Ditch watershed

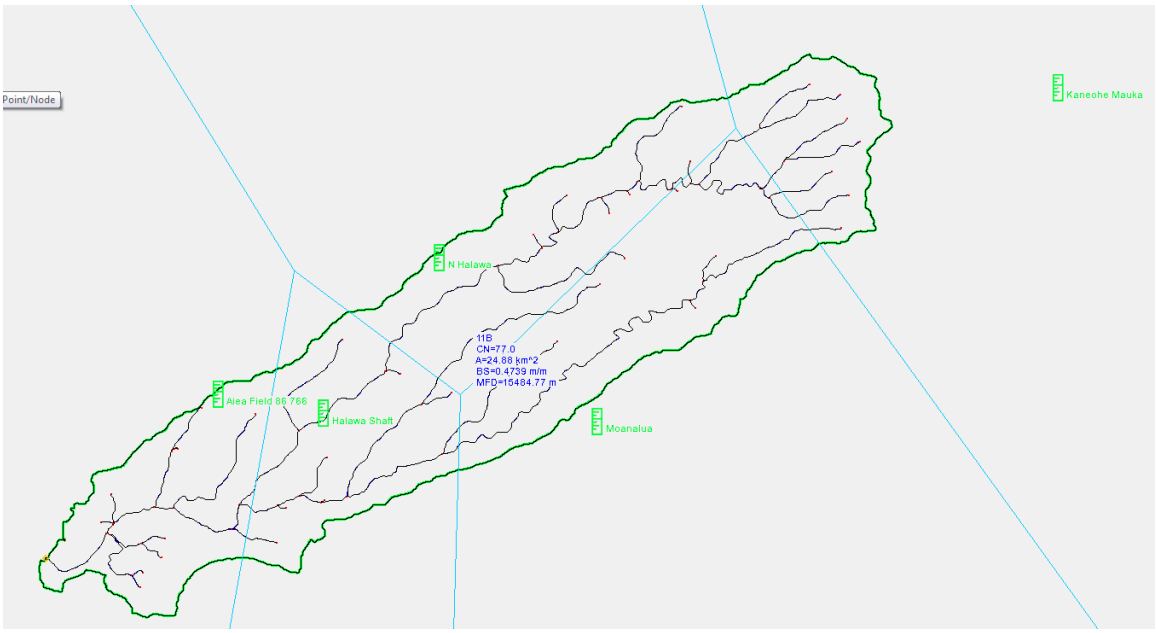

Figure 3-31 Drainage pathways and rain gage locations for Halawa Stream watershed

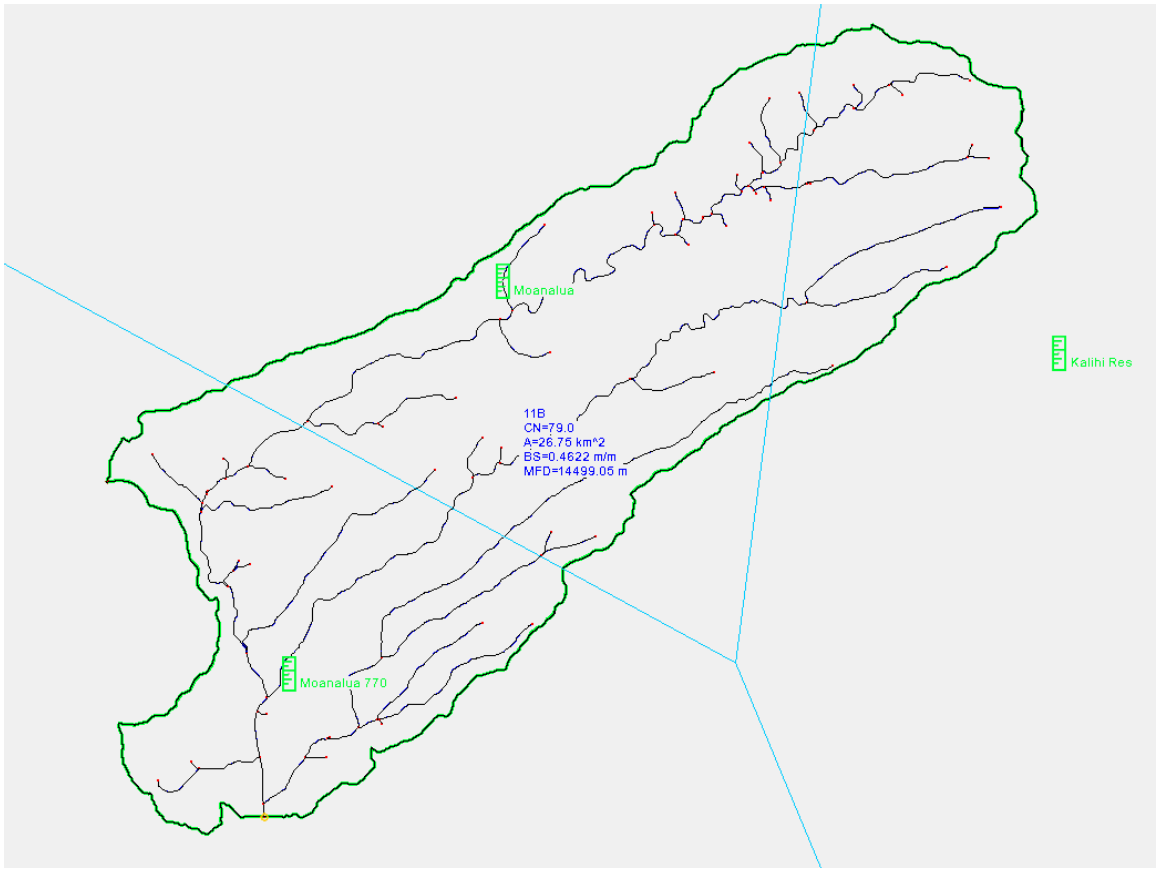

Figure 3-32 Drainage pathways and rain gage locations for Moanalua Stream watershed

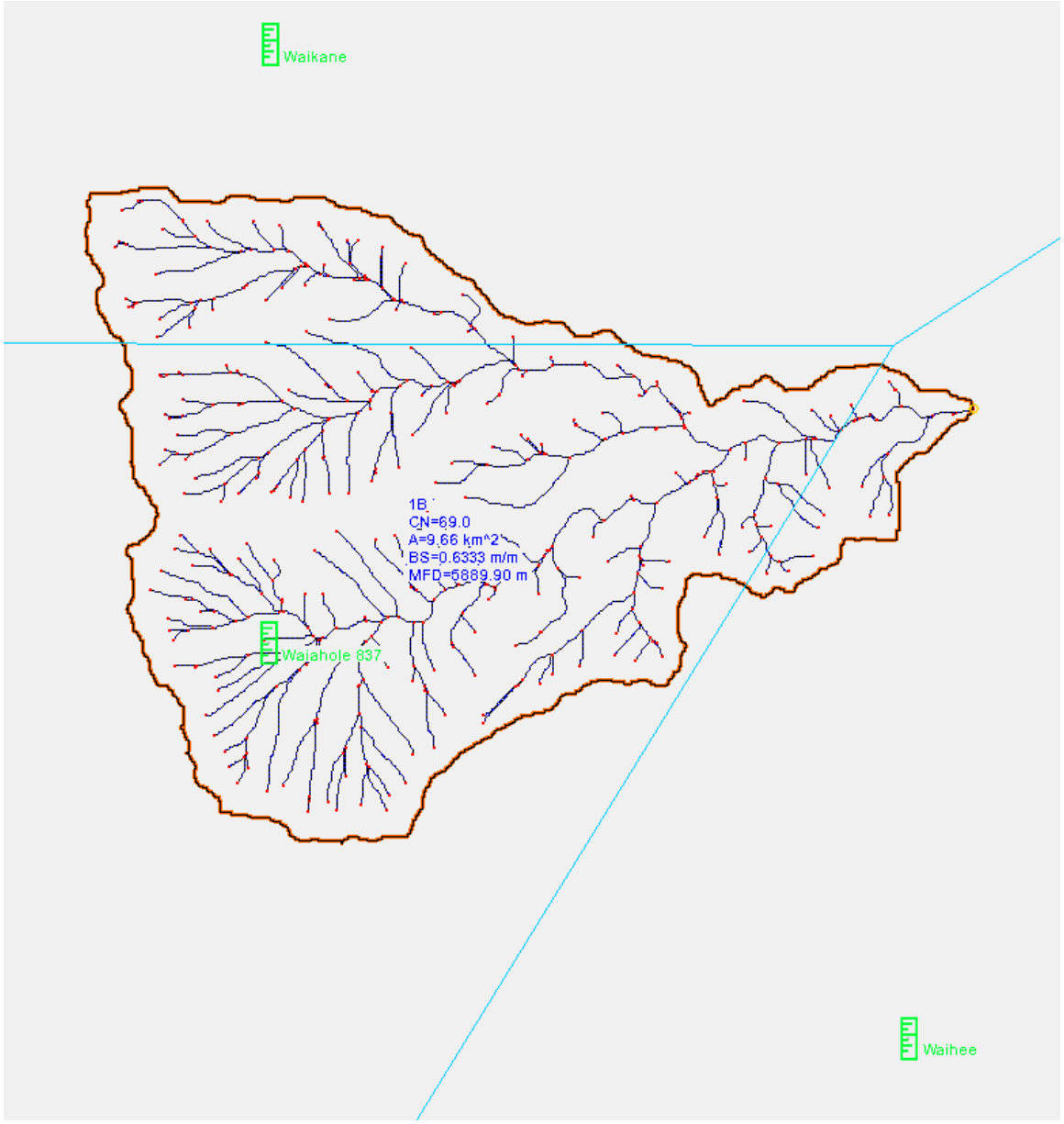

Figure 3-33 Drainage pathways and rain gage locations for Waiahole Stream watershed

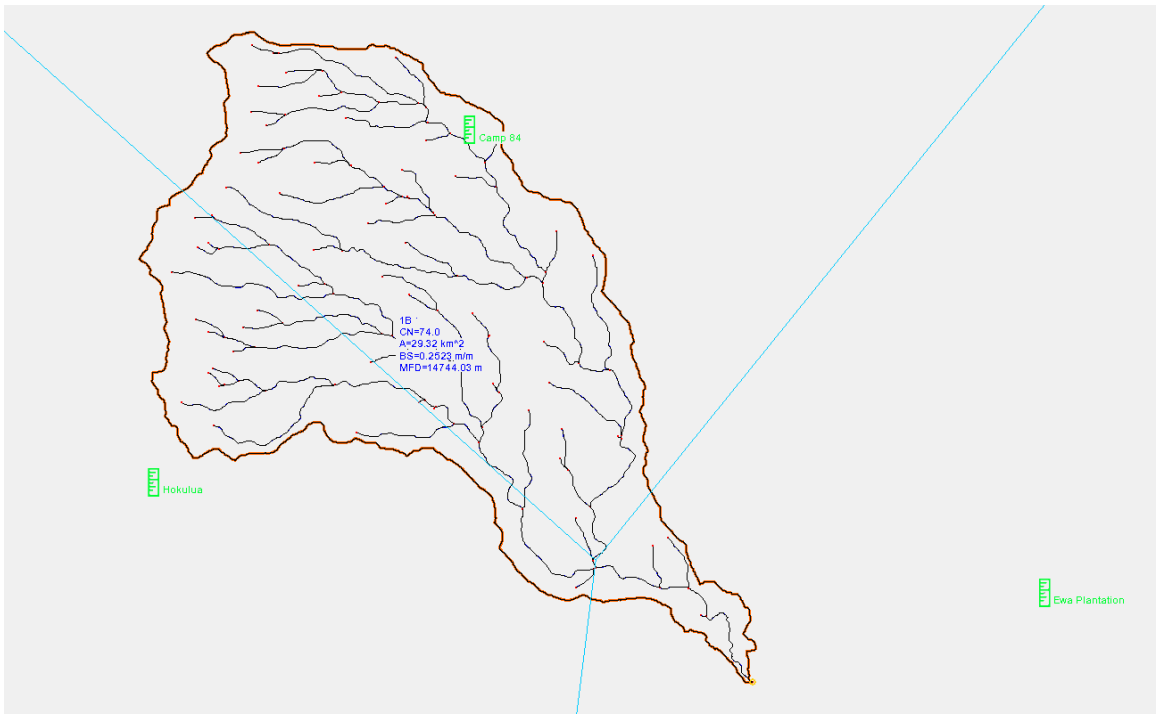

Figure 3-34 Drainage pathways and rain gage locations for West Loch Stream watershed

It should be noted that while the techniques used to generate each model were validated by the Manoa-Palolo watershed HEC-HMS composite model, each individual model could not be validated because of insufficient stream records. Therefore the result of the HEC-HMS model for each ungaged watershed should be used with caution. The 100 year discharge for each of the ungaged watersheds is listed in Table 3-18. The hydrographs generated using the NOAA Atlas 14 6 hour rainfall distribution are shown in Figure 3-35 through Figure 3-39. The hydrographs generated using the SCS Type 1 distribution and 24 hour rainfall are shown in Figure 3-40 through Figure 3-44.

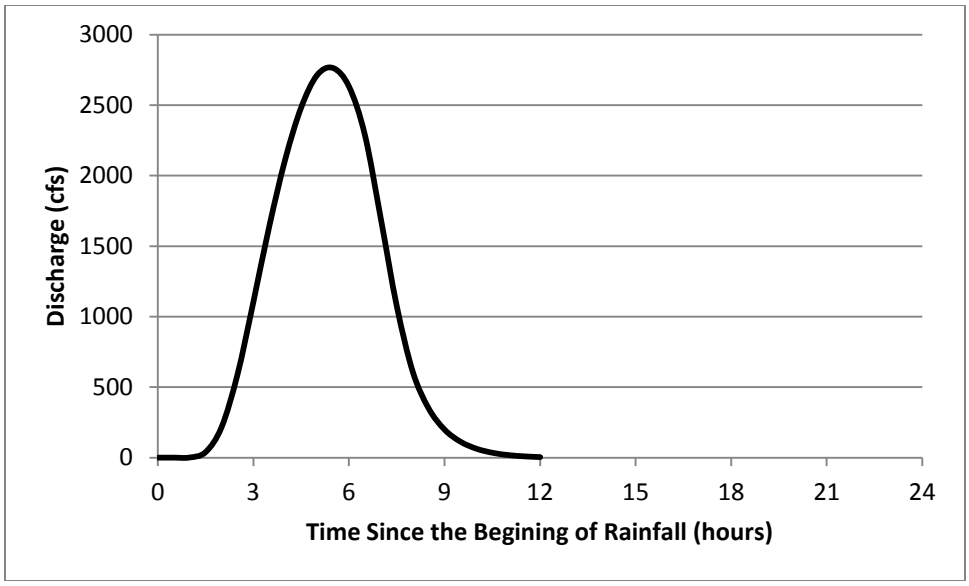

Figure 3-35 Hydrograph for the 100 year flood in the Kaoli Ditch generated using the HEC-HMS composite model and 6 hour NOAA Atlas 14 rainfall distribution

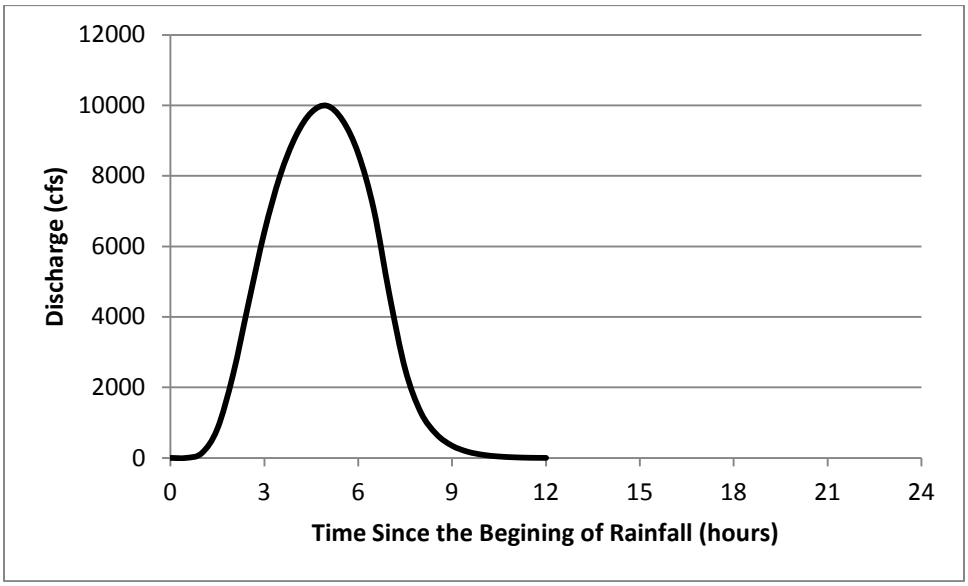

Figure 3-36 Hydrograph for the 100 year flood in the Halawa Stream generated using the HEC-HMS composite model and 6 hour NOAA Atlas 14 rainfall distribution

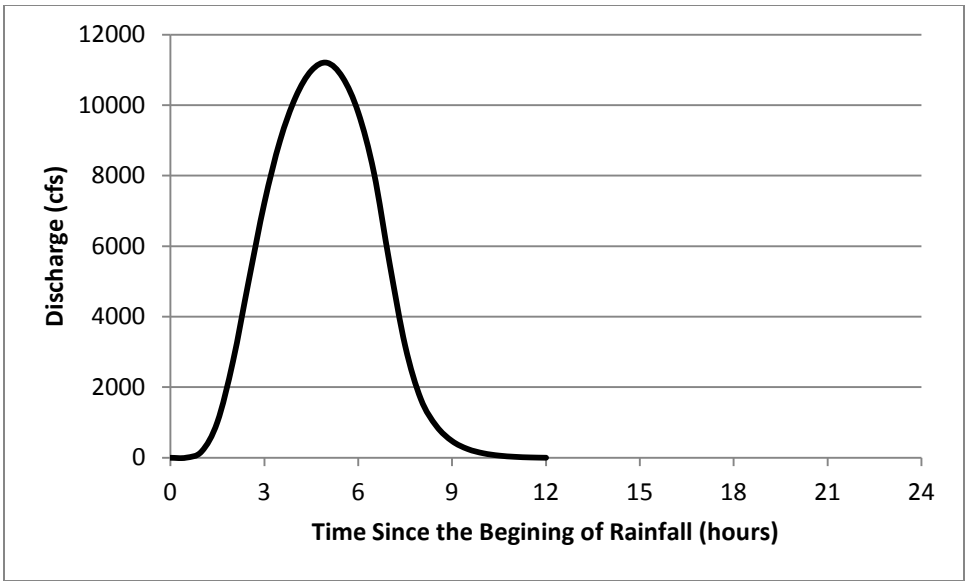

Figure 3-37 Hydrograph for the 100 year flood in the Moanalua Stream generated using the HEC-HMS composite model and 6 hour NOAA Atlas 14 rainfall distribution

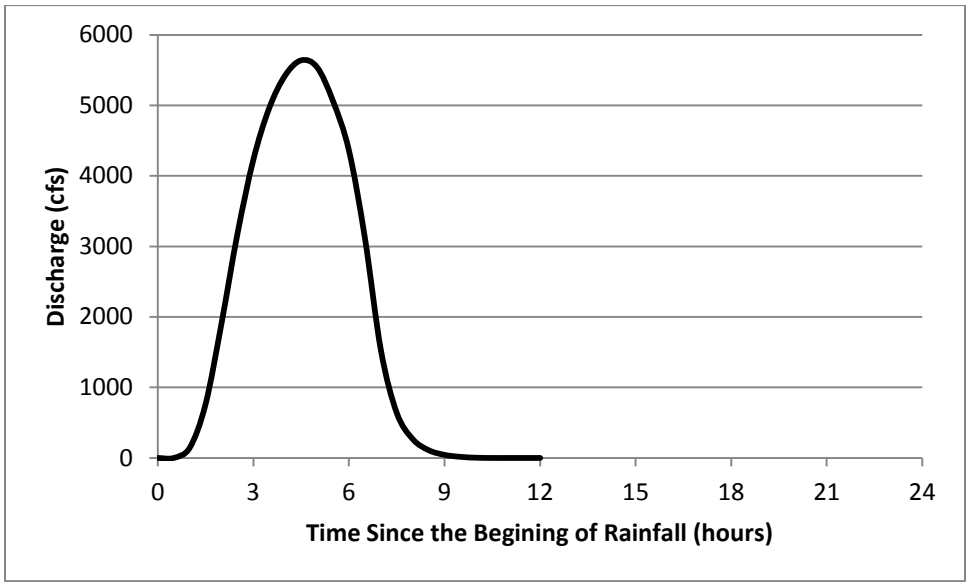

Figure 3-38 Hydrograph for the 100 year flood in the Waiahole Stream generated using the HEC-HMS composite model and 6 hour NOAA Atlas 14 rainfall distribution

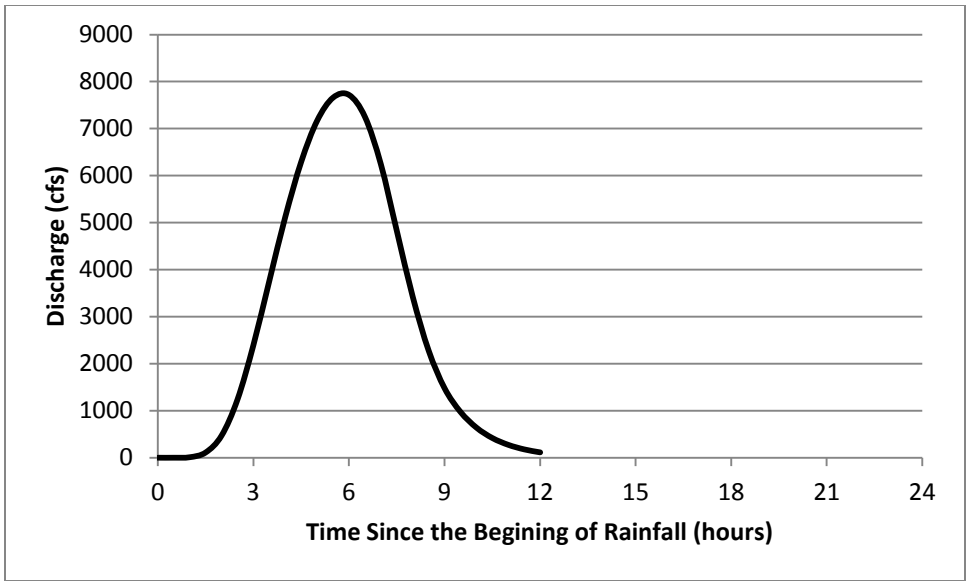

Figure 3-39 Hydrograph for the 100 year flood in the West Loch Stream generated using the HEC-HMS composite model and 6 hour NOAA Atlas 14 rainfall distribution

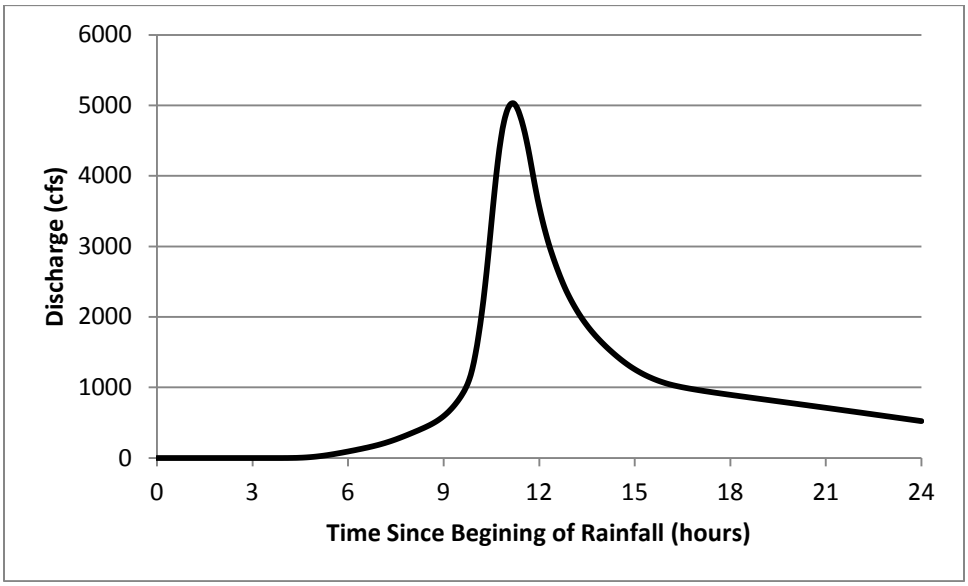

Figure 3-40 Hydrograph for the 100 year flood in the Kaoli Ditch generated using the HEC-HMS composite model and 24 hour Type 1 rainfall distribution

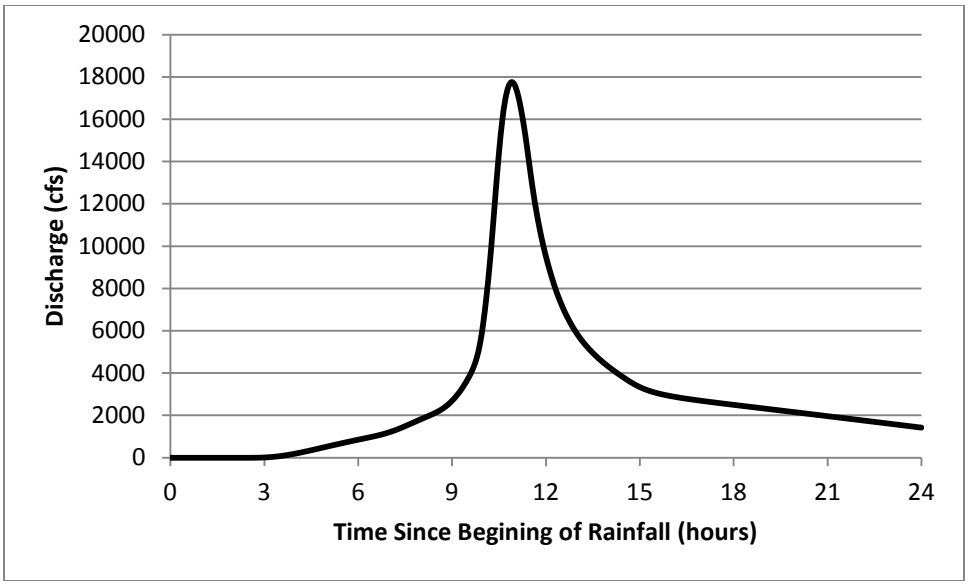

Figure 3-41 Hydrograph for the 100 year flood in the Halawa Stream generated using the HEC-HMS composite model and 24 hour Type 1 rainfall distribution

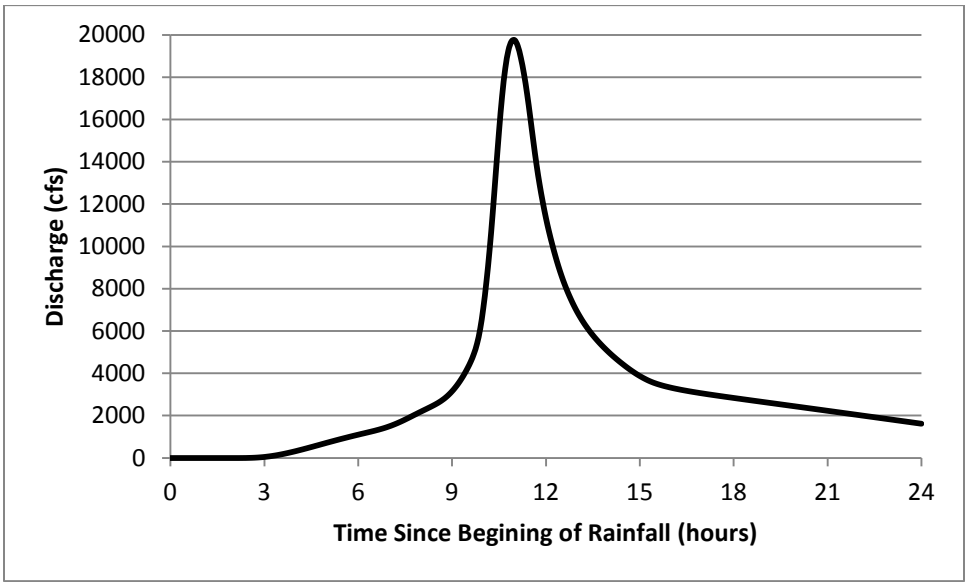

Figure 3-42 Hydrograph for the 100 year flood in the Moanalua Stream generated using the HEC-HMS composite model and 24 hour Type 1 rainfall distribution

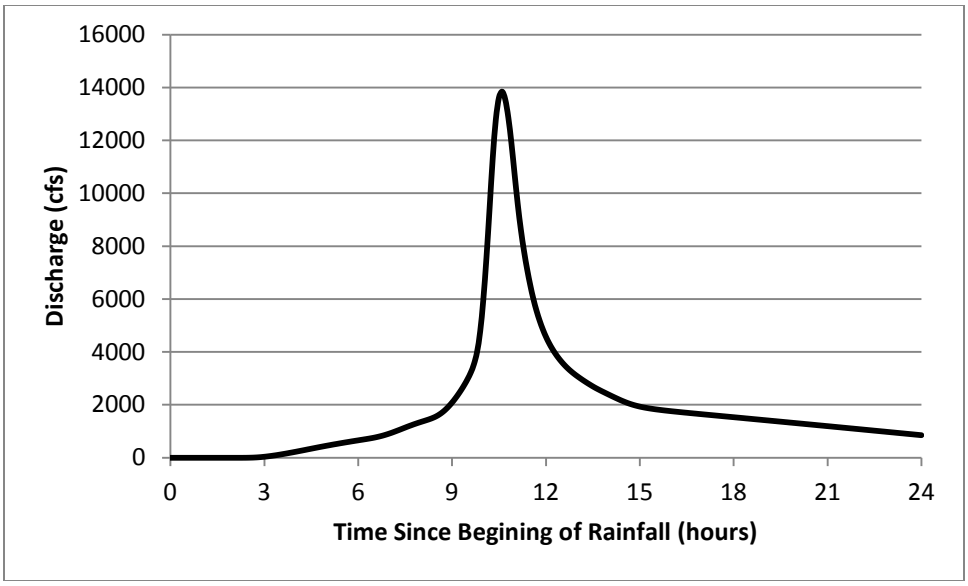

Figure 3-43 Hydrograph for the 100 year flood in the Waiahole Stream generated using the HEC-HMS composite model and 24 hour Type 1 rainfall distribution

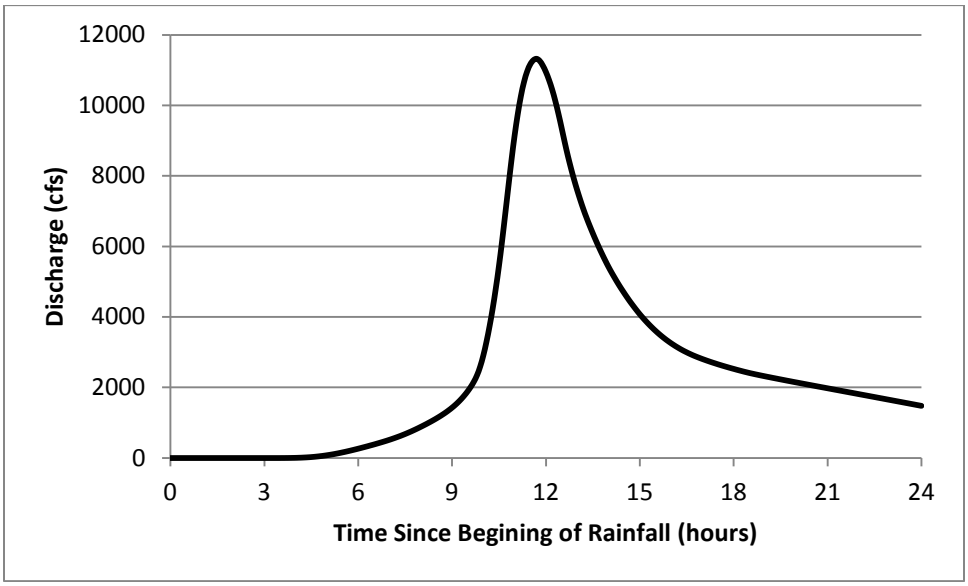

Figure 3-44 Hydrograph for the 100 year flood in the West Loch Stream generated using the HEC-HMS composite model and 24 hour Type 1 rainfall distribution

3.3.3 Comparison of the 100 Year Flood Predictions for the Ungaged Watersheds

The predicted 100 year discharge for both the USGS regional regression equations and the HEC-HMS composite model in all five ungaged watersheds are shown in Table 3-18. The results for the Halawa Stream, Moanalua Stream and West Loch Stream show very good agreement between the two methods. The respective HEC-HMS

model for Kaoli Ditch and Waiahole Stream predicts significantly lower than the corresponding USGS regional regression equations. Some of the discrepancy may be caused because the curve numbers used in the HEC-HMS model could not be validated and therefore may not accurately represent the respective watersheds. The rainfall distribution and duration in the HEC-HMS model may also account for a portion of this disparity. The spatial distribution of meterologic data for the Kaoli Ditch and Waiahole watershed models are both dominated by a single rain gage, with only a small contribution from other nearby rain gages. This may not accurately represent the rainfall gradient that exists in these watersheds. The discrepancy in 100 year peak flow predictions may also be caused by the USGS regional regression equation not adequately representing the conditions in the watershed. The USGS regional regression equations do not account for a significant number of variables that affect runoff that are included in HEC-HMS.

Table 3-18 Comparison of predicted 100 year discharge for ungaged watersheds

Stream	USGS Equation 100 Year Peak Flow (cfs)	HEC-HMS 100 Year Flow – 6 hour rainfall (cfs)	HEC-HMS 100 Year Flow – 24 hour rainfall (cfs)
Kaoli Ditch	4565	2764	5026
Halawa Stream	9840	9993	17759
Moanalua Stream	10311	11202	19747
Waiahole Stream	8454	5640	13842
West Loch Stream	8260	7714	11325

3.4 Preliminary Recommendation for Storm Duration for the 100-Year Flood

The literature review shows that there is no consensus regarding design storm duration for either rainfall of flood events. Certain regions are prone to long sustained storms, whereas others experience short and intense events. The rain gage analysis performed for the island of Oahu described in Table 3-2 shows that typical large rainfall events last between 3 and 13 hours.

The design scour event is based on the 100 year flood, not the 100 year rainfall. It is assumed that the 100 year rainfall will induce the 100 year flood, but this assumption is not always valid. Degree of soil saturation and debris blocking drainage pathways are two examples of conditions that can cause a relatively small rain event to induce a larger than expected flood. However these conditions cannot be predicted, therefore it is assumed that the 100 year rain event will induce the 100 year flood.

The duration of rainfall utilized to develop a design hydrograph with HEC-HMS in this study is 6 hours. This is approximately the average duration of rainfall of high intensity rainfall events on Oahu. The 6 hour duration rainfall also generates a peak flow that is consistent with the flow predicted through direct statistical analysis of the stream record in the Manoa-Palolo watershed. Future watershed analysis should include multiple hydrologic methods to predict the peak flow rate for a given drainage basin. The duration should be varied when the hydrologic method does not specify rainfall duration to determine the rainfall that will predict the peak flow rate for the design frequency flood event.

In this study, several different flood durations and hydrograph shapes will be investigated, including their effect on scour depth. Recorded hydrographs, hydrographs generated from HEC-HMS, triangular hydrographs and rectangular hydrographs will be analyzed. The sensitivity of the scour depth to hydrograph duration and shape may vary significantly based on streambed soil type. Non-cohesive soils have a high initial erosion rate and are likely to reach a depth close to maximum scour depth relatively quickly. Cohesive soils develop scour much slower than non-cohesive soils, so the shape and duration of the hydrograph are likely to have a much more significant impact on scour depth. A finalized recommendation of design hydrograph shape and duration will be made in Chapter 5 following an analysis of final scour depth in different soil types.

CHAPTER 4 FIELD AND LABORATORY STUDY OF SOIL PROPERTIES

Streambed soil properties are another critical input for scour prediction including the soil particle size distribution and erosion rate curve. The two bridges that are included in this study are the Kaelepulu Bridge and the Manoa-Palolo Bridge. The methods, procedure and results of field and laboratory study of the soil properties at these two sites are presented in the following sections in this chapter.

4.1. Field Sampling

Site investigation and field sampling was required to obtain soil properties from the sites where scour predictions will be evaluated. A sieve analysis is required to determine the median grain size (D_{50}) for the HEC-18 method. A Shelby tube sample is required to generate an EFA curve for the SRICOS-EFA method. The sampling at the Kaelepulu and Manoa-Palolo sites are described in the following sections.

4.1.1 Kaelepulu Field Sampling

The Kaelepulu stream at Kawailoa Rd is directly adjacent to the Kailua Beach Park. The stream bed soil is homogeneous beach sand. The stream experiences periodic sand plugging at the outlet due to tidal effects. This sand plugging prevents the Kaelepulu stream from draining to Kailua Bay at low flows when the outlet is plugged. A picture of the Kaelepulu Bridge is shown in Figure 4-1.

Figure 4-1 Kaelepulu Bridge, Kailua, HI

A Shelby tube was collected from the embankment next to the stream. The soil is relative homogeneous non-cohesive sand, and so traditional Shelby tube collection was not possible as the sample would fall from the tube as the tube was removed from the soil. The tube was pushed into the soil by hand as far as possible. A sledge hammer was utilized to drive the Shelby tube to full depth once the friction became too great to push the Shelby tube by hand. The soil around the Shelby tube was excavated, the bottom end of the Shelby tube was covered and the tube was removed by hand. Both ends were capped and the sample was returned to the lab.

4.1.2 Manoa-Palolo Field Sampling

The Manoa-Palolo Stream at the Kapiolani off-ramp from the H-1 freeway has highly heterogeneous non-cohesive soil. The soil surrounding the pier is coarse sand with gravel and cobbles. Fine non-cohesive soil exists in the stream and has vegetation growing. The fine soil is far enough away from the pier that it is unlikely to have a significant impact on scour depth. All soil samples from the location are coarse grained. The Manoa-Palolo Bridge is pictured in Figure 4-2, and the soil surrounding the pier of interest is shown in Figure 4-3. The construction plans for the bridge were obtained from the Hawaii Department of Transportation. The boring log for the Manoa-Palolo Bridge section is shown in Figure 4-4.

Figure 4-2 Manoa-Palolo Bridge, Honolulu, HI

Figure 4-3 Coarse sand with gravel and cobbles in the streambed of the Manoa-Palolo Stream

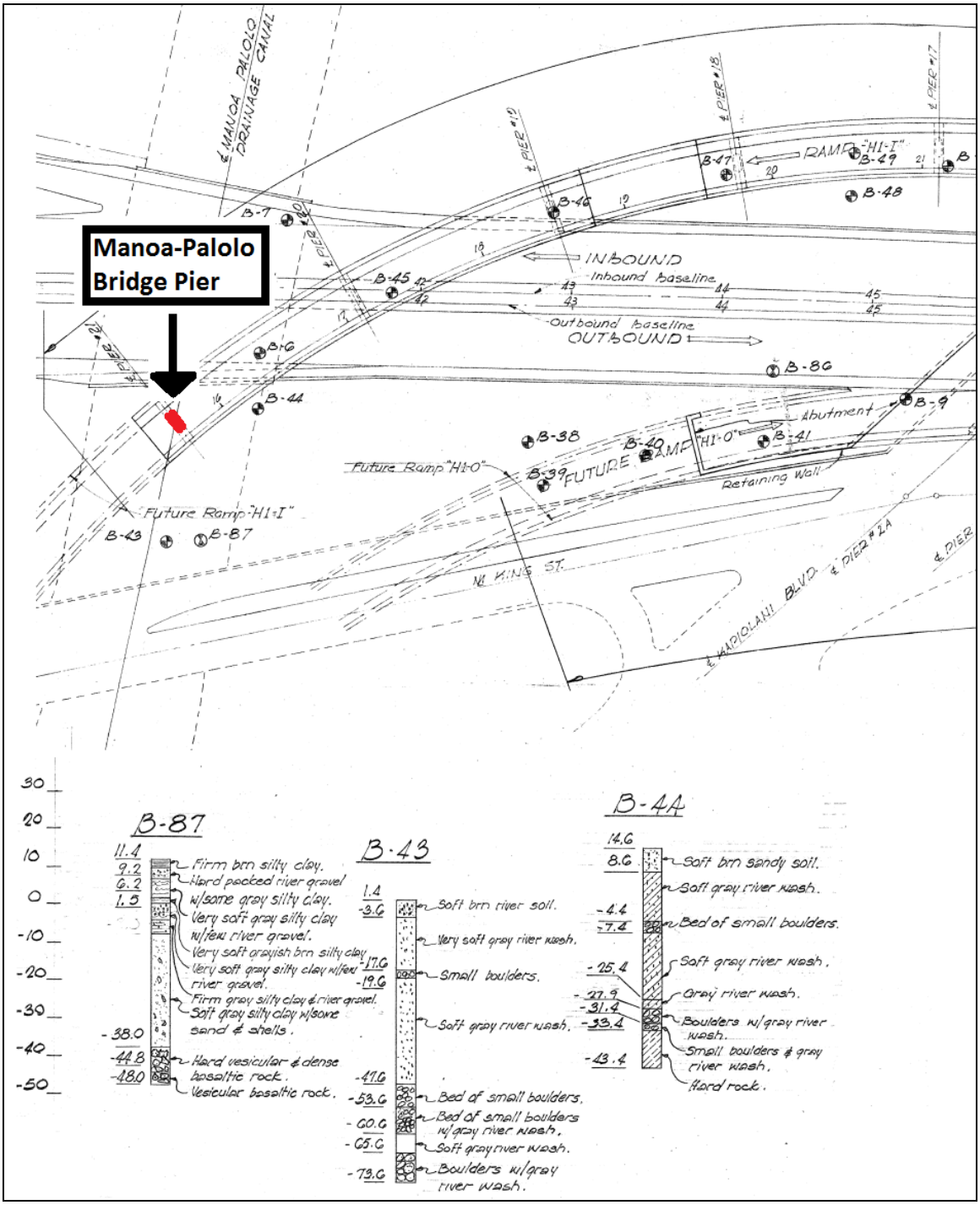

Figure 4-4 Boring logs from as-built plans of the Manoa-Palolo Bridge Pier, completed in 1965 by the Hawaii Department of Transportation

Soil was collected from the stream bed using a shovel for excavation. The soil was dried and analyzed using a sieve analysis. A sand-cone test to determine in-situ

density was completed on soil of the same layer as surrounding the pier, but above the stage of the stream.

The non-cohesive soil condition at the site prevented a Shelby tube from being collected using traditional methods. Therefore two different methods to obtain a Shelby tube that was representative of in-situ conditions were utilized. The dried soil collected for the sieve analysis was compacted into a Shelby tube in the lab to the in-situ density determined by the sand-cone test. The Shelby tube with the compacted soil was saturated and used to develop an EFA curve. A second Shelby tube was pushed into the soil to collect a sample through more direct means. The high friction of the soil prevented the tube from being pushed by hand for more than a few inches. A sledge hammer was used to drive the Shelby tube further into the soil. Numerous attempts were made to collect a sample, but the Shelby tube continued to encounter cobbles that prevented it from being driven to a sufficient depth to develop an EFA curve. The Shelby tube extraction was attempted at different locations surrounding the pier, as well as upstream and downstream in the same soil layer all with the same difficulties with cobbles. Once a location where the Shelby tube could be driven to a sufficient depth, the Shelby tube was extracted by shoveling the soil around the tube, covering the bottom of the tube, removing the sample by hand and capping both ends.

4.2 Lab Experiments to Determine Soil Particle Size Distribution

Soil samples were collected from both the stream bed and the stream bank at the Kaelepulu stream site. Soil was collected using a shovel and returned to the lab for analysis. The median grain size was 0.35 mm for the stream bed sample and 0.31 mm for the stream bank sample. It is of note that Masaki (2004) determined the median grain size to be 0.19 mm. The results of all three sieve analyses are shown in Figure 4-5. The difference in median grain size between the samples are likely the result of natural changes in the stream bed sediments caused by floods and tides over the 8 years between samples.

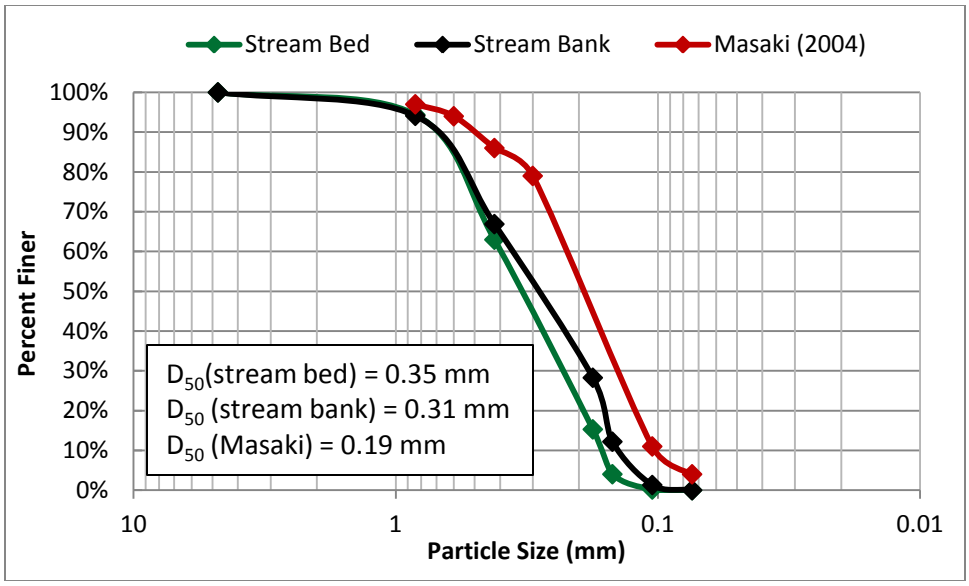

Figure 4-5 Grain size distribution for the Kaelepulu Stream

Soil was collected from the Manoa-Palolo Stream near the pier of interest using a shovel and bucket as described above. The soil was dried, and then a standard sieve analysis was conducted. The cobbles were excluded from the sieve analysis because a sieve analysis is typically conducted with about 0.5 kg of soil, and even a single cobble may represent an unrealistically large fraction of the sample. This may result in a median grain size that is slightly lower than field conditions, however fine non-cohesive grains erode more rapidly than the coarse grains, so this underestimation of median grain size is conservative. The median grain size for the Manoa-Palolo Stream was calculated to be 1.60 mm. The results of the sieve analysis are shown in Figure 4-6.

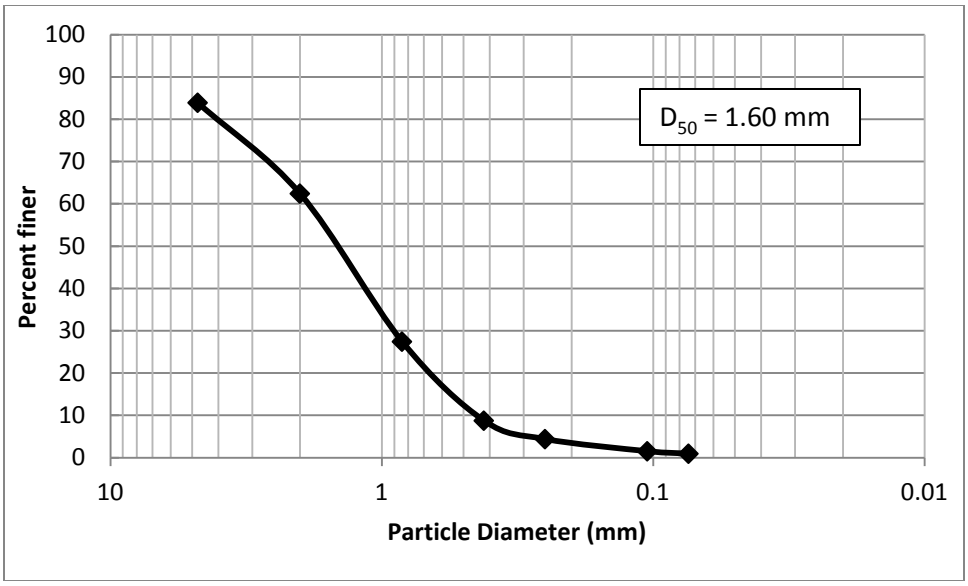

Figure 4-6 Grain size distribution for the Manoa-Palolo Stream

4.3. Lab Experiments to Determine Erosion Rate (EFA Curve)

An erosion function apparatus (EFA) is a critical piece of lab equipment for the SRICOS-EFA method. The EFA uses Shelby tubes collected from the location of interest, allowing in-situ conditions to be measured. An EFA allows the researcher to measure the erodability of the soil in relation to the shear stress applied to the soil. Details of the EFA and testing procedures will be discussed in the following sections.

4.3.1. The EFA Apparatus

An EFA consists of a horizontal rectangular conduit that has a circular hole in the bottom to allow a Shelby tube to be inserted. The conduit also has a viewing window around the area where a Shelby tube is inserted so the erosion can be monitored. A piston is located below the soil sample so that it can push the soil into the conduit. The flow in the conduit is controlled by a valve opening and closing, and the flow is measured by a velocimeter in a vertical PVC pipe downstream of the section where the soil erosion is monitored. A tank is attached to provide water to be pumped through the conduit, as well as a discharge point for water and eroded sediments after being pumped through the test section. This tank also has a sump pump to allow the water to be changed when the water

becomes too opaque with sediments, preventing the researcher from seeing the sample being eroded. A computer is attached to the EFA to allow for the recording of velocity and the amount of soil that has been pushed into the flow. A picture of an EFA is shown in Figure 4-7. For a complete description of the EFA components see Briaud et al. (1999).

Figure 4-7 Erosion function apparatus (EFA) (Briaud et al, 1999)

4.3.2. Measurement Procedure

The EFA measurement procedure requires an experienced. The Shelby tube must be loaded into the EFA with the soil sample flush with the bottom of the horizontal conduit. The flow can be initialized when the sample is in place, and when the velocity has stabilized at the desired quantity the test may begin.

The researcher shall protrude the sample 1 mm into the flow and start a timer. When the soil that is in the flow erodes, another millimeter shall be protruded into the conduit. In the case that the soil does not erode evenly across the surface, the researcher must use judgment as to when the sample should be raised by 1 mm. The front edge of the soil sample often erodes more rapidly than the rear edge, so one criteria to determine

when to raise the sample is to maintain an average height of 1 mm across the sample. This process shall continue until either 5 cm have been eroded, or 1 hour has elapsed. Once this procedure has concluded, the velocity is increased and the process repeated. The number of steps required varies based on soil characteristics, but a sufficient number of velocity steps to capture the shape of the erosion curve are required. For stiff clay, this may be as many as 8 steps ranging in velocity from 0.3 m/s to 6 m/s. For fine sand, the soil erodes too rapidly to be measured at higher velocities, so the curve may have to be defined with only 3 or 4 points.

After all measurements have been completed, an EFA curve can be constructed. Shear stress on the soil is calculated from the velocity in the conduit and erosion rate is calculated by dividing the amount of soil eroded at each velocity step by the duration of the velocity step. For additional details, see the EFA measurement procedure on constructing an EFA curve, see Briaud et al. (2004).

4.3.3. EFA Curve Results and Discussions

The friction between the Shelby tube and the sandy, non-cohesive soil is significantly greater than when clay-type soil is studied. This increase in friction created problems when trying to extract the soil sample from the Shelby tube using the piston that pushes the soil into the horizontal conduit of the EFA. Rather than pushing the soil into the conduit, the piston pushed the entire Shelby tube upwards and out of the clamp that holds the bottom of the Shelby tube in place. This problem occurred with soil from both locations. The problem was avoided by reducing the length of sample in the Shelby tube. Rather than a full 18 inch sample as recommended, a shorter sample of approximately 6-8 inches that could more easily be pushed by the piston was studied.

The Kaelepulu stream is characterized by an EFA curve generated from a Shelby tube driven into the bank of the stream bed. The soil in the bank was of the same type and had similar median grain size as adjacent to the pier structure, so this was assumed to be acceptable. The soil around the Shelby tube was excavated to allow the Shelby tube to be removed by hand. This was necessary because the site is non-cohesive and the sample

would fall out of the tube if it was removed using typical techniques. The EFA curve from Kaelepulu soil can be seen in Figure 4-8.

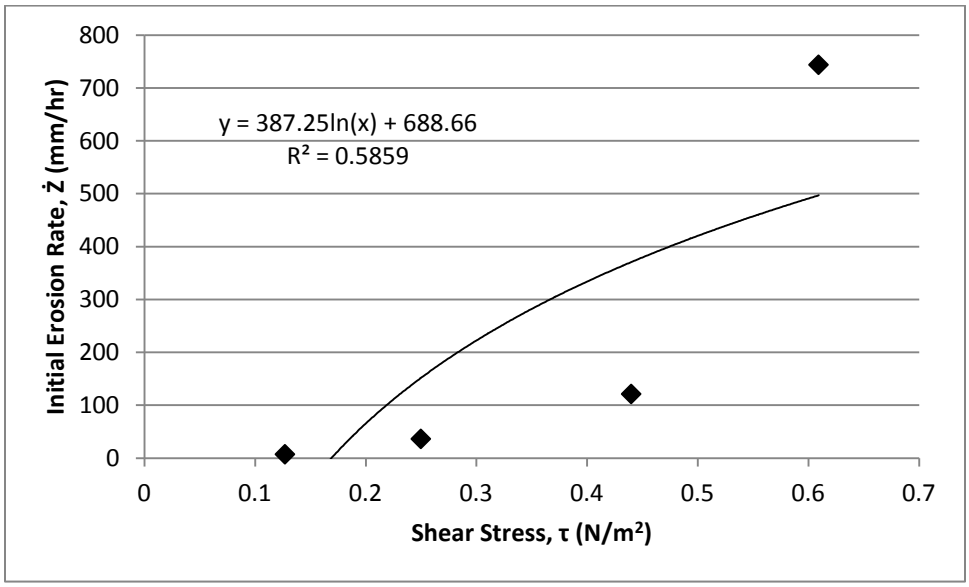

Figure 4-8 EFA curve for Kaelepulu from in-situ stream bank sample

Two different EFA curves were completed for the Manoa-Palolo location. The first was completed by collecting soil from the site in buckets and compacting the soil in the lab to the in-situ density. This lab compacted sample was collected from the soil directly adjacent to the downstream face of the pier of interest. The EFA curve for the lab compacted sample is shown in Figure 4-9. The second sample was obtained by driving a Shelby tube into the stream bed using a sledge hammer. Large gravel and cobbles prevented a Shelby tube from being driven to a sufficient depth adjacent to the pier, therefore the sample was collected approximately 150 feet upstream assuming the soil is of the same type. The EFA curve for the driven Shelby tube is shown in Figure 4-10. A typical EFA curve shows initial erosion rate increasing with shear stress. The Manoa-Palolo soil sample does not show this trend with all the data points. The soil is highly heterogeneous and includes gravel with the coarse sand. The gravel requires a longer duration to erode than sand and was non-uniformly present in the Shelby tube sample. This high degree of heterogeneity in the soil sample is likely the cause for the reduced

initial erosion rate with increased shear stress observed in some of the data points on the EFA curves.

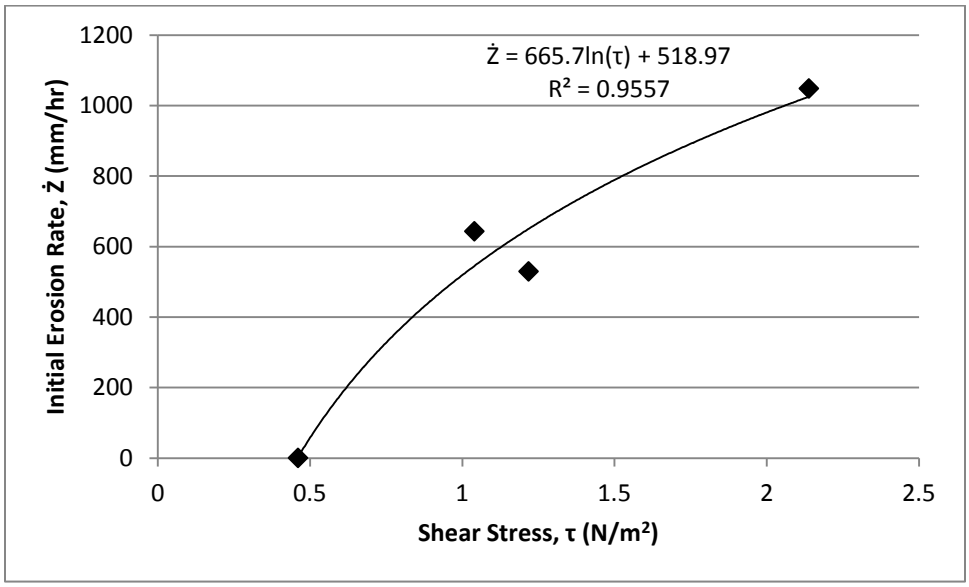

Figure 4-9 EFA curve for Manoa-Palolo from sample compacted in lab

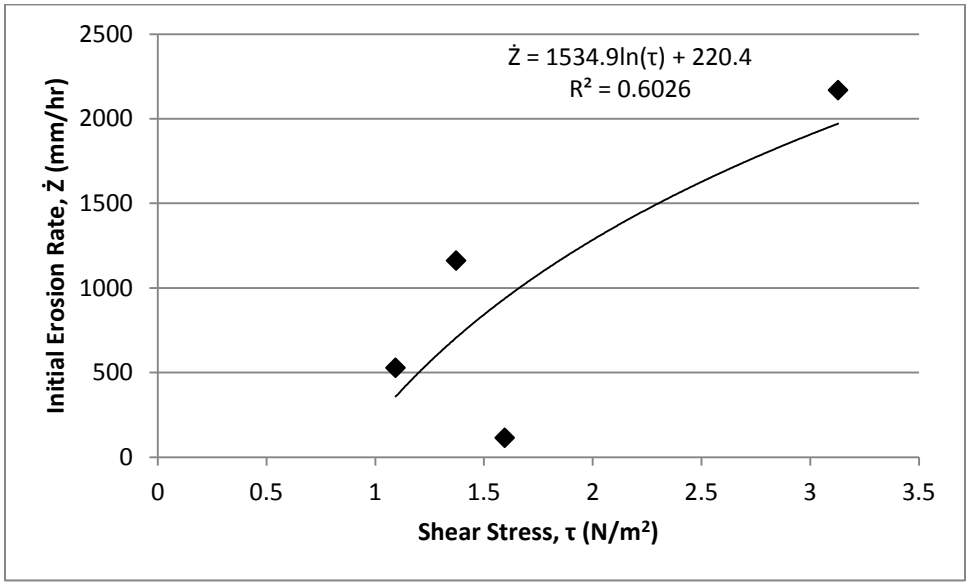

Figure 4-10 EFA curve for Manoa-Palolo from sample driven into streambed

Briaud et al. (2011) generated a graph of shear stress and erodibility for different classifications of soil, shown in Figure 4-11. This graph can be used either to estimate

erosion rate for a given classification of soil, or to verify that the EFA test completed is comparable to other similar soil types. The maximum shear stress and corresponding initial erosion rate for the January 2nd, 2004 flood of the Kaelepulu stream classify the soil as a High Erodibility II soil, which is consistent with the observed soil type. The maximum shear stress and initial erosion rate for Manoa-Palolo 100 year flood classify both EFA samples as Medium Erodibility III. These points are plotted on the erosion categories plot in Figure 4-12. The respective classification of all three EFA curves serves as validation of the collection and testing procedures. Therefore it can be assumed the EFA curves used to calculate scour are reasonable estimates and that atypical sampling procedures will not have a significant effect on initial erosion rate calculation in the SRICOS-EFA method.

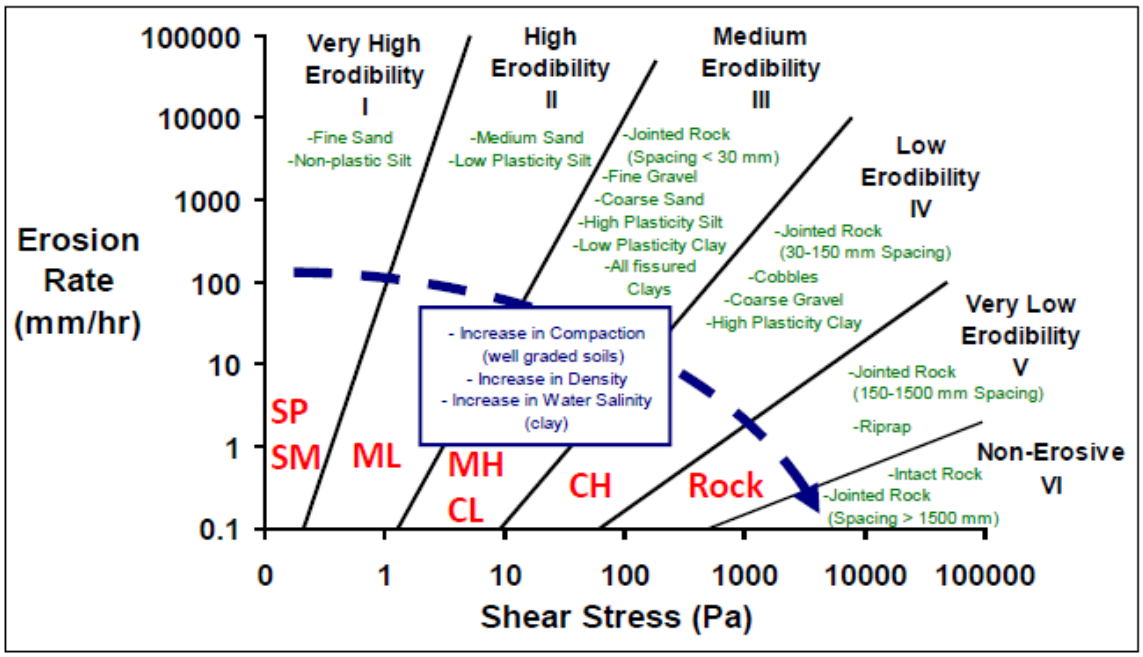

Figure 4-11 Erosion categories for soils and rocks (Briaud et al, 2011)

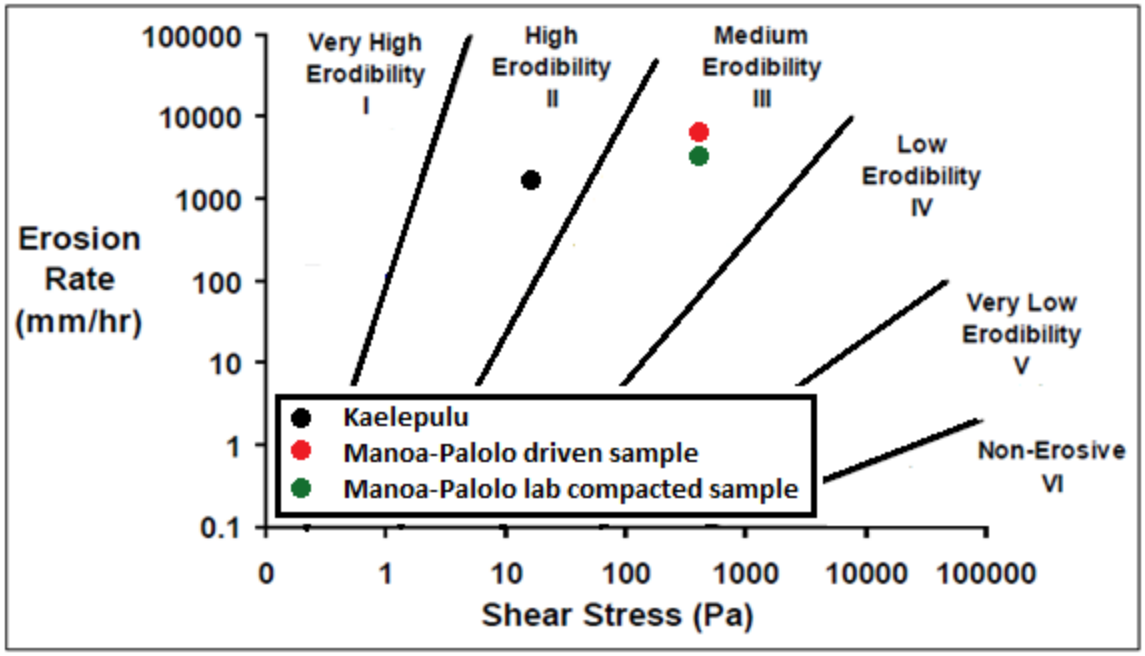

Figure 4-12 EFA curves plotted on erosion categories

Errors in the generation of an EFA curve are difficult to quantify. Collecting samples using a sledge hammer rather than pushing with a drill rig causes disturbance of the soil sample. Testing only the top layer of soil may not accurately represent the soil conditions to the full depth of scour. Errors may also occur in the EFA testing process. The decision of when to push a sample higher into the flow because a sample is highly heterogeneous is based on engineering judgment. The velocity in the EFA is not carefully controlled, and this variation in velocity may not be captured by an average velocity over the time that erosion is measured. However all these potential sources of error should not discredit the EFA results, as the erosion categories proposed by Briaud et al. (2011) are consistent with the observed in-situ soil conditions, shear stress and measured erosion rate.

CHAPTER 5 SCOUR PREDICTION RESULTS AND ANALYSIS

Both the existing HEC-18 method and the relatively new SRICOS-EFA method are applied to predict scour for the Kaelepulu Bridge and Manoa-Palolo Bridge on Oahu, Hawaii. The objective is to compare the predicted results between the two methods and also with the field data on scour depth for the Kaelepulu Stream in order to evaluate and validate the two methods. In addition, this study will analyze the effects of soil type, flood duration, hydrograph shape, and accuracy of velocity measurement on scour prediction. The results may help us to achieve a better understanding of bridge scour, an understanding of the accuracy of each scour prediction method, and which factors have a large effect on predicted scour depth.

5.1 Scour Prediction for Kaelepulu Bridge

The Kaelepulu Bridge was selected for this study because a scour event was recorded during a flood on January 2nd, 2004. This field measurement enables the evaluation and validation of the two different methods by comparing the predicted scour depth with the recorded scour depth.

5.1.1 The January 2004 Flood Event at Kaelepulu Bridge

A sliding magnetic collar type scour monitoring device was placed at a center pier of the Kaelepulu Bridge in 2003. On January 2nd, 2004 a scour event was recorded, with a total scour depth of 1 ft. The device has an accuracy of +/- 6 inches. The rainfall was recorded by a rain gage station near the Kaelepulu stream drainage area. The rainfall was converted to the hydrograph at the bridge using the Muskingum routing method (Masaki, 2004). This hydrograph and recorded pier scour elevation can be seen in Figure 5-1. This event is critical to the validation of the scour prediction methods as it is the only scour event recorded in real time in the state of Hawaii available for use in this study.

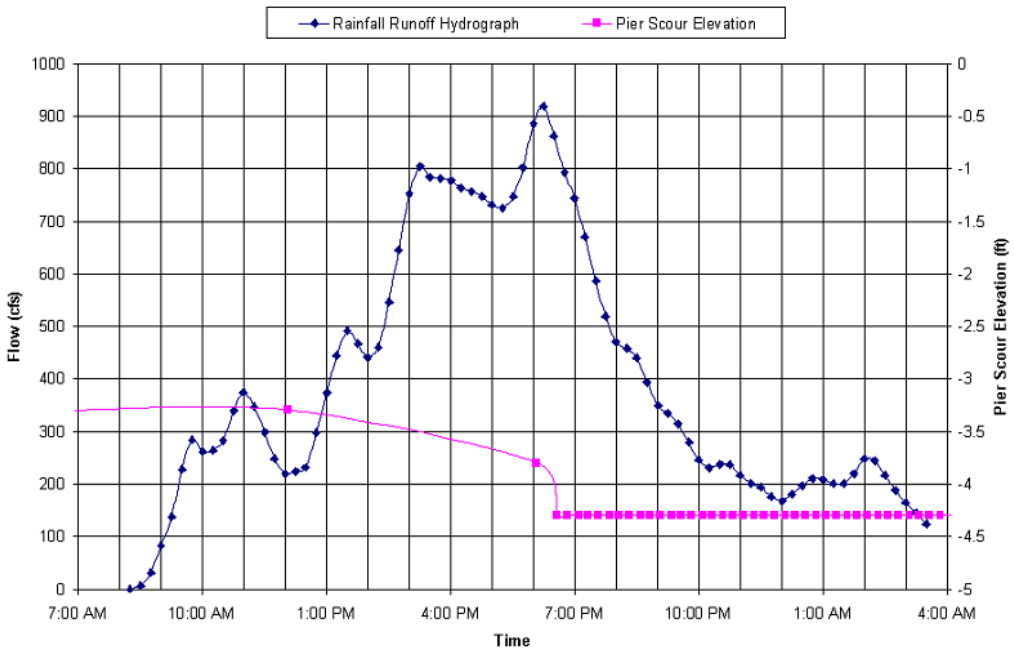

Figure 5-1 Recorded hydrograph and pier scour elevation for January 2nd, 2004 Kaelepulu Stream scour event (Masaki, 2004)

5.1.2 Predicted Scour Depth by HEC-18

Masaki (2004) used the HEC-RAS software and the peak stream flow from January 2nd, 2004 to compare the recorded scour with the depth predicted by the HEC-18 method. A HEC-RAS model was constructed from a site survey and historic bridge plans. Sieve analysis was utilized to obtain a median grain size required for the HEC-18 procedure. The peak flow rate was obtained from the hydrograph in Figure 5-1. The HEC-RAS software was utilized and the HEC-18 method predicted a scour depth of 11.03 ft.

5.1.3 Predicted Scour Depth by SRICOS-EFA

Nakamura (2010) used the recorded scour event to compare the accuracy of the SRICOS-EFA method with the recorded scour depth. The in-situ soil is non-cohesive, so the median grain size is believed to be the controlling parameter for scour development. Three different EFA curves were obtained from literature all of which had a relatively similar median grain size to the in-situ soil. The calculation was also simplified by

splitting the hydrograph into three flood events, each with a rectangular shape and constant flow rate. These three floods were considered a close approximation of the hydrograph shown in Figure 5-1. Nakamura (2010) predicted the following scour depths: 0.03 ft with silty clay D_{50}=0.03 mm; 4.89 ft with sand D_{50}=4.89 mm; 0.896 ft with fine sand D_{50}=0.13 mm.

The EFA curve generated from in-situ soil described in section 4.3.3 and shown in Figure 4-8 was also utilized to make a scour depth prediction using the SRICOS-EFA method. The hydrograph was split into 15 minute time steps generating 78 different flood events. This is the smallest time step that can be analyzed, as the rainfall data used in the Muskingum routing method to generate the hydrograph was collected at a 15 minute time interval. A scour depth of 4.20 feet was predicted using the EFA curve generated from in-situ soil and a hydrograph with 15 minute time intervals.

5.1.4 Comparison and Evaluation of the Kaelepulu Bridge Scour Predictions

The scour predictions for the Kaelepulu Bridge using all methods are summarized in Table 5-1. The HEC-18 method is a significant over prediction of the recorded scour depth. The only SRICOS-EFA method that results in a significant under prediction is generated from a soil with significantly different soil properties than the in situ soil and is likely not an accurate prediction for the site. The other SRICOS-EFA predictions are more reasonable predictions relative to the HEC-18 predicted scour depth.

Table 5-1 Comparison of all scour prediction for the January 2nd, 2004 flood of the Kaelepulu stream

	D_{50} (mm)	Scour Depth (ft)
Recorded scour depth (+/- 6 inch accuracy)		1 ft
HEC-18 method (Masaki, 2004)	0.19	11.03 ft
SRICOS-EFA method – silty clay (Nakamura, 2010)	0.01	0.03 ft
SRICOS-EFA method – sand (Nakamura, 2010)	0.3	4.89 ft
SRICOS-EFA method – fine sand (Nakamura, 2010)	0.13	0.896 ft
SRICOS-EFA method – in-situ soil: stream bank	0.31	4.20 ft

5.2 Scour Prediction for Manoa-Palolo Bridge

The Manoa-Palolo Bridge was used as a case study to make predictions for the 100 year scour depth without the benefit of recorded scour data. A HEC-RAS file of the entire Ala Wai watershed was obtained from Mr. Simon Li (Oceanit, 2008). The file was localized to only include the section of the Manoa-Palolo stream that contained the bridge of interest, with sufficient upstream and downstream reaches. Cross sections were added upstream and downstream of the Manoa-Palolo Bridge pier. The geometry of the bridge pier was added to the HEC-RAS file from bridge plans and a site survey. The pier has a pile foundation, with the depth to pile cap approximately 10.4 feet below the streambed. The depth of the pile tip is approximately 45.4 feet below the streambed. The effects of the pile cap and pile group, should they become exposed, were not considered in this analysis. The HEC-18 scour prediction for the 100 year flood event was predicted using HEC-RAS software assuming the 100 year flow rate is equal to 12568 cfs, the flow predicted using the Log-Pearson III statistical analysis. The Log-Pearson III 100 year flow rate was selected because it is based on stream records and fit the data better than the Gumbel distribution. The cross-section including the scour hole predicted by HEC-RAS is shown in Figure 5-2, and a summary of the input data and results are shown in Figure 5-3. The HEC-18 method predicted a 100 year scour depth of 18.71 feet for the Manoa-Palolo Bridge location.

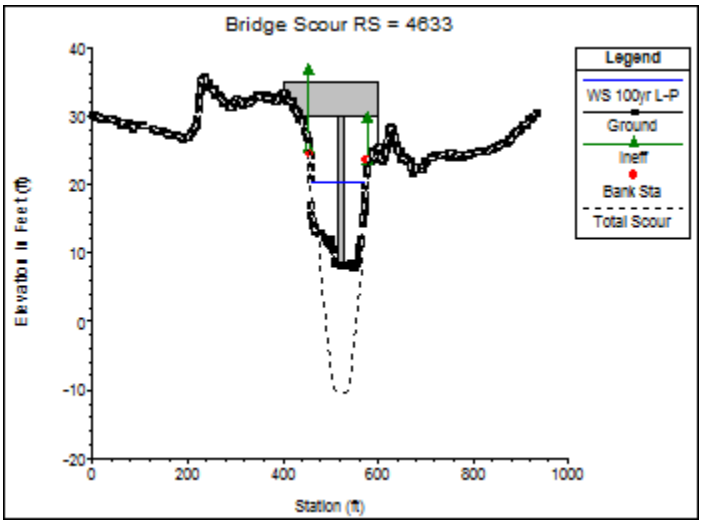

Figure 5-2 HEC-RAS bridge cross section for Manoa-Palolo with scour induced by 100 year flood

Pier Scour

All piers have the same scour depth

Input Data

Pier Shape:	Round nose
Pier Width (ft):	12.00
Grain Size D50 (mm):	1.60000
Depth Upstream (ft):	10.83
Velocity Upstream (ft/s):	9.79
K1 Nose Shape:	1.00
Pier Angle:	40.00
Pier Length (ft):	13.00
K2 Angle Coef:	0.97
K3 Bed Cond Coef:	1.10
Grain Size D90 (mm):	5.00000
K4 Armouring Coef:	1.00

Set K1 value to 1.0 because angle > 5 degrees

Results

Scour Depth Ys (ft):	18.71
Froude #:	0.52
Equation:	CSU equation

Figure 5-3 HEC-RAS output file for the Manoa-Palolo with scour induced by 100 year flood

The SRICOS-EFA method was also utilized to predict scour induced by the 100 year flood at the Manoa-Palolo Bridge location. A rectangular hydrograph with duration of 24 hours was selected as it is conservative and consistent with recommendations from the literature (Briaud et al., 2004, Ghelardi, 2004). The EFA curve utilized in this prediction was developed from a Shelby tube driven into the stream bed, shown in Figure 4-10. All geometric parameters were obtained from old bridge plans or site visits. The 100 year scour depth predicted by the SRICOS-EFA method for the Manoa-Palolo Bridge location is 19.61 feet.

The 100 year scour depth predicted by both the HEC-18 method and the SRICOS-EFA method are very close to each other. This is consistent with expectations because the soil is erodible so the time required for scour to develop is not a significant factor. It is of note that both scour predictions exceed the depth to the pile cap, classifying the Manoa-Palolo Bridge as scour critical. It is possible the scour induced by the 100 year flood will not develop to the depth predicted by either method as the pile cap is likely to armor the soil against scour. Once the depth to the pile cap is reached, the hole would need to widen to the extents of the pile cap, a minimum distance of 6 feet, before the scour hole could extend to a greater depth. If the predicted scour does develop to the full depth, the bridge pier would still be supported by the piles that extend approximately 25 feet deeper than the maximum predicted scour depth from the 100 year flood. A structural and geotechnical analysis of the soil and structure would be required to determine if the bridge could be stable and/or serviceable with an approximate 45% of the pile length above the soil surface.

5.3 Effect of Soil Property and Flood Duration on SRICOS-EFA Scour Prediction

The effect of different soil types under the same flood conditions was analyzed. The maximum scour depth as predicted by the SRICOS-EFA method is the same for all soil types, as this is a function of stream properties and bridge geometry. Theoretically all soils should scour to the same depth if given sufficient time to reach equilibrium. The Manoa-Palolo Bridge section was selected for the comparison. A rectangular hydrograph with flow rate equal to the 100 year event predicted using the Gumbel distribution was studied for all soil types. The duration of the rectangular hydrograph was varied to show the development of scour over time. In addition to the soil that is in-situ at the Manoa-Palolo site shown in Figure 4-10, the soil in-situ from the Kalepulu site shown in Figure 4-8 was also used in this comparison. Three EFA curves of different soil types from the literature were also included: high plasticity clay, sand with clay and silt, and clayey sand. The EFA curves for these soils can be seen in Figure 5-4, Figure 5-5 and Figure 5-6, respectively.

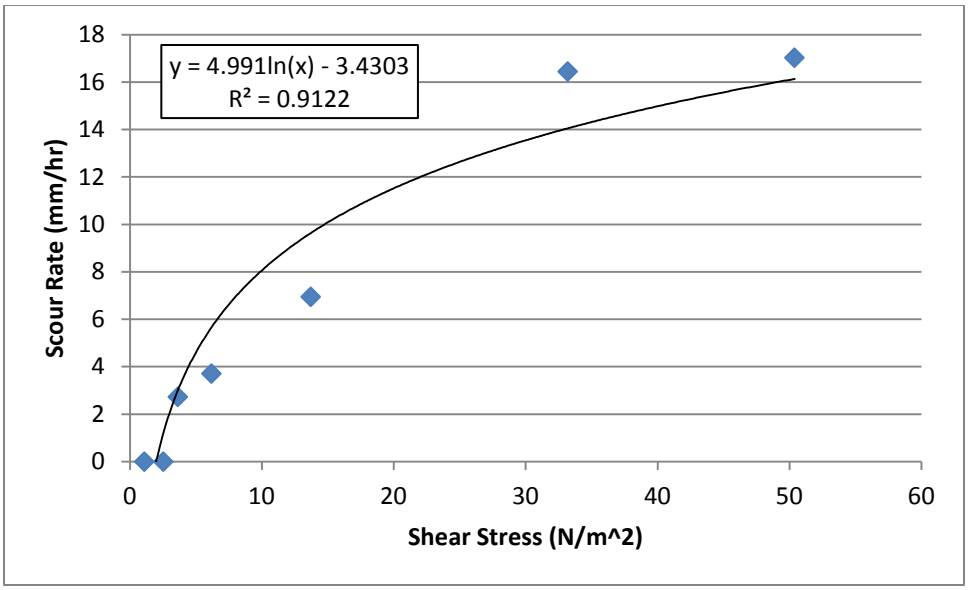

Figure 5-4 EFA curve for high plasticity clay (Kwak, 2000)

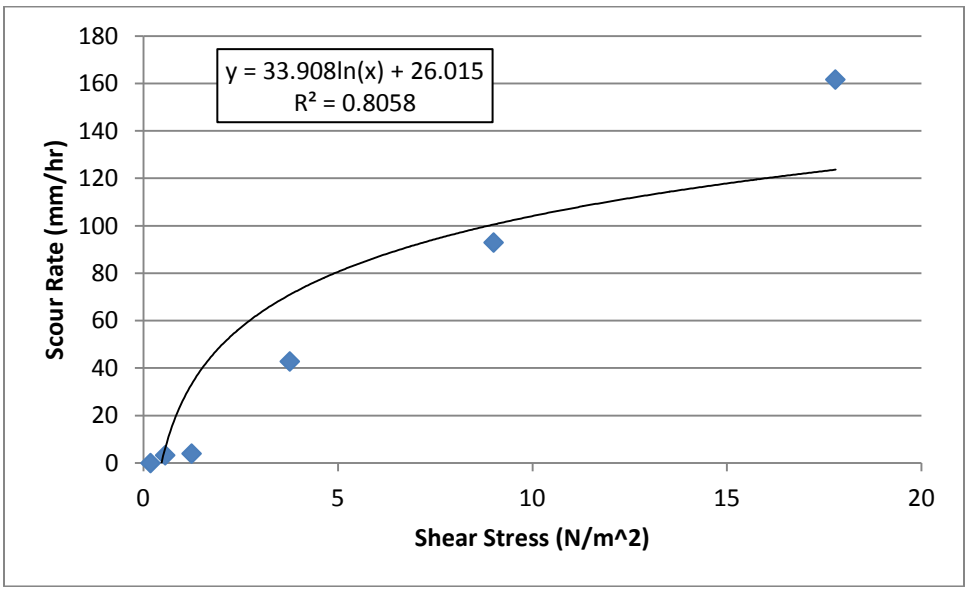

Figure 5-5 EFA curve for sand with clay and silt (Kwak, 2000)

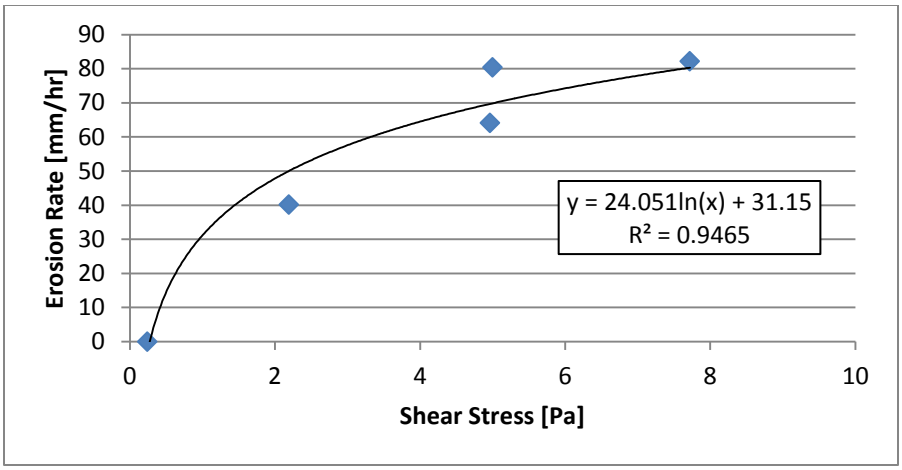

Figure 5-6 EFA curve for clayey sand (Kwak, 2000)

Figure 5-7 and Table 5-2 show the development of scour over time for the five different soil types with the Manoa-Palolo stream geometry and 100 year flow rate. It is clear that the coarser the material, the soil in-situ at both Manoa-Palolo and Kaelepulu, reach a depth close to their maximum scour depth rapidly and then do not show significant erosion. Both of the soils that include sands with some fines erode more slowly, but after 480 hours (20 days) reach nearly the same scour depth as the coarser materials. The high plasticity clay only scoured to 62% of the maximum scour depth at Manoa-Palolo after 20 days of constantly experiencing the 100 year discharge. The maximum scour depth of the high plasticity clay was reached at both the Manoa-Palolo and Kaelepulu soils in less than 4 hours. This confirms that cohesive soils are significantly more sensitive to hydrograph duration than non-cohesive materials.

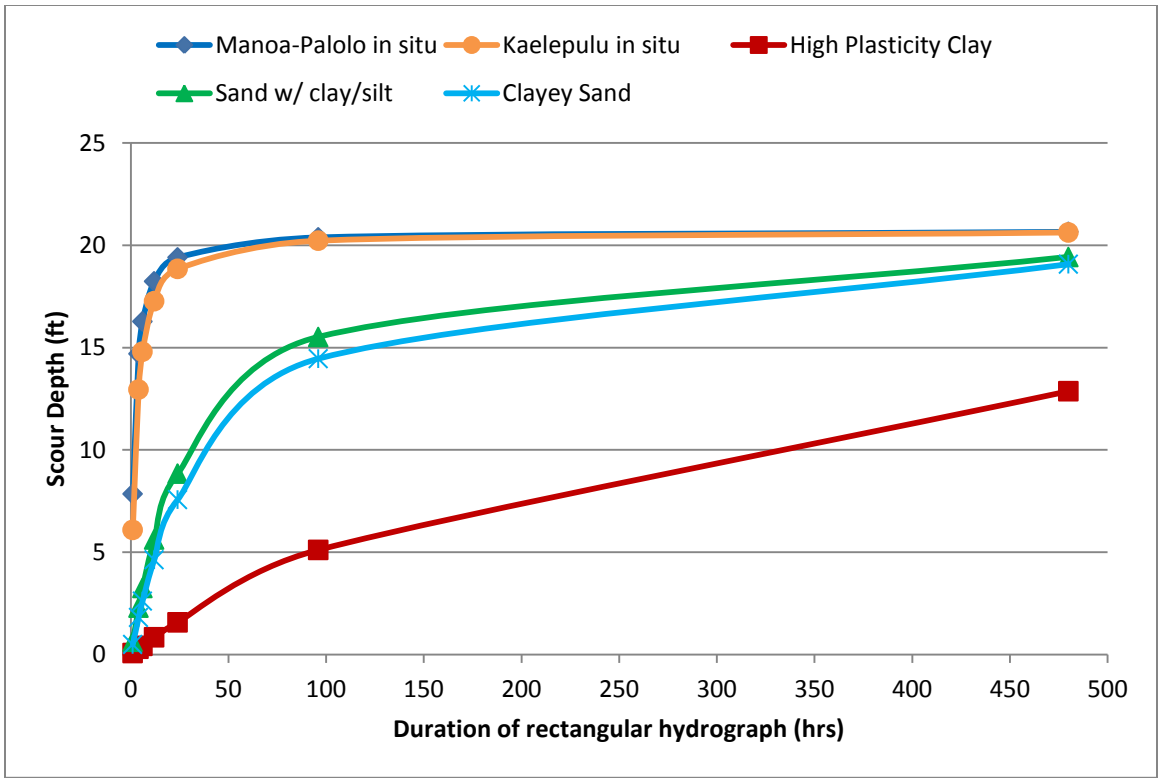

Figure 5-7 Comparison of scour development over time for different soil types with the Manoa-Palolo Bridge geometry and 100 year flow rate

Table 5-2 Scour depth (ft) variations with time and soil type

Rectangular Hydrograph Duration (hrs)	Manoa-Palolo in-situ soil	Kaelepulu in-situ	High Plasticity Clay	Sand with clay/silt	Clayey Sand
1	7.85	6.09	0.07	0.62	0.49
4	14.7	12.95	0.28	2.29	1.81
6	16.28	14.8	0.42	3.25	2.61
12	18.24	17.27	0.84	5.62	4.63
24	19.41	18.85	1.57	8.84	7.57
96	20.39	20.23	5.11	15.52	14.46
480	20.66	20.63	12.87	19.43	19.08

5.4 Effect of Hydrograph Shape and Flood Duration on Scour Prediction

The shape of a hydrograph can have a significant effect on the predicted scour depth. The Kaelepulu site was selected for this analysis. Two different soil types were tested: the in-situ soil with the EFA curve shown in Figure 4-8 and the high plasticity

clay with the EFA curve shown in Figure 5-4. The scour depth was predicted for 3 different hydrograph shapes shown in Figure 5-8: the recorded hydrograph from January 2nd, 2004 at the Kaelepulu site, a triangular hydrograph and rectangular hydrograph. The maximum flow rate and duration of all three hydrographs are the same to isolate the effect of hydrograph shape on predicted scour depth. The depth prediction for Kaelepulu in-situ soil can be seen in Figure 5-9 and the scour depth prediction for high plasticity clay can be seen in Figure 5-10.

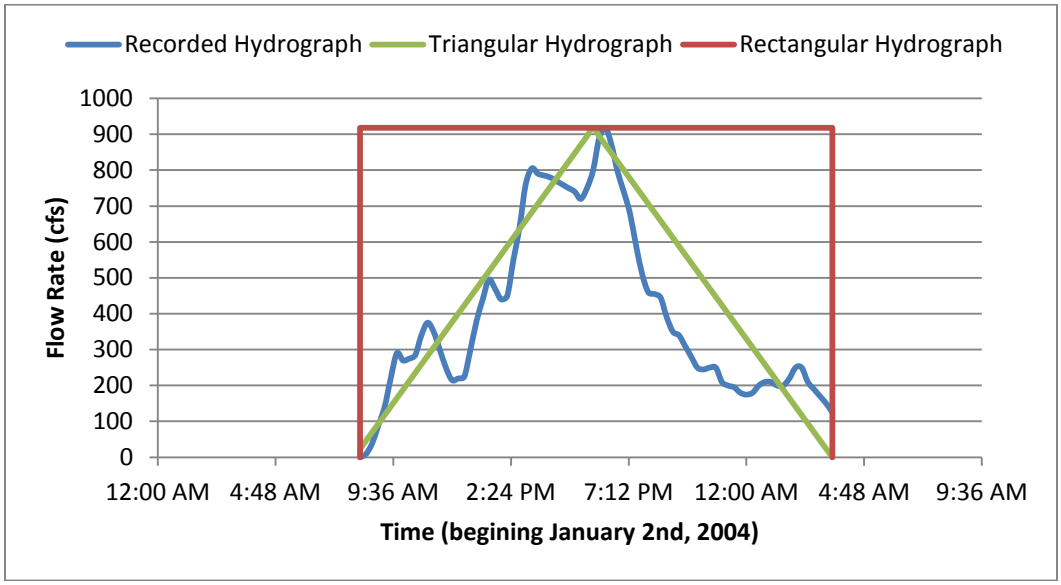

Figure 5-8 Hydrograph shapes used for scour depth comparison in Figure 5-9 and Figure 5-10

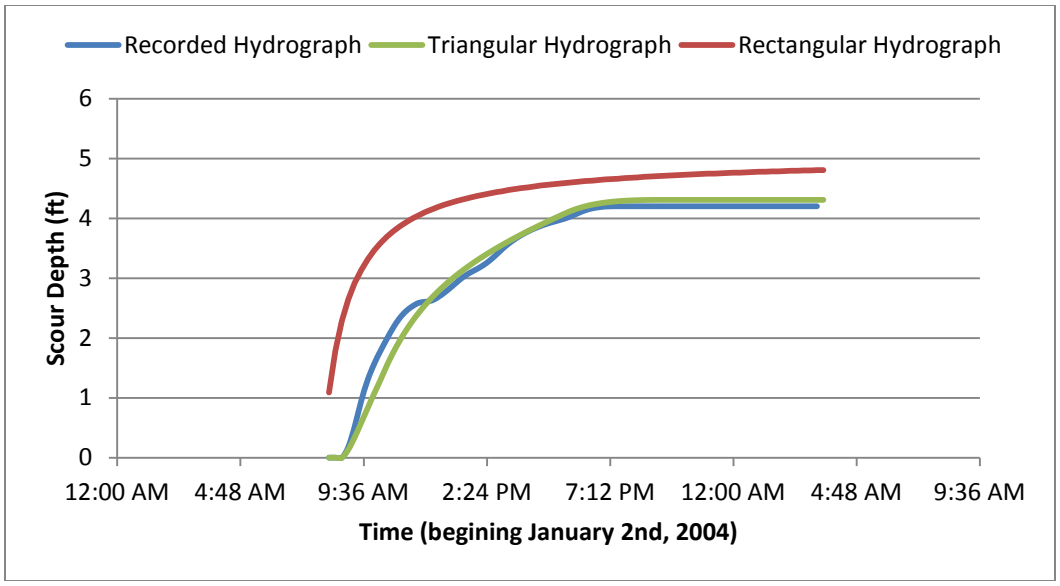

Figure 5-9 Predicted scour depth for different hydrograph shapes with Kaelepulu in-situ soil

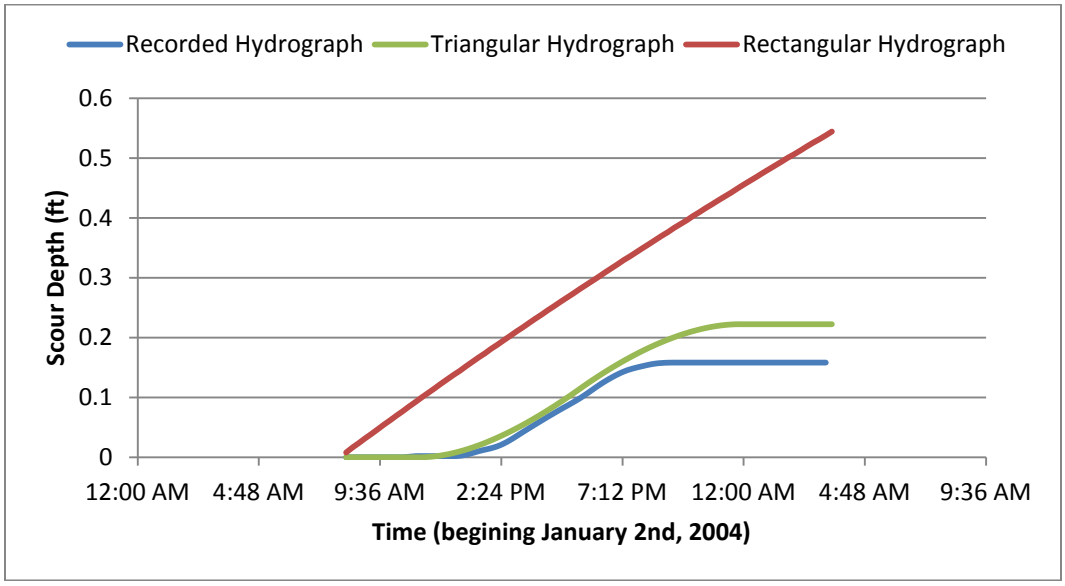

Figure 5-10 Predicted scour depth for different hydrograph shapes with high plasticity clay

The shape of hydrograph is shown to have an impact on predicted scour depth. The non-cohesive soil is significantly more erodible than the high plasticity clay. The difference in predicted scour depths for the non-cohesive soil is relatively small. The triangular hydrograph generates a scour development curve that almost mirrors the scour development curve of the recorded hydrograph. The rectangular hydrograph over predicts by approximately 14% relative to the recorded hydrograph but this is still a very close

estimate. The less erodible high plasticity clay shows a much greater effect of hydrograph shape on the scour development curve. The rectangular hydrograph over predicts the scour depth relative to the recorded hydrograph by a factor of nearly 3.5. The shape of the scour development curve is nearly linear whereas the recorded hydrograph scour development curve is hyperbolic. The triangular hydrograph is a closer approximation to the recorded hydrograph, over predicting the scour depth by a factor of 1.5, and nearly matching the shape of the scour development curve.

5.5 Representation of Hydrograph Curves by Rectangular Hydrographs

Stream gage records provide the most accurate representation of all the detailed characteristics of historic flood events. In many cases a stream gage record does not exist or is not sufficiently long to predict the flow rate of the required flood frequency. Methods such as the rational method and regional regression equations exist that can predict the peak flow rate for ungaged streams, but these methods do not generate a detailed hydrograph. A hydrologic model can be used to simulate a future flood event and generate a design hydrograph. However a design hydrograph has many limitations. As discussed in Chapter 3, discharge data is still required to validate that a model is an accurate representation of the conditions in a watershed. In the absence of this validation data any model result should be reviewed with caution. Representing a detailed design hydrograph generated by a hydrologic model by a simple rectangular hydrograph has the potential to simplify design calculations for both gaged and ungaged streams.

A rectangular hydrograph with the peak equal to the design flow has the potential to replace hydrographs developed by more complex hydrologic models. The duration of this rectangular hydrograph will have a significant impact on the final scour depth because the SRICOS-EFA method is a time dependent scour prediction method. Analysis is required to determine a duration that will yield conservative and realistic scour depth predictions. The scour depth for 10 different hydrograph curves, 6 developed from hydrologic models and 4 from recorded floods, was calculated using the SRICOS-EFA method. The time required to develop scour to the same depth, assuming the hydrograph was rectangular with the peak flow equal to the peak of the hydrograph curve, was then

calculated. Different soil types develop scour at different rates, and therefore this process was repeated with 3 different soil types. Both the Manoa-Palolo Bridge and Kaelepulu Bridge geometries were included to ensure that the effects of any single geometric parameter would be minimized.

Table 5-3 summarizes the included hydrographs and Table 5-4 describes the EFA curves that were varied in the rectangular hydrograph duration analysis. A total of 60 different scour depth predictions and peak flow durations are described in Table 5-5 through Table 5-16. A sample of the rectangular hydrograph analysis is plotted in Figure 5-11 showing the December 19, 2010 flood and the Manoa-Palolo Bridge geometry. The rectangular hydrograph duration is shown to increase as the soil become more cohesive while the predicted scour depth decreases as the soil becomes more cohesive.

Table 5-3 Hydrographs used in rectangular hydrograph duration analysis

Hydrograph	Abbreviation	Figure Number
Manoa-Palolo 100 year hydrograph	Manoa-Palolo	Figure 3-20
Kaoli Ditch 100 year hydrograph	Kaoli Ditch	Figure 3-35
Halawa Stream 100 year hydrograph	Halawa	Figure 3-36
Moanalua Stream 100 year hydrograph	Moanalua	Figure 3-37
Waiahole Stream 100 year hydrograph	Waiahole	Figure 3-38
West Loch Stream 100 year hydrograph	West Loch	Figure 3-39
January 2, 2004 flood; Kaelepulu Stream	1/2/04	Figure 5-1
December 19, 2010 flood; Manoa-Palolo Stream	12/19/10	Figure 3-15
March 5, 2012 flood; Manoa-Palolo Stream	3/5/12	Figure 3-17
May 2, 2011 flood; Manoa-Palolo Stream	5/2/11	Figure 3-16

Table 5-4 EFA curves used in rectangular hydrograph duration analysis

EFA curve	Figure Number
coarse sand	Figure 4-10
sand w/ silt & clay	Figure 5-5
high plasticity clay	Figure 5-4

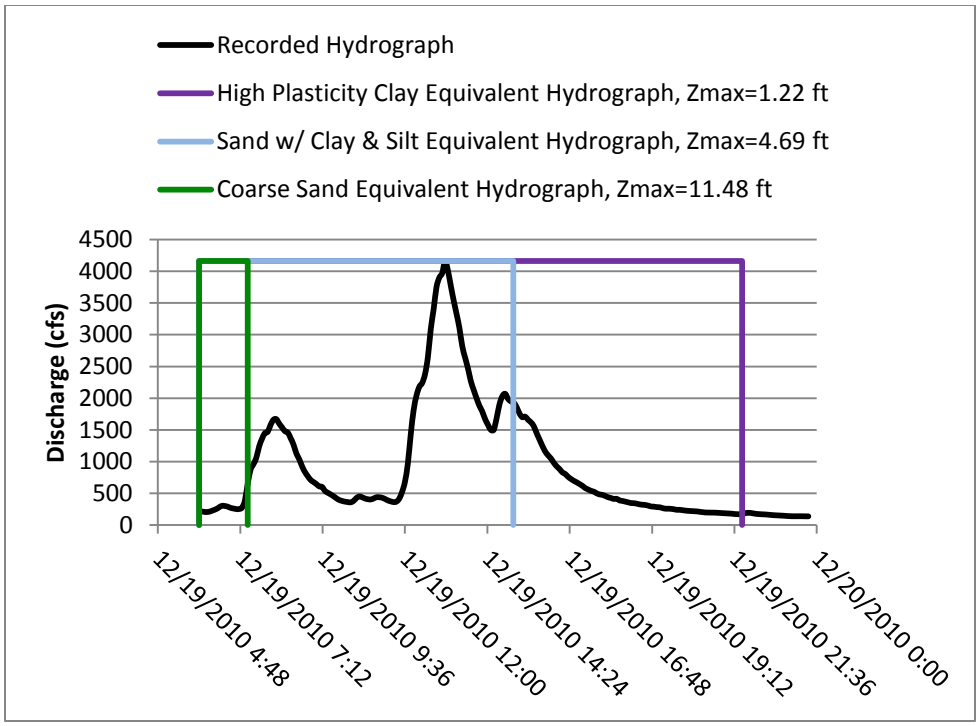

Figure 5-11 Duration required to scour to the same depth as the recorded hydrograph with varying soil type for the December 19, 2010 flood and Manoa-Palolo Bridge geometry

Table 5-5 Rectangular hydrograph duration analysis part 1

Bridge Geometry	Manoa-Palolo	Manoa-Palolo	Manoa-Palolo	Manoa-Palolo	Manoa-Palolo
Hydrograph	Manoa-Palolo	Kaoli Ditch	Halawa	Moanalua	Waiahole
EFA curve	coarse sand	coarse sand	coarse sand	coarse sand	coarse sand
SRICOS-EFA maximum scour depth (ft)	22.43	13.55	22.28	23.37	17.66
Scour developed over hydrograph (ft)	18.22	11.85	18.13	18.89	14.97
Percent of maximum scour that developed	81%	87%	81%	81%	85%
Rectangular hydrograph duration (hrs)	3.68	3.04	3.69	3.78	3.41

Table 5-6 Rectangular hydrograph duration analysis part 2

Bridge Geometry	Manoa-Palolo	Manoa-Palolo	Manoa-Palolo	Manoa-Palolo	Manoa-Palolo
Hydrograph	West Loch	1/2/04	12/19/10	3/5/12	5/2/11
EFA curve	coarse sand	coarse sand	coarse sand	coarse sand	coarse sand
SRICOS-EFA maximum scour depth (ft)	20.02	9.21	15.72	16.87	13.41
Scour developed over hydrograph (ft)	16.59	8.26	11.48	11.44	8.7
Percent of maximum scour that developed	83%	90%	73%	68%	65%
Rectangular hydrograph duration (hrs)	3.53	2.51	1.42	1.22	0.8

Table 5-7 Rectangular hydrograph duration analysis part 3

Bridge Geometry	Manoa-Palolo	Manoa-Palolo	Manoa-Palolo	Manoa-Palolo	Manoa-Palolo
Hydrograph	Manoa-Palolo	Kaoli Ditch	Halawa	Moanalua	Waiahole
EFA curve	high plasticity clay	high plasticity clay	high plasticity clay	high plasticity clay	high plasticity clay
SRICOS-EFA maximum scour depth (ft)	22.44	13.55	22.28	23.37	17.66
Scour developed over hydrograph (ft)	0.64	0.66	0.7	0.71	0.63
Percent of maximum scour that developed	3%	5%	3%	3%	4%
Rectangular hydrograph duration (hrs)	9.14	7.95	10	10.29	8.17

Table 5-8 Rectangular hydrograph duration analysis part 4

Bridge Geometry	Manoa-Palolo	Manoa-Palolo	Manoa-Palolo	Manoa-Palolo	Manoa-Palolo
Hydrograph	West Loch	Kaelepulu	12/19/2010	3/4/2012	5/2/2011
EFA curve	high plasticity clay	high plasticity clay	high plasticity clay	high plasticity clay	high plasticity clay
SRICOS-EFA maximum scour depth (ft)	20.02	9.21	15.72	16.87	13.41
Scour developed over hydrograph (ft)	0.81	1.23	1.22	0.9	0.38
Percent of maximum scour that developed	4%	13%	8%	5%	3%
Rectangular hydrograph duration (hrs)	11.16	15.93	15.82	11.67	4.47

Table 5-9 Rectangular hydrograph duration analysis part 5

Bridge Geometry	Manoa-Palolo	Manoa-Palolo	Manoa-Palolo	Manoa-Palolo	Manoa-Palolo
Hydrograph	Manoa-Palolo	Kaoli Ditch	Halawa	Moanalua	Waiahole
EFA curve	sand w/ clay & silt	sand w/ clay & silt	sand w/ clay & silt	sand w/ clay & silt	sand w/ clay & silt
SRICOS-EFA maximum scour depth (ft)	22.44	13.55	22.28	23.37	17.66
Scour developed over hydrograph (ft)	3.91	3.56	4.09	4.18	3.72
Percent of maximum scour that developed	17%	26%	18%	18%	21%
Rectangular hydrograph duration (hrs)	7.27	6.4	7.67	7.89	6.69

Table 5-10 Rectangular hydrograph duration analysis part 6

Bridge Geometry	Manoa-Palolo	Manoa-Palolo	Manoa-Palolo	Manoa-Palolo	Manoa-Palolo
Hydrograph	West Loch	Kaelepulu	12/19/2010	3/4/2012	5/2/2011
EFA curve	sand w/ clay & silt	sand w/ clay & silt	sand w/ clay & silt	sand w/ clay & silt	sand w/ clay & silt
SRICOS-EFA maximum scour depth (ft)	20.02	9.21	15.72	19.87	13.41
Scour developed over hydrograph (ft)	4.4	4.22	4.69	3.61	1.99
Percent of maximum scour that developed	22%	46%	30%	18%	15%
Rectangular hydrograph duration (hrs)	8.35	10.14	9.16	6.42	3.09

Table 5-11 Rectangular hydrograph duration analysis part 7

Bridge Geometry	Kaelepulu	Kaelepulu	Kaelepulu	Kaelepulu	Kaelepulu
Hydrograph	Manoa-Palolo	Kaoli Ditch	Halawa	Moanalua	Waiahole
EFA curve	coarse sand	coarse sand	coarse sand	coarse sand	coarse sand
SRICOS-EFA maximum scour depth (ft)	21.7	8.46	21.4	23.53	13.66
Scour developed over hydrograph (ft)	17.61	7.34	17.38	18.97	11.56
Percent of maximum scour that developed	81%	87%	81%	81%	85%
Rectangular hydrograph duration (hrs)	2.64	2.34	2.62	2.7	2.5

Table 5-12 Rectangular hydrograph duration analysis part 8

Bridge Geometry	Kaelepulu	Kaelepulu	Kaelepulu	Kaelepulu	Kaelepulu
Hydrograph	West Loch	Kaelepulu	12/19/2010	3/4/2012	5/2/2011
EFA curve	coarse sand	coarse sand	coarse sand	coarse sand	coarse sand
SRICOS-EFA maximum scour depth (ft)	17.36	5.03	11	12.53	8.31
Scour developed over hydrograph (ft)	14.36	4.49	7.78	8.35	5.04
Percent of maximum scour that developed	83%	89%	71%	67%	61%
Rectangular hydrograph duration (hrs)	2.52	3.01	0.96	0.86	0.54

Table 5-13 Rectangular hydrograph duration analysis part 9

Bridge Geometry	Kaelepulu	Kaelepulu	Kaelepulu	Kaelepulu	Kaelepulu
Hydrograph	Manoa-Palolo	Kaoli Ditch	Halawa	Moanalua	Waiahole
EFA curve	high plasticity clay	high plasticity clay	high plasticity clay	high plasticity clay	high plasticity clay
SRICOS-EFA maximum scour depth (ft)	21.7	8.46	21.4	23.53	13.66
Scour developed over hydrograph (ft)	0.52	0.28	0.55	0.58	0.41
Percent of maximum scour that developed	2%	3%	3%	2%	3%
Rectangular hydrograph duration (hrs)	5.2	4.46	5.5	5.7	4.96

Table 5-14 Rectangular hydrograph duration analysis part 10

Bridge Geometry	Kaelepulu	Kaelepulu	Kaelepulu	Kaelepulu	Kaelepulu
Hydrograph	West Loch	Kaelepulu	12/19/2010	3/4/2012	5/2/2011
EFA curve	high plasticity clay	high plasticity clay	high plasticity clay	high plasticity clay	high plasticity clay
SRICOS-EFA maximum scour depth (ft)	17.36	5.03	11	12.53	8.31
Scour developed over hydrograph (ft)	0.53	0.16	0.35	0.19	0.06
Percent of maximum scour that developed	3%	3%	3%	2%	1%
Rectangular hydrograph duration (hrs)	5.87	5.13	4.81	2.36	0.98

Table 5-15 Rectangular hydrograph duration analysis part 11

Bridge Geometry	Kaelepulu	Kaelepulu	Kaelepulu	Kaelepulu	Kaelepulu
Hydrograph	Manoa-Palolo	Kaoli Ditch	Halawa	Moanalua	Waiahole
EFA curve	sand w/ clay & silt	sand w/ clay & silt	sand w/ clay & silt	sand w/ clay & silt	sand w/ clay & silt
SRICOS-EFA maximum scour depth (ft)	21.7	8.46	21.4	23.53	13.66
Scour developed over hydrograph (ft)	3.58	2.08	3.63	3.85	2.81
Percent of maximum scour that developed	16%	25%	17%	16%	21%
Rectangular hydrograph duration (hrs)	5.03	4.63	5.15	5.28	4.8

Table 5-16 Rectangular hydrograph duration analysis part 12

Bridge Geometry	Kaelepulu	Kaelepulu	Kaelepulu	Kaelepulu	Kaelepulu
Hydrograph	West Loch	Kaelepulu	12/19/2010	3/4/2012	5/2/2011
EFA curve	sand w/ clay & silt	sand w/ clay & silt	sand w/ clay & silt	sand w/ clay & silt	sand w/ clay & silt
SRICOS-EFA maximum scour depth (ft)	17.36	5.03	11	12.53	8.31
Scour developed over hydrograph (ft)	3.44	1.87	2.59	1.61	0.7
Percent of maximum scour that developed	20%	37%	24%	13%	8%
Rectangular hydrograph duration (hrs)	5.37	7.98	5.02	2.58	1.3

Bridge geometry does not have a significant impact on the percent of maximum scour that will develop over a given hydrograph. This is consistent with expectations, as the geometry will affect the maximum scour depth but should have little effect on the development of scour over time.

The maximum scour depth for a given hydrograph and geometry is controlled by the peak flow rate of the given hydrograph. As expected, the hydrographs with a larger peak flow have a greater maximum scour depth. The shape of the hydrograph curve and whether it was observed or modeled appears to have a relatively small effect on the percent of maximum scour depth that was developed within a given soil type. Hydrograph curves with a longer duration of elevated flow were observed to require a rectangular hydrograph with a longer duration to generate the same scour depth relative to hydrograph curves that were shorter in duration.

Soil type is observed to have the most significant impact on both the depth of scour developed over the duration of a hydrograph and the rectangular hydrograph duration required to generate the same scour depth. The non-cohesive coarse sand is observed to generate the greatest depth of scour in the shortest duration. The high plasticity clay developed a very small depth of scour over a hydrograph and required a significantly longer duration to achieve the same depth with a rectangular hydrograph. The sand with silt and clay, which has cohesive strength between the coarse sand and high plasticity clay, was observed to scour to a depth between the coarse sand and high plasticity clay over the same hydrograph. The rectangular hydrograph duration required

to scour to the same depth as the full hydrograph for the sand with silt and clay was also observed to fall between the duration required for the high plasticity clay and the coarse sand.

5.6 Sensitivity Analysis of Input Parameters on Predicted Scour Depth

A sensitivity analysis was conducted to determine which parameters have the most significant effect on the final scour depth. The Manoa-Palolo Bridge geometry was selected for this analysis. Two hydrographs were included in the sensitivity analysis, the Manoa-Palolo 100 year flood generated using HEC-HMS composite model, shown in Figure 3-20, and a 12 hour rectangular hydrograph with the same peak flow rate. Two EFA curves were also selected for this analysis, the coarse sand from the Manoa-Palolo stream shown in Figure 4-10 and high plasticity clay shown in Figure 5-4. For each parameter studied in this sensitivity analysis a total of 4 scour depths were calculated, one for each combination of hydrograph and EFA curve. The maximum percent change in scour for each parameter is shown in Table 5-17. Geometric parameters were not included in this sensitivity analysis as they are likely to be known with a high degree of certainty in either a design scenario or review of an existing structure.

Table 5-17 Results of SRICOS-EFA sensitivity analysis

Parameter Varied	Percent Change in Parameter	Maximum Percent Change in Scour Depth
Peak Flow	-10%	-3.96%
Hydrograph Duration	-10%	-9.46%
EFA measured velocity	-10%	4.82%
EFA Measured Erosion Rate	-10%	-9.64%
Manning's Roughness Coefficient	-10%	7.23%
Hydraulic Radius	-10%	-3.61%

Accurately estimating peak flow of a design flood event is important; however there is a high degree of uncertainty in hydrologic studies. The SRICOS-EFA method yields a scour depth that varies less than the change in peak flow. Non-cohesive soils that

are close to reaching the maximum scour depth are more sensitive to variations in peak flow than cohesive soils.

The duration of hydrograph has a significant effect on the scour depth particularly in cohesive soils. Scour develops along a hyperbolic curve, approaching an asymptote equal to the maximum scour depth. Hydrograph duration has the most significant effect early in the development of the scour depth, before the scour approaches the maximum scour depth. Therefore cohesive soils which develop scour more slowly are likely to be more sensitive to hydrograph duration than non-cohesive soils.

The erosion function apparatus regulates flow velocity by opening and closing a valve, and the velocity is measured in the pipe after the soil sample is exposed to the flow. The recorded velocity does not remain exactly constant but fluctuates due to the mechanical nature of the pump and velocity meter. The effect of this fluctuation on scour depth is relatively minimal. While the maximum percent change in scour depth shown in Table 5-17 is 4.82%, the largest absolute difference in scour depth is less than 0.1 feet.

A researcher is required to observe the rate a sample is eroded during an EFA test. The researcher is required to determine when to further protrude a sample into the flow which can produce inconsistency between samples and researchers. The percent change in the depth of scour is nearly equal to the percent error in determining the erosion rate. An experienced researcher should conduct all EFA testing to consistently and accurately determine the erosion rate. Conducting multiple EFA tests for a single soil type will also increase the reliability of an EFA curve.

Manning’s roughness coefficient and the hydraulic radius of a stream are required to accurately convert flow rate into velocity. Manning’s roughness coefficient requires an experienced hydrologist to determine the roughness of the stream bed by observation. Inaccurately determining Manning’s roughness coefficient will significantly affect the velocity input to SRICOS-EFA which can lead to a highly inaccurate scour depth calculation. The hydraulic radius is related to the geometry of a stream and the stream stage for a given flood event. Hydraulic radius can be calculated with a high degree of certainty given a proper stream survey. Inaccuracy in determining hydraulic radius will affect the scour depth, but to a lesser extent than Manning’s roughness coefficient.

5.7 Hydrograph Recommendation for the Design Scour Event using SRICOS-EFA

The design scour depth calculated using the SRICOS-EFA method for a non-cohesive soil may be approximated as Z_{max}, without requiring a full SRICOS-EFA analysis. The actual scour depth for the design flood is likely between 60% and 90% of Z_{max}, but this overestimation can serve as a reasonable factor of safety. If a reduced factor of safety is desired a rectangular hydrograph with peak equal to the design flow rate and duration equal to either 12 or 24 hours can be utilized for a full SRICOS-EFA calculation. The design scour depth calculated using the HEC-18 manual is likely to yield comparable results.

The design scour depth calculated using the SRICOS-EFA method for a soil with cohesion may be approximated as either 25% of Z_{max} or the scour depth generated by a rectangular hydrograph with peak equal to the design flow and 12 hour duration, whichever is greater. One of these two scenarios should yield a conservative design scour depth for a single design flood event, as shown in Table 5-5 through Table 5-16. If an additional factor of safety is desired, a rectangular hydrograph with 24 hour duration rather than 12 hour duration is acceptable. It should be noted that this recommendation is based on the analysis of 3 EFA curves, only one of which was developed from a cohesive soil. This recommendation may not be valid for cohesive soils that do not have an EFA curve similar to Figure 5-4. The HEC-18 manual is the current FHWA design standard and is also acceptable method that will likely generate a conservative result, but some may consider the result overly conservative particularly in soils with a high cohesive strength or significant armoring of the soil. This is supported by comparing the results in Figure 5-7 with the HEC-18 design scour depth discussed in Section 5.2.

The recommendation for a 12 hour rectangular hydrograph is consistent with the rainfall duration analysis in Chapter 3. Table 3-1 shows the average duration of a high intensity rainfall event on Oahu is 6.72 hours. A rainfall of approximately 6 hours will yield a flood that recedes in approximately 12 hours, as supported by the HEC-HMS 100 year flood design hydrographs for 6 different watersheds on Oahu. Changing the shape from a curve to a rectangle with constant peak flow serves as a factor of safety. The

magnitude of this factor of safety will depend on soil type, but the change in shape is likely to increase the design scour depth by a factor between 1.1 and 3.5 according to Figure 5-9 and Figure 5-10. All design scour depths should be evaluated with caution. Engineers should consider multiple hydrologic methods to predict peak flow and multiple hydrographs with characteristics consistent with the local watershed in SRICOS-EFA calculations. A conservative scour depth should always be utilized in bridge design to ensure public safety.

Chapter 6 SUMMARY AND CONCLUSIONS

6.1 Summary

Predicting floods with the 100 year return period is significant because both the HEC-18 and SRICOS-EFA scour prediction methods require a design event like the 100 year flood. The Manoa-Palolo watershed was the primary focus of this flood frequency analysis as this allowed for indirect predictive methods to be compared with a statistical analysis on the stream gage record. The 100 year flow rate for the Manoa-Palolo Stream predicted using 6 different methods is shown in Table 3-16. The statistical analysis that was conducted included 43 years of annual peak discharge data. A longer stream gage record, and accounting for the effects of climate change over time, may result in an improved statistical flood frequency analysis. The USGS regional regression equations provided an estimate of the flood frequency but have a large standard error introduced by representing a large and diverse hydrologic region by a single simple equation. The other indirect methods of predicting the 100 year flood all required converting rainfall to stream discharge. This is not always accurate because hydraulic factors, such as a blocked bridge or culvert, may cause a rain event to induce a flood much larger than expected. However this is the best information that is available in a design scenario and was utilized in this flood frequency analysis. Both the HEC-HMS software and TR-55 method were found to be very sensitive to certain parameters including number of sub-basins, curve number, rainfall distribution, lag time, time of concentration and travel time. The HEC-HMS software could be validated by historic flood events, but this validation is not possible for watersheds without a stream gage. The rational method was also studied; however this method requires a very small drainage area. The result is that a large basin must be sub-divided many times, and the error associated with parameters that require estimation and cannot be validated is potentially compounded. The HEC-HMS software that utilized a composite model, SCS runoff curve number was used as the loss rate method and the SCS unit hydrograph as the transform method was selected for predicting peak flow rates for ungaged watersheds. Even though the existing hydrologic design manuals typically recommend using sub-divisions to increase the accuracy of

predictions, the results of this study indicate that in certain situations a composite area may provide better predictions than using sub-divisions. Since hydrologic modeling involves a high degree of uncertainty, this issue requires further investigation. The HEC-HMS software allows for variations in rainfall while utilizing a composite model, both spatially and temporally, that the TR-55 method does not allow. A composite model requires fewer parameters to be estimated than a model including sub-basins which is beneficial for a model that cannot be validated by historic flood events.

The hydrologic analysis was applied to the SRICOS-EFA and HEC-18 methods to compare and evaluate the predicted scour depths. The January 2nd, 2004 flood in the Kaelepulu Stream was the only scour event recorded in real time available that occurred in the state of Hawaii and was used to compare the two methods to a recorded event. The SRICOS-EFA method was found to be closer approximation of the recorded scour depth than the HEC-18 method for the January 2nd, 2004 scour event. Predicted scour depth induced by the 100 year flood in the Manoa-Palolo Stream was also evaluated. Both methods were found to have very comparable scour depth predictions for the 100 year flood in the Manoa-Palolo Stream. This is consistent with expectations since the soil is non-cohesive, the design flood duration is long, and the time dependence of scour development is not expected to have a significant impact on the SRICOS-EFA predicted scour depth. Parameters that have a significant effect on the SRICOS-EFA method predicted scour depth were evaluated. Soil type, or more specifically the shape of the EFA curve, was found to have a significant impact on predicted scour depth. The duration required for a rectangular hydrograph to scour to the same depth as a hydrograph curve was studied using the SRICOS-EFA method and three EFA curves. The coarse sand was found to require a short duration equivalent rectangular hydrograph and scour to a relatively large depth, whereas the high plasticity clay was found to require a very long duration equivalent rectangular hydrograph and erode to a relatively small depth. The information regarding the duration of rectangular hydrograph required to scour to the same depth as a hydrograph curve was used to make a recommendation for the type of hydrograph that can be utilized with the SRICOS-EFA method to yield a reasonable and conservative design scour depth and is discussed in section 5.7.

6.2 Conclusions

1. The SRICOS-EFA method was more accurate in predicting the recorded scour depth than the HEC-18 method for the January 2nd, 2004 flood event in the Kaelepulu Stream.
2. The predicted scour depth induced by the 100 year flood in the Manoa-Palolo Stream, which has a streambed characterized by coarse sand and gravel, is very comparable between the HEC-18 and SRICOS-EFA methods.
3. For the SRCIOS-EFA method, soils with a large initial erosion rate are less sensitive to variations in hydrograph shape and duration than soils with a small initial erosion rate.
4. A large degree of uncertainty exists in flood frequency analysis. Multiple methods should be considered in evaluating flood frequency. The best hydrologic method for predicting flood frequency may depend on the watershed characteristics, type of information available, the limitations of each hydrologic method, and which method can best represent the field conditions.

6.3 Recommendations for Future Research

1. Research focused on generating a rainfall distribution suitable for predicting peak flow that will also generate a design hydrograph and is representative of hydrologic conditions in Hawaii would be beneficial to engineering design.
2. Further investigation into the ideal size of a drainage area or sub-basin for the HEC-HMS and TR-55 methods is necessary. A method to validate parameters required for both methods in ungaged watersheds would also be beneficial.
3. Continued evaluation of a reasonable and conservative design hydrograph for the SRICOS-EFA method is necessary. This should include an increased number of EFA curves, particularly focused on different cohesive soils.
4. Utilizing scour monitoring equipment to record more scour events in the state of Hawaii is important. Increasing the number of scour events that are recorded will allow for a more detailed comparison between the recorded and predicted scour

depth using the SRICOS-EFA method, the HEC-18 method, or some other scour prediction method not considered in this research.

5. Development of a method to predict the initial erosion rate without requiring site specific sampling and EFA testing would allow for a simpler scour design process. This method should include a wide range of soil types, including non-cohesive soils that cannot be sampled using conventional methods for collecting a Shelby tube sample. The initial erosion rate determined by an EFA curve has a significant impact on the SRICOS-EFA predicted scour depth, and such a method should correlate well with EFA curves generated from site specific samples.

REFERENCES

Arneson, L. A., Zevenbergen, L. W., Lagasse, P. F., & Clopper, P. E. (2012). *Evalutaing Scour at Bridges Fifth Edition.* Washington D.C.: Federal Highway Administration.

Bateni, S. M., Borghei, S. M., & Jeng, D. S. (2007). Neural network and neuro-fuzzy assessments for scour depth around bridge piers. *Engineering Applications of Artificial Intelligence*, 401-414.

Briaud, J. L., Chen, H. C., Kwak, K. W., Han, S. W., & Ting, F. C. (2001). Multiflood and multilayer method for scour rate prediction at bridge piers. *Journal of Geotechnical and Geoenvironmental Engineering, 127*(2), 114-125.

Briaud, J. L., Ting, F. C., Chen, H. C., Gudavalli, R., Perugu, S., & Wei, G. (1999). SRICOS: prediction of scour rate in cohesive soils at bridge piers. *Journal of Geotechnical and Geoenvironmental Engineering, 125*(4), 237-246.

Briaud, J.-L., Chen, H.-C., Chang, K.-A., Oh, S., Chen, S., Wang, J., . . . Ting, F. (2011). *The SRICOS-EFA Method.* College Station, TX: Texas A&M University.

Briaud, J.-L., Chen, H.-C., Li, Y., Nurtjahyo, P., & Wang, J. (2004). *Pier and Contraction Scour in Cohesive Soils.* Washington, D.C.: Transportation Research Board.

Calappi, T., Miller, C. J., & Carpenter, D. (2010). Revisiting the HEC-18 Scour Equation. *Fifth International Conference on Scour and Erosion* (pp. 1102-1109). San Francisco, CA, USA: ASCE.

Choi, S.-U., & Cheong, S. (2006). Prediction of Local Scour Around Bridge Piers Using Artifial Neural Networks. *Journal of the American Water Resources Association*, 487-494.

Chu, P.-S., Zhao, X., Ruan, Y., & Grubbs, M. (2009). Extreme Rainfall Events in the Hawaiian Islands. *Journal of Applied Meteorology and Climatology, 48*(3), 502-516.

City and County of Honolulu. (2000). *Rules relating to storm drainage standards.* Honolulu, HI: City and County of Honolulu Department of Planning and Permitting.

Cleveland, T. G., Thompson, D. B., Fang, X., & He, X. (2008). Synthesis of Unit Hydrographs from a Digital Elevation Model. *Journal of Irrigation and Drainage Engineering*, 212-221.

Conaway, J. S. (2007). Analysis of Real-Time Streambed Scour Data From Bridges in Alaska. *World Environmental and Water Resources Congress.* ASCE.

Debnath, K., & Chaudhuri, S. (2010). Bridge Pier Scour in Clay-Sand Mixed Sediments at Near-Threshold Velocity for Sand. *Journal of Hydraulic Engineering*, 597-609.

Federal Highway Administration. (1988). *Revisions to the National Bridge Inspection Standards (NBIS).* McLean, VA.

Feldman, A. D. (2000). *Hydrologic Modeling System HEC-HMS Technical Reference Manual.* Washington, DC: US Army Corps of Engineers.

Firat, M., & Gungor, M. (2009). Generalized Regression Neural Networks and Feed Forward Neural Networks for Predictoin of Scour Depth Around Bridge Piers. *Advances in Engineering Software*, 731-737.

Ghelardi, V. M. (2004). *Estimation of Long Term Bridge Pier Scour in Cohesive Soils at Maryland Bridges Using EFA/SRICOS.* College Park, MD: University of Maryland: Master's Thesis.

Giambelluca, T. W., Chen, Q., Frazier, A. G., Price, J. P., Chen, Y.-L., Chu, P.-S., . . . Delparte, D. M. (2012). Online Rainfall Atlas of Hawai'i. *Bull. Amer. Meteor. Soc.*, doi: 10.1175/BAMS-D-11-00228.1.

Govindasamy, A. V., Briaud, J. L., Chen, H. C., Delphia, J., Elsbury, K., Gardoni, P., . . . Olivera, F. (2008). Simplified Method for Estimating Scour at Bridges. *GeoCongress*, (pp. 385-393).

Govindasamy, A. V., Briaud, J. L., Kim, D., Olivera, F., Gardoni, P., & Delphia, J. (2010). Observational Method for Estimating Future Scour Depth at Existing Bridges. *Fifth International Conference on Scour and Erosion* (pp. 41-65). San Francisco, CA, USA: ASCE.

Hager, W. H., & Unger, J. (2010). Bridge Pier Scour under Flood Waves. *Journal of Hydraulic Engineering*, 842-847.

Hawaii Department of Transportation Highways Division. (2010). *Design Criteria for Highway Drainage.* Honolulu, HI: State of Hawaii.

Huang, W., Yang, Q., & Xiao, H. (2009). CFD modeling of scale effects on turbulence flow and scour around bridge piers. *Computers & Fluids*, 1050-1058.

Inglis, C. C. (1949). *The behavior and control of rivers and canals: Poona, India.* Poona Research Station: Central Water Power Irrigation and Navigation Report 13, Part II.

Inglis, S. C. (1949). *The behavior and control of rivers and canals: Poona, India.* Poona Research Station. Central Water Power Irrigation and Navigation Report.

Jackson, K. S. (1996). *Evaluation of bridge scour data at selected sites in Ohio.* Columbus, OH: US Geologic Survey Water Resources Investigation Report 97-4182.

Jackson, K. S. (1996). *Evaluation of Bridge-Scour Data at Selected Sites in Ohio.* Columbus, OH: US Geologic Survey Water Resources Investigation Report 97-4182.

Jiang, J., Ganju, N. K., & Mehta, A. J. (2004). Estimation of Contraction Scour in Riverbed Using SERF. *Journal of Waterway, Port, Coastal and Ocean Engineering*, 215-218.

Kaya, A. (2010). Artificial Neural Network Study of Observed Pattern of Scour Depth Around Bridge Piers. *Computers and Geotechnics*, 413-418.

Kimoto, A., Canfield, H. E., & Stewart, D. (2011). Comparison of Synthetic Design Storms with Observed Storms in Southern Arizona. *Jounral of Hydrologic Engineering*, 935-941.

Kwak, K. (2000). *Prediction of Scour depth Versus Time for Bridge Piers in Cohesive Soils in the CAse of Multi-Flood and Multi-Layer Soil Systems.* College Station, TX: Dissertation: Texas A&M University.

Larsen, R. J., Francis, C. K., & Jones, A. L. (2011). Flow Velocity and Pier Scour Prediction in a Compound Channel: Big Sioux River Bridge at Flandreau, South Dakota. *Journal of Hydraulic Engineering*, 595-605.

Lau, D., & Gali, S. (2010). How "Critical" is Critical Duration in Determining Flodd Risk, Flood Damages and Stormwater Management Solutions. *Watersheed Management*, (pp. 1214-1225).

Laursen, E. M., & Toch, A. (1956). *Scour around bridge piers and abutments.* Ames, Iowa: Iowa Highway Research Board.

Laursen, E. M., & Toch, A. (1956). *Scour around bridge piers and abutments.* Iowa Highway Research Board Bulletin 4.

Lee, T. L., Jeng, D. S., Zhang, G. H., & Hong, J. H. (2007). Neural Network Modelling for Estimation of Scour Depth Around Bridge Piers. *Journal of Hydrodynamics*, 378-386.

Levy, B., & McCuen, R. (1999). Assessment of Storm Duration for Hydrologic Design. *Journal of Hydrologic Engineering*, 209-213.

Lu, J.-Y., Hong, J.-H., Su, C.-C., Wang, C.-Y., & Lai, J.-S. (2008). Field Measurments and Simulation of Bridge Scour Depth Variations during Floods. *Journal of Hydraulic Engineering*, 810-821.

Masaki, G. (2004). *Scour Monitoring and Prediction for Selected Highway Bridges on Oahu.* Honolulu, HI: University of Hawaii at Manoa: Master's Thesis.

Masaki, G., Teng, M. H., Cheng, E. D., & Matsuda, C. (2005). A validation study of the empirical bridge scour equations. *In Proceedings of the Joint ASME/ASCE/SES Conference on Mechanics and Materials.* Baton Rouge, Louisiana.

Melville, B. W., & Chiew, Y. M. (1999). Time scale for local scour at bridge piers. *J. Hydraul. Eng., 125*(1), 59-65.

Miller, R. L., & Wilson, J. T. (1996). *Evaluation of scour at selected bridge sites in Indiana.* Indianapolis, IN: US Geologic Survey Water Resources Invesigation Report 95-4259.

Miller, R. L., & Wilson, J. T. (1996). *Evaluation of Scour at Selected Bridge Sites in Indiana.* Indianapolis, IN: US Geological Survey Water-Resources Investigations Report 95-4259.

Miyagi, M. (2010). *Preliminary Testing of an Active Control Device for Mitigating Sand Blocakge Inside Coastal Highway Culverts and a Watershed Modeling System Simulation of the Kaaawa Watershed.* Honolulu, HI: Univesity of Hawaii at Manoa - Master's Thesis.

Najafzadeh, M., & Barani, G.-A. (2011). Comparison of group method of data handling based genetic programming and back propagation systems to predict scour depth around bridge piers. *Scientia Iranica*, 1207-1213.

Nakamura, J. (2010). *Evaluation and Compaison of teh HEC-18 and NCHRP-516 Methods for Predicting Scour at the Kaelepulu Bridge in Kailua,HI for January 2, 2004 Storm.* Honolulu, HI: University of Hawaii at Manoa: Master of Science Plan B Thesis.

National Oceanic and Atmospheric Administration. (2012). *Climate Data Online*. Retrieved from National Climatic Data Center: http://www.ncdc.noaa.gov/cdo-web/

National Weather Service. (2013). *Hawai'i Archived Hydronet Data*. Retrieved from National Weather Service Forecast Office: http://www.prh.noaa.gov/hnl/hydro/hydronet/hydronet-data.php

Natural Resources Conservation Service. (1986). *Urban Hydrology for Small Watersheds TR-55.* Conservation Engineering Division. United States Department of Agriculture.

Oceanit. (2008). *Final Drainage Evaluation Report Ala Wai Canal Watershed Project.* Honolulu, HI.

Oki, D. S., Rosa, S. N., & Yeung, C. W. (2010). *Flood-Frequency Estimates for Streams on Kaua'i, O'ahu, Moloka'i, Maui, and Hawai'i, State of Hawai'i.* Reston, VA: US Geologic Survey Scientific Investigations Report 2010-5035.

Perica, S., Martin, D., Lin, B., Parzybok, T., Riley, D., Yekta, M., . . . Bonnin, G. (2011). *Precipitation-Frequency Atlas of the United States, Volume 4, Version 3: Hawaiian Islands.* Silver Spring, MD: NOAA National Weather Service, NOAA Atlas 14.

Polasik, S. D. (2005). Tacoma Narrows Bridge Hydraulic Analysis. *Metropolis and Beyond.* New York, NY, USA.

Sturm, T. W., Ettema, R., & Melville, B. W. (2011). *Evaluation of bridge scour research: abutment and contraction scour processes and prediction.* NCHRP Web-only Document 181.

Tecca, N., Nakamura, J., Masaki, G., & Teng, M. H. (2012). *Evaluation of two different methods for predicting flood induced bridge scour.* South Bend, IN: In Proceedings of the 2012 Joint Conference of the Engineering Mechanics Institute and the 11th ASCE Joint Specialty Conference on Probabilistic Mechanics and Structural Reliability.

Tregnaghi, M., Marion, A., Bottacin-Busolin, A., & Tait, S. J. (2011). Modelling time varying scouring at bed sills. *Earth Surface Processes and Landforms*, 1761-1769.

USGS. (2013). *USGS 16247100 Manoa-Palolo Drainage Canal at Moiliili, Oahu, HI*. Retrieved from National Water Information System: Web Interface: http://nwis.waterdata.usgs.gov/nwis/nwisman/?site_no=16247100&agency_cd=USGS

Yu, X., Tao, J., & Yu, X. (2011). Comparison Study on Computer Simulations for Bridge Scour Estimation. *GeoRisk* (pp. 1125-1132). ASCE.

Zevenbergen, L. W., Thorne, C. R., Spitz, W. J., & Huang, X. (2011). *Evaluation of bridge scour research: geomorphic processes and predictions.* NCHRP Web-only document 177.

Zounemat-Kermani, M., Beheshti, A.-A., & Ataie-Ashtiani, B. (2009). Estimation of current-induced scour depth around pile groups using neural network and adaptive neuro-fuzzy inference system. *Applied Soft Computing*, 746-755.